Chapter 1
Diffusion and Point Defects in Silicon Materials

Hartmut Bracht

Abstract This chapter aims to provide a basic understanding on the complex diffusion behavior of self-, dopant-, and selected metal atoms in silicon (Si). The complexity of diffusion in Si becomes evident in the shape of self- and foreign-atom diffusion profiles that evolves under specific experimental conditions. Diffusion studies attempt to determine from the diffusion behavior not only the mechanisms of atomic transport but also the type of the point defects involved. This information is of pivotal interest to control the diffusion and activation of dopants during the fabrication of Si-based devices and, from a more fundamental scientific point of view, for comparison to the predictions of theoretical calculations on the properties of point defects in Si. In general, diffusion research relies both on experimental methods to accurately determine diffusion profiles established under well-defined conditions. The analysis of diffusion profiles that can be based on either analytical or numerical solutions of the considered diffusion-reaction equations provides first information about possible diffusion mechanisms. To identify the mechanisms of diffusion, studies under different experimental conditions have to be performed. This chapter on diffusion in Si starts with an introduction on the significance of diffusion research in semiconductors to determine the properties of atomic defects. Diffusion in solids is treated from a phenomenological and atomistic point of view. Experiments designed to investigate the diffusion of self- and foreign atoms are presented and typical self- and foreign-atom profiles obtained after diffusion annealing under specific conditions are illustrated. The mathematical treatment of diffusion-reaction mechanisms is introduced to understand the shape of diffusion profiles and the meaning of the diffusion coefficient deduced from experiments. Modeling of self-, dopant-, and metal-atom diffusion is described that aims at a consistent interpretation of atomic transport processes in Si based on unified properties of the native point defects involved. Finally, till unsolved questions on the properties of point defects in bulk Si and on the diffusion behavior in three-dimensional confined Si structures are addressed.

H. Bracht (✉)
Institute of Materials Physics, University of Münster, Wilhelm-Klemm-Str. 10, 48149 Münster, Germany
e-mail: bracht@uni-muenster.de

© Springer Japan 2015

Y. Yoshida, G. Langouche (eds.), *Defects and Impurities in Silicon Materials*,
Lecture Notes in Physics 916, DOI 10.1007/978-4-431-55800-2_1

Keywords Self-diffusion • Dopant diffusion • Metal diffusion • Point defects in silicon • Reaction mechanism • Isotope structures

1.1 Introduction

Over the last six decades our daily life has been revolutionized by the invention of Si-based electronic devices. The key for this development was the preparation and growth of high purity single crystals as well as the ability to control the impurity level, i.e., the defects incorporated in Si on the atomic scale. Till these days the defect density determines the integrity of Si devices for e.g. electronic and photovoltaic applications [1]. Further improvement of Si-based electronic devices requires an in-depth understanding on the properties of atomic defects and their interactions. The properties of atomic defects concern their type, structure, and charge states as well as their thermodynamic properties, i.e., their free enthalpy of formation and migration. Although atomistic calculations based on density functional theory (DFT) [2–15], tight binding molecular dynamics (TBMD) [16–19] and molecular dynamics (MD) simulations [20–23] were and are still increasingly used to predict the stability, mobility, and electronic properties of defects, the relevance of the theoretical results must finally be verified experimentally, since it remains unclear, how far theoretical data, mostly deduced for zero Kelvin, are also applicable for higher temperatures.

Theoretical calculations of the structure and formation energy of point defects in solids are most valuable for comparison with spectroscopic results gained e.g. from electron paramagnetic resonance (EPR) studies [24–26], optical methods such as infrared (IR) and photoluminescence spectroscopy [27], deep level transient spectroscopy (DLTS) [28], and perturbed angular correlation (PAC) experiments [29]. These methods provide results for temperatures which range from cryogenic to room temperature. More general applicable spectroscopic methods for studying point defects at temperatures relevant for device processing are hardly available. An exception is the positron annihilation spectroscopy (PAS) [30–32] and the Mössbauer spectroscopy (MS) [33]. Whereas the former method is highly capable for the investigation of vacancy-like defects in condensed matter, the latter method is mainly applicable to investigate the preferred incorporation of iron (Fe). Unfortunately PAS fails in the case of Si because the concentration of vacancies in thermal equilibrium is below the detection limit of the method [34]. On the other hand MS can provide valuable information about the occupancy of Fe on interstitial and substitutional lattice sites [35] but this method is less suited for studying diffusion phenomena in general as MS is practically restricted to the radioactive isotope ^{57}Fe.

Another capable method for studying point defect properties at elevated temperatures is diffusion in solids. This is highlighted by the present contribution that explains the origin of characteristic diffusion profiles in Si and describes what kind of information can be deduced from the diffusion of self- and foreign-atoms.

First a phenomenological and microscopic description of diffusion in solids is given in Sects. 1.3 and 1.4. Then the diffusion mechanisms mostly relevant for elemental semiconductors are presented. Direct and indirect diffusion mechanisms are introduced that highlight the significance of native point defects in atomic transport processes. The mathematical description of diffusion in solids with emphasis on Si is presented considering diffusion both under electronically intrinsic and extrinsic doping conditions. Examples on self-, dopant and metal diffusion experiments are given. The analyses of the experimental diffusion profiles provide valuable information about the properties of the point defects involved in the diffusion process. These examples also demonstrate the methods that are widely used to analyze diffusion in semiconductors. Special emphasis is paid to the interrelation between self- and foreign-atom diffusion that becomes directly evident in the fast diffusion of some mainly substitutionally dissolved metals and the simultaneous diffusion of self- and dopant atoms in isotopically modulated Si structures. Overall, diffusion studies pursue the goal to identify the mechanisms of diffusion and to determine the properties of the point defects involved. This understanding on the diffusion and interaction of point defects in semiconductors is of fundamental significance to control the diffusion and the electrical activation of dopants in the fabrication of electronic devices. Accordingly, point defects in semiconductors can be considered as the "salt of the soup". They not only determine the atomic transport but also the electronic, optical, and mechanical properties of semiconductors.

1.2 Defects in Semiconductors

Defects in elemental semiconductors such as Si and germanium (Ge) significantly affect their electrical properties. The same holds for binary group III–V (GaAs, GaSb, GaN, etc.), group II-VI (ZnO, ZnSe, CdTe, etc.) and ternary and quaternary compound semiconductors. Point defects such as impurities, which are mainly dissolved on lattice sites and introduce shallow acceptor or donor centers, make the material highly conductive and therewith suitable for electronic applications. In addition, defects which give rise to deep level centers affect the electrical properties of semiconductors. Such defects, like Au in Si, act as recombination centers for electrons and holes and are commonly used to reduce the lifetime of minority electrons and holes in high frequency devices. On the other hand high concentrations of deep level centers are undesirable because the effective doping concentration of the material would be strongly reduced by these compensating centers.

During the fabrication of electronic devices appropriate processing steps have to be performed to minimize the concentration of unintentionally introduced defects. In Si device technology, the concentration of detrimental transition metal contaminants (Fe, Cu, etc.) are reduced by gettering treatments. Transition metal precipitates and also D-defects in silicon wafers, the latter are considered to be vacancy clusters [36, 37], are responsible for the degradation of the gate oxide integrity of MOS structures [38–40]. This illustrates that not only the incorporation

of point defects but also the formation of extended defects such as dislocations, stacking faults and agglomerates of foreign atoms or native point defects must be controlled during wafer processing and, in particular, already during Si crystal growth.

Charged native point defects in Si are generally not considered to alter the electrical properties of the material significantly. Their concentration is believed to be sufficiently low as this is supported by direct measurements of the native defect concentration with positron annihilation experiments [34] and results deduced from diffusion studies (see e.g. [41]). However, compared to elemental semiconductors the concentration of native point defects in compound semiconductors can be several orders of magnitude higher because the formation of these defects depends on the partial pressure of the components over the compound [42–44].

The controlled incorporation of point defects in semiconductors is one of the main tasks in the production of electronic devices. Homogeneous doping is generally achieved by adding a controlled amount of the dopant element to the melt or to the gas phase of epitaxial layer deposition systems. However, the fabrication of electronic devices like diodes, transistors, or complex integrated circuits requires spatially inhomogeneous dopant distributions. Such distributions are formed by the deposition of dopants on or implantation beneath the surface followed by a high temperature diffusion step. In order to tune the semiconductor devices to the desired functionality the diffusion induced dopant distribution must be predictable and as accurate as possible. This requires a detailed knowledge of the atomic mechanisms of dopant diffusion that comprises information on the type of native point defects involved in dopant diffusion, their charge states and formation and migration enthalpies and entropies.

The diffusion mechanisms considered in this chapter are mainly representative for self- and foreign-atom diffusion in Si. It is noteworthy that the mechanisms are also applicable to diffusion in other elemental semiconductors and even to diffusion in compound semiconductors since the atomic transport in semiconductor compounds is often restricted to the sublattice of one of the constituents.

Before the atomic transport of self- and foreign-atoms in Si is treated in Sect. 1.5, first a phenomenological and atomistic view on diffusion is given in the following.

1.3 Phenomenological Treatment of Diffusion

Diffusion describes a process where an initial inhomogeneous distribution of matter in a media becomes homogenously distributed. Accordingly diffusion is reflected by the transport of matter. This transport acts in the direction to remove existing concentration gradients [45]. In many diffusion processes the concentration C_{A} of a foreign-atom A is low compared to the number density C_o of the matrix atoms, i.e., $C_{\mathrm{A}} \leq 10^{-2}$at%. In this nearly ideal dilution Fick's first law

$$\mathbf{j}_{\mathrm{A}}(\mathbf{r}, t) = -D_{\mathrm{A}}\, \nabla C_{\mathrm{A}}(\mathbf{r}, t) \tag{1.1}$$

describes the transport of a particle A in an existing concentration gradient (see e.g. [46]). $\mathbf{j}_\mathrm{A}$ denotes the diffusion flux in units of $[m^{-2}s^{-1}]$, D_A the diffusion coefficient in units of $[m^2s^{-1}]$, and C_A the number density, i.e. concentration, in units of $[m^{-3}]$. $\nabla = (\frac{\partial}{\partial x}, \frac{\partial}{\partial y}, \frac{\partial}{\partial z})$ is the nabla operator in the unit $[m^{-1}]$. The minus sign in Eq. (1.1) considers that the particle transport is opposite to the direction of the concentration gradient. In general, D_A is a second order tensor because the particle flux $\mathbf{j}_\mathrm{A}$ and concentration gradient ∇C_A can be directed differently. In crystals with cubic symmetry, such as in Si and Ge, the diffusion is isotrop and accordingly the diffusion coefficient is a scalar quantity.

In the case the number of particles is conserved during diffusion of A, i.e., no loss of particles occurs due to e.g. aggregation, segregation or other interactions with defects in the lattice, the combination of the continuity equation

$$\frac{\partial C_\mathrm{A}(\mathbf{r}, t)}{\partial t} = -\nabla \cdot \mathbf{j}_\mathrm{A}(\mathbf{r}, t) \tag{1.2}$$

with Fick's first law (1.1) yields Fick's second law

$$\frac{\partial C_\mathrm{A}(\mathbf{r}, t)}{\partial t} = \nabla \cdot (D_\mathrm{A} \, \nabla C_\mathrm{A}(\mathbf{r}, t)). \tag{1.3}$$

For a concentration- and location-independent diffusion coefficient D_A can be placed before the nabla operator and we obtain

$$\frac{\partial C_\mathrm{A}(\mathbf{r}, t)}{\partial t} = D_\mathrm{A} \, \Delta C_\mathrm{A}(\mathbf{r}, t) \tag{1.4}$$

where $\Delta = \frac{\partial^2}{\partial x^2} + \frac{\partial^2}{\partial y^2} + \frac{\partial^2}{\partial z^2}$ represents the Laplace operator in units of $[m^{-2}]$. Considering only diffusion in x-direction that is often realized by the diffusion of an element A into a solid from an infinite source on top of the surface or in experiments that consider the diffusion induced intermixing of layered structures, Fick's second law reads

$$\frac{\partial C_\mathrm{A}(x, t)}{\partial t} = D_\mathrm{A} \, \frac{\partial^2 C_\mathrm{A}(x, t)}{\partial x^2}. \tag{1.5}$$

The solution of this second order linear partial differential equation is given by

$$C_\mathrm{A}(x, t) = C_\mathrm{A}^\circ \operatorname{erfc} \frac{x}{2\sqrt{D_\mathrm{A} t}} \tag{1.6}$$

in the case of diffusion into a semi-infinite solid with constant surface concentration $C_\mathrm{A}(x = 0, t) = C_\mathrm{A}^\circ$. erfc in Eq. (1.6) represents the complementary error function (erfc $= 1 -$ erf). Solution (1.6) is typical for concentration-independent diffusion processes. Other solutions of Eq. (1.5) for different initial and boundary conditions

are given in textbooks [46, 47] or can be calculated with the method of separation of variables as well as by means of Laplace and Fourier transforms.

Concentration profiles described by Eq. (1.6) are expected for the diffusion of particles A into a solid under constant surface concentrations when the type of the particle does not change during diffusion. This, strictly speaking, only holds for mainly interstitial dissolved foreign-atoms such as hydrogen (H) and copper (Cu) in Si. These interstitial foreign atoms diffuse via interstitial lattice sites and remain interstitial atoms during their diffusive jump from one interstice to another. The interstitial mechanism of diffusion is considered in Sect. 1.5.1. In the case the type of the particle changes in the diffusion process, due to interaction of A with other defects, Fick's law of diffusion are no longer valid because the number of particles is not conserved. Accordingly, the corresponding diffusion equations have to consider defect reactions. This increases significantly the mathematical complexity to calculate the solution of the differential equations, that is, in most cases the system of underlying diffusion equations can only be solved numerically. Typical examples of elements A that exhibit a complex diffusion behavior are n- and p-type dopant atoms in Si such as P and B, respectively, as well as amphoteric foreign-atoms such as Au and Zn in Si that occupy both interstitial and substitutional lattice sites. Diffusion processes that involve defect reactions are treated in Sect. 1.5.2. Analytical solutions of the differential equation system are derived for conditions that can be realized experimentally.

In the following Sect. 1.4 diffusion in solids is treated from an atomistic point of view. Subsequently, the mechanisms of diffusion are divided in direct and indirect mechanisms and treated in Sect. 1.5 with special emphasis on the most relevant mechanisms for Si.

1.4 Atomistic Description of Diffusion

The fundamental process of diffusion of atomic components is a jump between two adjacent lattice sites. Since the site exchange is associated with a deformation of the environment, the particle has to overcome a saddle point between the potential minimum of the initial and final position. The magnitude of the barrier is given by the difference in the free enthalpy between minimum and saddle point. Accordingly, the particle has to overcome an activation enthalpy to perform a successful diffusion jump. From this treatment of diffusive jumps an exponential temperature dependence of the diffusion coefficient D_{A} is deduced that is described by an Arrhenius equation

$$D_{\mathrm{A}} = D_{\mathrm{A}}^{\circ} \exp\left(-\frac{Q_{\mathrm{A}}}{k_{\mathrm{B}} T}\right) \tag{1.7}$$

where k_{B} and T are the Boltzmann constant and absolute temperature, respectively. D_{A}° is the pre-exponential factor, that is a product of the jump distant squared, the

jump frequency, the correlation factor, an entropy term and a geometry factor. The specific expressions of D_{A}° and the activation enthalpy Q depend on the underlying diffusion mechanisms that are described in the next Sect. 1.5. In logarithmic representation Eq. (1.7) describes a linear relation between $\log D_{\mathrm{A}}$ and $\frac{1}{T}$. Deviations from the Arrhenius equation can be due to a simultaneous occurrence of different contributions to diffusion or due to a temperature dependent activation enthalpy $Q(T)$.

1.5 Diffusion Mechanisms

Diffusion in solids can, in general, be described by means of direct and indirect diffusion mechanisms. Characteristic of the direct diffusion of atoms is that no native point defects are involved to assist the migration of the atom. On the other hand, native point defects are required for the indirect diffusion of atoms. In the following the diffusion of an atom A via direct and indirect diffusion mechanisms and the corresponding diffusion coefficients are considered.

1.5.1 Direct Diffusion Mechanisms

The interstitial diffusion is schematically illustrated in Fig. 1.1. This mechanism represents the direct diffusion of an interstitial foreign-atom A_i and describes the jump of interstitially dissolved foreign-atoms to the neighboring interstitial position as indicated by the arrows in Fig. 1.1.

In diluted systems the concentration of interstitial foreign-atoms is small compared to available interstitial sites. Then the interstitial diffusion is a purely statistical process. For cubic crystals the following diffusion coefficient D_{A_i} of the

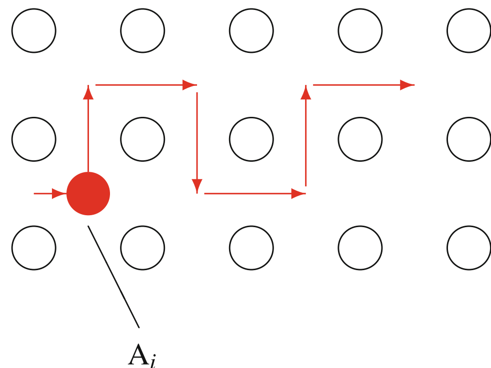

Fig. 1.1 Interstitial mechanism of the diffusion of interstitially dissolved foreign-atoms A_i

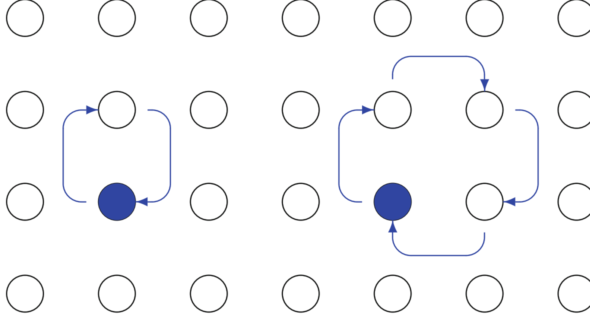

Fig. 1.2 Direct diffusion of substitutional atoms (self- or foreign-atoms) via a direct exchange

interstitial foreign-atom is derived [46, 48]

$$D_{A_i} = D^{\circ}_{A_i} \exp\left(-\frac{H^{M}_{A_i}}{k_B T}\right) \tag{1.8}$$

with the pre-exponential factor

$$D^{\circ}_{A_i} = g_{A_i} a_o^2 \nu_o \exp\left(\frac{S^{M}_{A_i}}{k_B}\right). \tag{1.9}$$

The geometry factor g_{A_i} includes the crystal structure and details about the atomistic diffusion process. In the case of direct diffusion via the interstice of a crystal with diamond structure the geometry factor equals $1/8$. a_o and ν_o are the lattice constant (Si: 5.431×10^{-10} m) and attempt frequency. The latter quantity is of the order of the Debye frequency ($\approx 10^{13}\,\mathrm{s}^{-1}$). The activation enthalpy of direct interstitial diffusion in Eq. (1.8) equals the migration enthalpy $H^{M}_{A_i}$ of the interstitial foreign-atom. This quantity is of the order of 1 eV or even less. $S^{M}_{A_i}$ in Eq. (1.9) represents the corresponding migration entropy. Typical examples for interstitial diffusors in Si are hydrogen (H) and copper (Cu) (see [49, 50] and references therein).

The exchange of two atoms on substitutional sites or the exchange of atoms along a ring describe the direct diffusion of substitutional atoms. This is illustrated in Fig. 1.2. So far no experimental evidence has been found for this direct mechanism of diffusion in Si indicating that the diffusion of A_s via indirect mechanisms is energetically more favorable.

1.5.2 *Indirect Diffusion Mechanisms*

Native point defects such as vacancies (V) and self-interstitials (I) are always present even in single crystalline, high purity dislocation-free Si wafers. This is

a consequence of the Gibbs free energy of the crystal under thermal equilibrium which is minimized when native defects are formed (see e.g. [46]). Diffusion mechanisms that involve native point defects as diffusion vehicle are called indirect mechanisms. Both the diffusion of self-atoms, i.e. self-diffusion, and the diffusion of substitutional foreign-atoms are mediated by native point defects. In the following the indirect mechanisms of self- and foreign-atom diffusion are introduced that are most relevant for Si.

1.5.2.1 Self-Diffusion

Vacancy Mechanism

The diffusion of self-atoms requires native point defects as diffusion vehicle. The mechanism involving vacancies is the so called vacancy mechanism that is schematically shown in Fig. 1.3.

In order that self-diffusion via vacancies can proceed, a vacancy must exist next to a tagged matrix atom. The probability to find a vacancy at a next nearest neighbor site is given by the concentration C_V^{eq} of V in thermal equilibrium normalized by the number density C_o of the matrix atoms (Si: $C_o = 5 \times 10^{22}\,\mathrm{cm}^{-3}$). For thermal equilibrium conditions the vacancy concentration at a specific temperature is given by

$$C_V^{\mathrm{eq}} = C_o \exp\left(-\frac{G_V^F}{k_B\,T}\right) \tag{1.10}$$

with the Gibbs free energy of vacancy formation G_V^F. This energy is interrelated via $G_V^F = H_V^F - T\,S_V^F$ with the formation enthalpy H_V^F and entropy S_V^F of V. Considering the jump of the vacancy in the case of tracer self-diffusion experiments the site exchange of the vacancy proceeds with equal probability to any next nearest

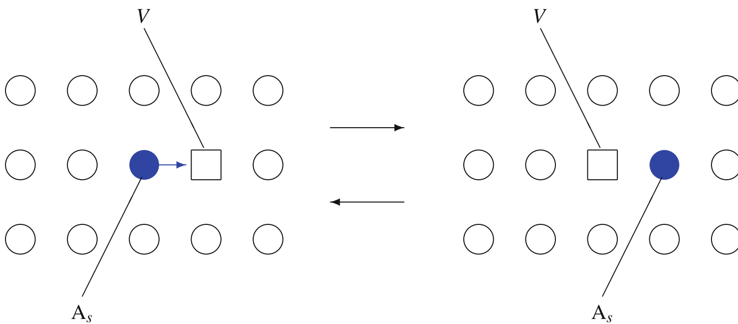

Fig. 1.3 Diffusion of self- and foreign-atoms via the vacancy mechanism. Radioactive or enriched stable isotopes can be used as suitable marker atoms (•)

neighbor site. In contrast, the jump of the tracer atom occurs with higher probability into the vacancy. The so called correlation factor f_V accounts for the preferred backward jump of the tracer atom. For solids with diamond structure the correlation factor for self-diffusion via V is exactly $f_V = 0.5$ [51].

The activation enthalpy $H_V^{SD} = H_V^F + H_V^M$ of self-diffusion via vacancies comprises both the enthalpy of formation H_V^F and migration H_V^M of the vacancy. In crystals with cubic symmetry the temperature dependence of the tracer self-diffusion coefficient is given by the following Arrhenius expression (see e.g. [46, 48])

$$D_V^{SD} = \frac{1}{C_o} f_V \, C_V^{\mathrm{eq}} \, D_V = D_{Vo}^{SD} \exp\left(-\frac{H_V^{SD}}{k_B \, T}\right) \tag{1.11}$$

with the pre-exponential factor

$$D_{Vo}^{SD} = f_V \, g_V \, a_o^2 \, \nu_o \exp\left(\frac{S_V^{SD}}{k_B}\right). \tag{1.12}$$

The pre-exponential factor depends on the activation entropy $S_V^{SD} = S_V^F + S_V^M$ of self-diffusion via V that reflects the sum of the entropy of vacancy formation S_V^F and migration S_V^M. The other parameters in Eq. (1.11) have the same meaning as in Eq. (1.9). The geometry factor equals 1/8 for the case of self-diffusion via V in a diamond structure. The vacancy mechanism controls self-diffusion in Ge [52] and in many crystalline metals [53, 54].

Interstitialcy Mechanism

An other indirect mechanism of self-diffusion is the so called interstitialcy mechanism. This mechanism is schematically illustrated in Fig. 1.4 and relevant in particular for self-diffusion in Si [49].

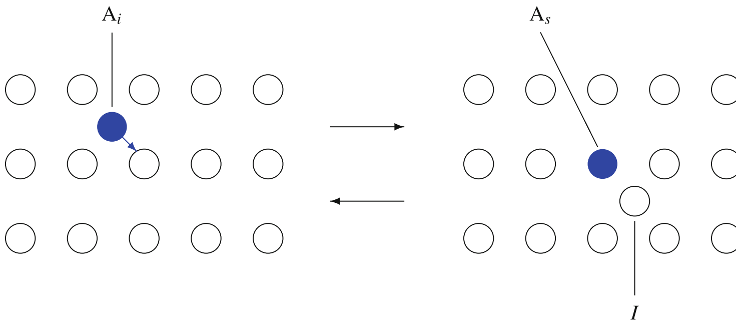

Fig. 1.4 The interstitialcy mechanism of self- and foreign-atom diffusion

In case of the interstitialcy mechanism a self-interstitial (I) mediates the diffusion of the matrix atoms, i.e., a self-interstitial pushes a neighboring host atom into the next interstitial position. Thereby the former self-interstitial becomes substitutional and forms a new self-interstitial. Subsequently the diffusion process is repeated with the newly formed I. In analogy to self-diffusion via V, self-diffusion via I is described by an Arrhenius expression

$$D_I^{SD} = \frac{1}{C_o} f_I \, C_I^{\mathrm{eq}} \, D_I = D_{Io}^{SD} \exp\left(-\frac{H_I^{SD}}{k_B\,T}\right) \tag{1.13}$$

with the pre-exponential factor

$$D_{Io}^{SD} = f_I \, g_I \, a_o^2 \, \nu_o \exp\left(\frac{S_I^{SD}}{k_B}\right) \tag{1.14}$$

and

$$H_I^{SD} = H_I^F + H_I^M \quad , \quad S_I^{SD} = S_I^F + S_I^M \tag{1.15}$$

as well as with the concentration of I in thermal equilibrium

$$C_I^{\mathrm{eq}} = C_o \exp\left(-\frac{G_I^F}{k_B\,T}\right) \tag{1.16}$$

where C_o represents the number of interstitial lattice sites. The parameters f_I, g_I, ν_o and the thermodynamic quantities H_I^F, H_I^M, S_I^F, S_I^M, and G_I^F have a corresponding meaning as the quantities in Eqs. (1.10), (1.11), and (1.12).

The diffusion of the tracer atom via the interstitialcy mechanism is also correlated. Starting with a tracer atom in interstitial position the first diffusional jump of the tracer atom occurs with equal probability in all possible directions. After the site exchange the tracer atom occupies a substitutional lattice site with a self-interstitial in close vicinity. Accordingly, a backward jump of the tracer atom is highly probable [48].

The correlation factor for self-diffusion via the interstitialcy mechanism for a crystalline solid with diamond structure was calculated by Compaan and Haven [55] to $f_I = 0.7273$. This factor corresponds to self-interstitials occupying tetrahedral interstitial lattice sites of the diamond structure. The geometry factor follows to $g_I = 1/4$ in this model considering next nearest neighbor jumps. More recent theoretical calculations of f_I consider that self-interstitials in the diamond lattice can exist in various configurations. In addition to tetrahedral interstitials also self-atoms on hexagonal interstices as well as split-interstitials, where two self-atoms share one lattice site, are predicted by theory. Accordingly, self-diffusion can proceed via different self-interstitial defects with their corresponding correlation factor. Following recent theoretical calculations the split interstitial is the most stable defect among the various possible self-interstitial configurations [5, 11, 20, 23]. For

this configuration a correlation factor of $f_I = 0.59$ [56] was deduced. In the case the dominant configuration of I changes with temperature, f_I becomes temperature dependent [57]. The correlation factor f_I for interstitial-mediated self-diffusion in Si was calculated to change from 0.64 to 0.80 for temperatures between 1000 and 1100 °C [57]. This represents a change of f_I within 20 % in the considered temperature range that is hardly resolved due to the limited accuracy of self-diffusion experiments.

Whereas self-diffusion in closely packed metals and germanium is fully described by the vacancy mechanism, both the vacancy and interstitialcy mechanism contribute to self-diffusion in Si [58–67]. Till today the individual contributions of V and I to Si self-diffusion are a matter of debate [65–67].

1.5.2.2 Foreign-Atom Diffusion

The vacancy and interstitialcy mechanisms illustrated in Figs. 1.3 and 1.4 also describe the indirect diffusion of mainly substitutionally dissolved foreign-atoms. Isolated V and I approach substitutional impurities and form next-nearest AV and AI defect pairs due to Coulomb attraction and/or minimizing local strain. Theses processes are described by the following reactions

$$\mathrm{A}_s + V \rightleftharpoons \mathrm{A}V \tag{1.17}$$

$$\mathrm{A}_s + I \rightleftharpoons \mathrm{A}I. \tag{1.18}$$

It is emphasized that for a long-range migration of $\mathrm{A_s}$ via the vacancy mechanism, the AV pair must partially dissociate, and the vacancy has to diffuse to at least a third-nearest neighbor site in the diamond lattice and return to the substitutional impurity along a different path to complete the diffusion step. In the case that the interaction potential between the vacancy and the dopant extends beyond the third-nearest neighbor site, complete dissociation of the AV complex becomes less probable, and A and V diffuse as a pair [68]. This vacancy-assisted diffusion mechanism is also called E-center mechanism [69]. Dopant diffusion via the interstitialcy mechanism only occurs if the AI pair does not dissociate.

The activation enthalpy Q_A of foreign-atom diffusion via reactions (1.17) and (1.18) reflects the sum of the migration $H^M_{\mathrm{A}X}$ and formation enthalpy $H^F_{\mathrm{A}X}$ of the dopant-defect AX pair ($X \in \{V, I\}$) that mediates dopant diffusion, i.e., $Q_\mathrm{A} = H^F_{\mathrm{A}X} + H^M_{\mathrm{A}X}$. Depending on the binding energy $H^B_{\mathrm{A}X}$ between the dopant and the native defect X, the formation enthalpy $H^F_{\mathrm{A}X}$ can be higher or lower than the formation enthalpy H^F_X of the isolated defect. For $H^F_{\mathrm{A}X} > H^F_X$ ($H^F_{\mathrm{A}X} < H^F_X$) a repulsive (attractive) interaction between A and X exists. The binding energy $H^B_{\mathrm{A}X}$ is the difference in energy to form an isolated defect X and a dopant-defect pair AX, i.e., $H^B_{\mathrm{A}X} = H^F_X - H^F_{\mathrm{A}X}$. This shows that Q_A comprises $H^M_{\mathrm{A}X}$, H^F_X and $H^B_{\mathrm{A}X}$ and,

accordingly, the temperature dependence of D_A reads

$$D_\mathrm{A} = D_\mathrm{A}^\circ \exp\left(-\frac{H_\mathrm{AX}^M + H_X^F - H_\mathrm{AX}^B}{k_B T}\right) \tag{1.19}$$

with the pre-exponential factor

$$D_\mathrm{A}^\circ = f\, g\, a_o^2\, \nu_o \exp\left(\frac{S_\mathrm{AX}^M + S_X^F - S_\mathrm{AX}^B}{k_B}\right). \tag{1.20}$$

The correlation factor f is now a complicated quantity which considers temperature-dependent site exchange frequencies under the impact of nearby foreign-atoms [70].

According to Eq. (1.19) the activation enthalpy Q_A of dopant diffusion via the vacancy (interstitialcy) mechanism is $Q_\mathrm{A} = H_\mathrm{AV}^M + H_V^F - H_\mathrm{AV}^B$ ($Q_\mathrm{A} = H_\mathrm{AI}^M + H_I^F - H_\mathrm{AI}^B$). Following Hu's analysis of dopant diffusion via vacancies, the activation enthalpy can be further decomposed as [71]

$$Q_\mathrm{A} = \underbrace{H_V^\mathrm{F} - \Delta H_1}_{H_\mathrm{AV}^\mathrm{F}} + \underbrace{H_V^\mathrm{M} + \Delta H_1 - \Delta H_3}_{H_\mathrm{AV}^\mathrm{M}}, \tag{1.21}$$

where H_V^F and H_V^M are the formation and migration enthalpy of vacancies far away from the dopant. The potential energy landscape of the vacancy as assumed by Hu [71] and Dunham and Wu [72] is illustrated in Fig. 1.5. ΔH_1, ΔH_2, and ΔH_3 denote the difference in potential energy of a vacancy far away and on first, second, and third nearest neighbor site from the dopant, respectively, with $\Delta H_1 = H_\mathrm{AV}^B$.

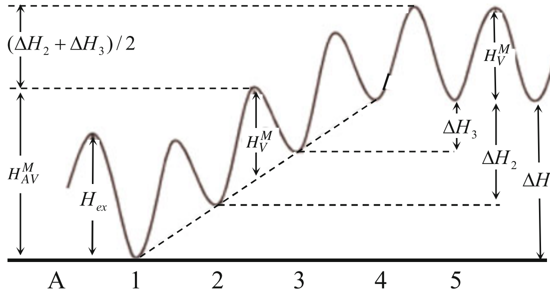

Fig. 1.5 Potential energy landscape of a vacancy close and far away from a dopant A [75]. H_{AV}^M and H_V^M are the migration enthalpy of the dopant-vacancy pair and the isolated vacancy, respectively. ΔH_1, ΔH_2, and ΔH_3 denote the difference in potential energy of a vacancy far away and on first, second, and third nearest neighbor site from the dopant, respectively. H_{ex} is the enthalpy barrier for site exchange between dopant and vacancy

The more recent analysis of vacancy-mediated diffusion in a diamond structure performed by Dunham and Wu [72] lead to the following modification of Hu's approach

$$Q_{\mathrm{A}} = H_V^{\mathrm{F}} + H_V^{\mathrm{M}} - \frac{\Delta H_2 + \Delta H_3}{2}$$
$$= H_V^{\mathrm{F}} + H_V^{\mathrm{M}} - \overline{\Delta H_{23}}. \tag{1.22}$$

Equation (1.22) accounts for a reduction in the migration barrier of the vacancy associated with changes in the binding energy between the sites. According to Dunham and Wu the difference between the activation enthalpy of self-diffusion $H_V^{SD} = H_V^F + H_V^M$ and dopant diffusion Q_{A} is the average of the vacancy binding energy $\overline{\Delta H_{23}}$ at the second and third nearest neighbor site from the dopant with respect to a vacancy far away (see Eq. (1.22)).

The binding energy between the dopant and the vacancy significantly affects the diffusion behavior of dopants, i.e., the higher the binding energy the lower is the activation enthalpy of dopant diffusion compared to self-diffusion. This becomes e.g. clearly evident in the diffusion behavior of n-type dopants such as phosphorus (P), arsenic (As) and antimony (Sb) in Ge [73]. The diffusion activation enthalpy of P, As, and Sb decreases from P to Sb although the size of the dopants increases from P to Sb. This peculiar diffusion behavior reflects in accordance with theoretical calculations [74] a binding energy between the n-type dopant and the vacancy in Ge that increases with increasing atomic size. A prerequisite for diffusion via the vacancy mechanism is that the AV pair must at least partially dissociate. In the diamond lattice the vacancy has to move to at least a third nearest neighbor site before it returns to the dopant to complete one diffusion step. Otherwise, as the V moves away from the donor atom the AV pair dissociates. In that case the donor atom is effectively immobilized and an interaction with another vacancy is required to migrate further [74].

The description of dopant diffusion demonstrates that the interaction of the dopant with the native defect strongly affects the diffusion activation enthalpy. An attractive (repulsive) interaction will result in an activation enthalpy that is lower (higher) compared to the activation enthalpy of self-diffusion. This also demonstrates that a comparison of dopant diffusion to self-diffusion is mandatory to understand the dopant diffusion in more detail.

In addition to the vacancy and interstitialcy mechanisms (1.17) and (1.18) the reactions

$$\mathrm{A}I + V \rightleftharpoons \mathrm{A}_s \tag{1.23}$$

$$\mathrm{A}V + I \rightleftharpoons \mathrm{A}_s \tag{1.24}$$

are considered for modeling dopant diffusion in Si [64, 76]. These reactions describe a dopant-defect pair assisted recombination of V and I that provide additional ways of recombination beside direct recombination of V and I via the Frenkel-pair

reaction

$$V + I \rightleftharpoons \phi. \tag{1.25}$$

In Si some foreign-atoms such as gold (Au), platinum (Pt), and zinc (Zn) are incorporated both on interstitial and substitutional sites (see [49, 50] and references therein). The diffusion of these hybrid elements is a combination of direct and indirect diffusion. The diffusion of the atom in the interstitial configuration significantly exceeds the diffusion of the atom in the substitutional configuration, that is, the indirect diffusion of A_s can be neglected and the binding energy between foreign-atom and native defect is circumstantial. In the following diffusion models are introduced that describe the diffusion of hybrid elements.

Interstitial-Substitutional Diffusion Mechanisms

The treatment of interstitial-substitutional exchange mechanisms is reasonable for elements that are dissolved both on interstitial and substitutional sites. The transformation from the interstitial configuration A_i to the substitutional configuration A_s can only take place by means of a native point defect. The defect involved can be the vacancy as well as the self-interstitial. This is expressed on the one hand by the dissociative mechanism, that describes the A_i-A_s transformation via V, and on the other hand via the kick-out mechanism, that involves a self-interstitial for the A_i-A_s transformation

$$A_i + V \rightleftharpoons A_s \tag{1.26}$$

$$A_i \rightleftharpoons A_s + I. \tag{1.27}$$

These transformation reactions are schematically illustrated in Figs. 1.6 and 1.7. The figures reflect the diffusion behavior of hybrid elements which are mainly dissolved on substitutional sites but are highly mobile as interstitial defects A_i.

The dissociative mechanism was first proposed by Frank and Turnbull [77] to explain the diffusion behavior of copper (Cu) in Ge. Today this mechanism forms the basis for modeling the diffusion of various transition metals such as iron (Fe), cobalt (Co), and nickel (Ni) in Ge as well as to explain the diffusion behavior of Cu, silver (Ag) and gold (Au) in Ge. In particular, Cu diffusion experiments are well suited to extract information not only about the uncorrelated Ge self-diffusion coefficient [78–80] but also about the concentration and diffusivity of vacancies in Ge [81].

Gösele et al. [82] introduced the kick-out diffusion model (see Fig. 1.7) to explain the diffusion behavior of Au in Si. Based on reaction (1.27) Au diffusion profiles are consistently described and confirm the impact of self-interstitials I on Au diffusion in Si [83–86].

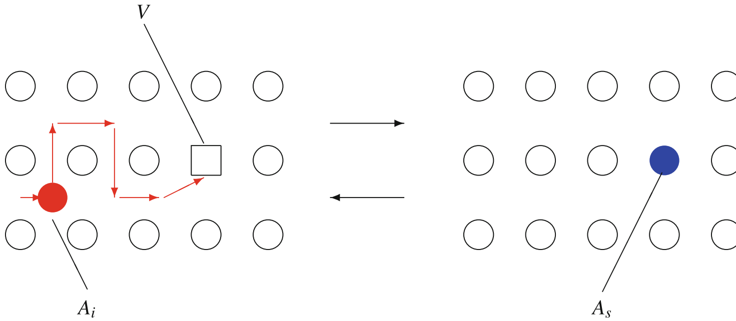

Fig. 1.6 Dissociative mechanism of the diffusion of foreign atoms that occupy both interstitial (*red filled circle*) and substitutional (*blue filled circle*) lattice sites. The interstitial-substitutional exchange is mediated by means of a vacancy V

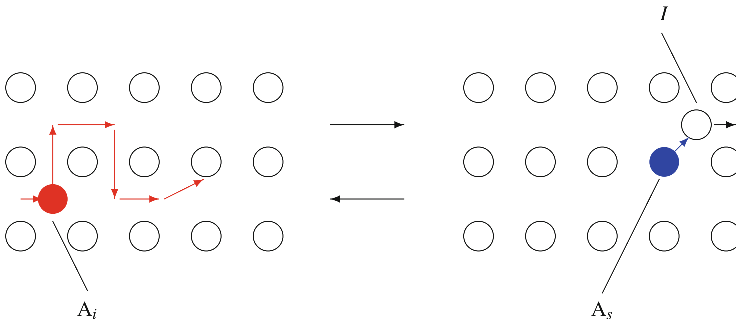

Fig. 1.7 Kick-out mechanism of the diffusion of foreign atoms that occupy both interstitial (*red filled circle*) and substitutional (*blue filled circle*) lattice sites. The interstitial-substitutional exchange is mediated by means of a self-interstitial I

In the following section the mathematical treatment of diffusion is introduced. Special emphasis is given to the diffusion of hybrid and dopant elements. The maximum solubility of typical hybrid elements such as Au, Pt, and Zn is of the order of 10^{17} cm^{-3} at about 1573 K and decreases to about 10^{15} cm^{-3} at 1173 K (see [50] and references therein). The incorporation of these hybrid elements introduces electronic defect states within the band gap of Si [50]. Due to their low solubility the free carrier concentration established at the particular diffusion temperature is not significantly affected. Accordingly, the diffusion of the hybrid elements can be considered to occur under spatial homogenous doping conditions, i.e, constant position of the Fermi level E_f. In the case when hybrid diffusion in undoped Si is considered, the diffusion occurs under electronically intrinsic conditions and the Fermi level is at its intrinsic position, i.e., at midgap position. In contrast, the maximum solubility of n- and p-type dopants in Si such as P, As, and B reaches a few atomic percent. The electron and hole concentration introduced by these dopants exceeds the intrinsic carrier concentration even at 1573 K. Accordingly,

the position of the Fermi level changes along the dopant diffusion profile that is established when dopant diffusion proceeds from an infinite source into undoped Si. The dopant profile gives rise to an internal electric field that affects the diffusion of charged mobile defects. In the following the mathematical treatment of diffusion under both intrinsic and extrinsic diffusion conditions is considered.

1.6 Mathematical Description of Diffusion

The first paragraph of this section, i.e. Sect. 1.6.1, treats the mathematical description of the diffusion of hybrid elements in Si. The diffusion of these elements is fully described on the basis of interstitial-substitutional exchange mechanisms, i.e., the dissociative and kick-out mechanisms illustrated in Figs. 1.6 and 1.7 and formulated by the reactions (1.26) and (1.27). Possible charge states of the point defects involved are not considered because the position of the Fermi level is not affected during the diffusion of hybrid elements in Si.

The second paragraph, i.e. Sect. 1.6.2, treats the diffusion of n- and p-type dopant atoms in Si whose incorporation on mainly substitutional lattice site cause extrinsic doping conditions even at high temperatures. To demonstrate the impact of extrinsic doping on diffusion and the formation of point defects the simultaneous diffusion of self- and dopant atoms in Si is treated that can be realized experimentally by dopant diffusion in isotopically controlled Si multilayer structures. The diffusion mechanisms relevant for dopant diffusion are the vacancy and interstitialcy mechanisms illustrated in Figs. 1.3 and 1.4 and formulated by the reactions (1.17) and (1.18), respectively. In addition dopant-defect pair assisted recombination reactions (1.23) and (1.24) and possible charge states of the point defects involved in these reactions are taken into account to accurately describe and predict dopant diffusion in Si.

1.6.1 Diffusion of Hybrid Atoms

The full reactions representing the dissociative and kick-out mechanisms must consider beside the point defects indicated in reactions (1.26) and (1.27) also unoccupied interstitial sites Z and substitutional sites O occupied by the host atom. In case of the dissociative model a vacancy V is annihilated via the transformation of an interstitial foreign-atom to a substitutional foreign-atom and concurrently an unoccupied interstitial position is formed. On the other hand, in case of the kick-out reaction a substitutional lattice atom O is transformed to a self-interstitial I. Thus

reactions (1.26) and (1.27) are fully described by

$$A_i + V \underset{k_{-1}}{\overset{k_{+1}}{\rightleftharpoons}} A_s + Z \tag{1.28}$$

$$A_i + O \underset{k_{-2}}{\overset{k_{+2}}{\rightleftharpoons}} A_s + I. \tag{1.29}$$

k_{+1}, k_{-1} and k_{+2}, k_{-2} represent the forward and backward reaction rates of the particular reaction in units of $[m^3 s^{-1}]$. The law of mass action for the reactions (1.28) and (1.29) combines the reaction rates with the equilibrium concentrations C_X^{eq} of the reaction partners. This yields

$$K_1 = \frac{k_{+1}}{k_{-1}} = \frac{C_{\mathrm{A}_s}^{\mathrm{eq}}\, C_o}{C_{\mathrm{A}_i}^{\mathrm{eq}}\, C_V^{\mathrm{eq}}} \tag{1.30}$$

$$K_2 = \frac{k_{+2}}{k_{-2}} = \frac{C_{\mathrm{A}_s}^{\mathrm{eq}}\, C_I^{\mathrm{eq}}}{C_{\mathrm{A}_i}^{\mathrm{eq}}\, C_o} \tag{1.31}$$

with the equilibrium constants K_1 and K_2 for the dissociative and kick-out reactions (1.28) and (1.29), respectively. $C_o = 5 \times 10^{22}\,\mathrm{cm}^{-3}$ is the concentration or atom density of Si atoms on substitutional lattice site that also equals the concentration of interstitial sites in Si. The concentration of interstitial and substitutional foreign-atoms is generally much lower than C_o. Accordingly, the concentration of matrix atoms and interstices remains nearly constant. In dynamical equilibrium the temporal change of the educts equals that of the products, i.e.,

$$k_{+1} C_{\mathrm{A}_i} C_V = k_{-1} C_{\mathrm{A}_s} C_o \tag{1.32}$$

$$k_{+2} C_{\mathrm{A}_i} C_o = k_{-2} C_{\mathrm{A}_s} C_I. \tag{1.33}$$

The formation of substitutional dissolved foreign-atoms per time unit via reactions (1.28) and (1.29) thus reads

$$\frac{\partial C_{\mathrm{A}_s}}{\partial t} = k_{+1} C_{\mathrm{A}_i} C_V - k_{-1} C_o C_{\mathrm{A}_s} + k_{+2} C_{\mathrm{A}_i} C_o - k_{-2} C_{\mathrm{A}_s} C_I. \tag{1.34}$$

The concentrations $C_X(\mathbf{r}, t)$ of the reactants $X \in \{\mathrm{A}_s, \mathrm{A}_i, V, I\}$ change not only by the exchange reactions but also by diffusion (see Eq. (1.3)). The following equations represent the full differential equation system that describes the diffusion

of foreign-atoms in Si via the interstitial-substitutional exchange mechanisms (1.28) and (1.29)

$$\frac{\partial C_{\mathrm{A}_s}}{\partial t} = \nabla \cdot (D_{\mathrm{A}_s} \nabla C_{\mathrm{A}_s}(\mathbf{r},t)) + k_{+1} C_{\mathrm{A}_i} C_V - k_{-1} C_o C_{\mathrm{A}_s} + k_{+2} C_{\mathrm{A}_i} C_o - k_{-2} C_{\mathrm{A}_s} C_I \quad (1.35)$$

$$\frac{\partial C_{\mathrm{A}_i}}{\partial t} = \nabla \cdot (D_{\mathrm{A}_i} \nabla C_{\mathrm{A}_i}(\mathbf{r},t)) - k_{+1} C_{\mathrm{A}_i} C_V + k_{-1} C_o C_{\mathrm{A}_s} - k_{+2} C_{\mathrm{A}_i} C_o + k_{-2} C_{\mathrm{A}_s} C_I \quad (1.36)$$

$$\frac{\partial C_V}{\partial t} = \nabla \cdot (D_V \nabla C_V(\mathbf{r},t)) - k_{+1} C_{\mathrm{A}_i} C_V + k_{-1} C_o C_{\mathrm{A}_s} + k_V (C_V^{eq} - C_V) \quad (1.37)$$

$$\frac{\partial C_I}{\partial t} = \nabla \cdot (D_I \nabla C_I(\mathbf{r},t)) + k_{+2} C_{\mathrm{A}_i} C_o - k_{-2} C_{\mathrm{A}_s} C_I + k_I (C_I^{eq} - C_I). \quad (1.38)$$

These differential equations and Eqs. (1.30) and (1.31) represent the full equation system to describe the diffusion of hybrid elements in Si. One rate constant of each reaction can be replaced by means of the corresponding mass action equation (see Eqs. (1.30) and (1.31)). The terms $k_V(C_V^{\mathrm{eq}} - C_V)$ and $k_I(C_I^{\mathrm{eq}} - C_I)$ consider the formation and annihilation of V and I at internal sources and sinks of the crystal [82]. Stacking faults [87, 88], dislocations [86, 88], swirls [89] and defect clusters can act as sources and sinks of native defects. The quantities k_V and k_I denote the effectiveness of sources and sinks and strongly depend on the defect structure of the crystal. Considering a diffusion controlled supply or annihilation of native point defects the quantities k_V and k_I are described by [82]

$$k_V = \gamma_V \, \rho_V \, D_V \quad (1.39)$$

$$k_I = \gamma_I \, \rho_I \, D_I \quad (1.40)$$

where $\rho_{V,I}$ represents the density of the source and sink of the native defects in units of [m^{-2}]. The constants $\gamma_{V,I}$ characterize the effectiveness of e.g. dislocations and are of the order of 1 [90].

The coupled, nonlinear partial differential equations (1.35), (1.36), (1.37), and (1.38) describe the full mathematical treatment of foreign-atom diffusion via interstitial-substitutional exchange mechanisms (1.28) and (1.29) in three dimensions. Analytical solutions of this system of equations can be derived for specific conditions, i.e., for sufficient long diffusion times and appropriate boundary and initial conditions. Solutions for more general conditions can be calculated numerically. In the following analytical solutions of the differential equation system are derived for diffusion in one dimension.

1.6.1.1 Reduced Differential Equation System

In order to discuss analytical solutions of the differential equations (1.35), (1.36), (1.37), and (1.38) that describe the diffusion of hybrid elements such as Au [83–86, 91] and Zn [41, 91–94] in Si under special experimental conditions the equation system is reduced to one dimension, i.e., ($\nabla \rightarrow \frac{\partial}{\partial x}$ and $C(\mathbf{r},t) \rightarrow C(x,t)$). This reduction is justified when the diffusion of foreign-atoms into Si crystal proceeds from a large surface covered with the foreign-atom of interest or from the gas phase. Moreover, the diffusion coefficients D_{A_s}, D_{A_i}, D_V, and D_I are moved in front of the differentiation. This approach requires concentration- and depth-independent diffusion coefficients. This is justified in the case of hybrid elements whose solubility is small in Si compared to the intrinsic carrier concentration at typical diffusion temperatures. Accordingly, the free carrier concentration introduced by the diffusion and incorporation of the hybrid elements in Si does not significantly affect the position of the Fermi level, that is, the Fermi level stays at its position under electronically intrinsic conditions. The other case when the free carrier concentration introduced by the foreign-atoms exceeds the intrinsic carrier concentration is treated in Sect. 1.6.2. Under the considered intrinsic conditions the equilibrium concentrations of the point defects involved in reactions (1.28) and (1.29) represent their concentrations for electronic intrinsic conditions. The equilibrium constants K_1 and K_2 are concentration independent and their temperature dependence is described by an Arrhenius equation [68].

The direct diffusion D_{A_s} of the substitutional foreign-atom A_s via direct exchange with a lattice atom or the ring mechanism (see Fig. 1.2) can be neglected compared to the indirect diffusion of A via the interstitial-substitutional exchange, i.e., $D_{\mathrm{A}_s} \approx 0$ effectively holds. Introducing normalized concentrations $\widetilde{C}_{\mathrm{X}} = C_{\mathrm{X}}/C_{\mathrm{X}}^{\mathrm{eq}}$ with $X \in \{\mathrm{A}_s, \mathrm{A}_i, V, I\}$, reduced diffusivities $D_{\mathrm{X}}^{*} = C_{\mathrm{X}}^{\mathrm{eq}} D_{\mathrm{X}}/C_{\mathrm{A}_s^{\mathrm{m}}}^{\mathrm{eq}}$, and considering Eqs. (1.30) and (1.31), the following differential equation system is obtained

$$\frac{\partial \widetilde{C}_{\mathrm{A}_s}}{\partial t} = \left(\frac{\partial \widetilde{C}_{\mathrm{A}_s}}{\partial t}\right)_V + \left(\frac{\partial \widetilde{C}_{\mathrm{A}_s}}{\partial t}\right)_I \tag{1.41}$$

$$\frac{C_{\mathrm{A}_i}^{\mathrm{eq}}}{C_{\mathrm{A}_s}^{\mathrm{eq}}} \frac{\partial \widetilde{C}_i}{\partial t} = D_{\mathrm{A}_i}^{*} \frac{\partial^2 \widetilde{C}_{\mathrm{A}_i}}{\partial x^2} - \left(\frac{\partial \widetilde{C}_{\mathrm{A}_s}}{\partial t}\right)_V - \left(\frac{\partial \widetilde{C}_{\mathrm{A}_s}}{\partial t}\right)_I \tag{1.42}$$

$$\frac{C_V^{\mathrm{eq}}}{C_{\mathrm{A}_s}^{\mathrm{eq}}} \frac{\partial \widetilde{C}_V}{\partial t} = D_V^{*} \frac{\partial^2 \widetilde{C}_V}{\partial x^2} - \left(\frac{\partial \widetilde{C}_{\mathrm{A}_s}}{\partial t}\right)_V + k_V(1 - \widetilde{C}_V) \tag{1.43}$$

$$\frac{C_I^{\mathrm{eq}}}{C_{\mathrm{A}_s}^{\mathrm{eq}}} \frac{\partial \widetilde{C}_I}{\partial t} = D_I^{*} \frac{\partial^2 \widetilde{C}_I}{\partial x^2} + \left(\frac{\partial \widetilde{C}_{\mathrm{A}_s}}{\partial t}\right)_I + k_I(1 - \widetilde{C}_I) \tag{1.44}$$

with

$$\left(\frac{\partial \widetilde{C}_{\mathrm{A}_s}}{\partial t}\right)_V = k_{-1} C_o (\widetilde{C}_{\mathrm{A}_i} \widetilde{C}_V - \widetilde{C}_{\mathrm{A}_s}) \tag{1.45}$$

$$\left(\frac{\partial \widetilde{C}_{\mathrm{A}_s}}{\partial t}\right)_I = k_{-2} C_I^{eq} (\widetilde{C}_{\mathrm{A}_i} - \widetilde{C}_{\mathrm{A}_s} \widetilde{C}_I). \tag{1.46}$$

Equations (1.41), (1.42), (1.43), (1.44), (1.45), and (1.46) form the basis for the simulation of the diffusion of Au, Pt, and Zn in Si. In the following section, solutions of the above differential equations are discussed that represent special cases of practical significance. These examples also demonstrate the benefit of the reduced equation system with the model parameters $D^*_{\mathrm{A}_i}$, D^*_V, and D^*_I. These parameters mainly affect the diffusion behavior of hybrid atoms after sufficient long diffusion times. Finally, in Sect. 1.6.1.5 numerical solutions are presented to demonstrate the significance of the model parameters for the time evolution of the concentration profiles.

1.6.1.2 Dominance of the Dissociative Mechanism

The reaction rate constants k_{+1}, k_{-1}, k_{+2}, and k_{-2} of the interstitial-substitutional exchange reactions (1.28) and (1.29) determine the process that mediates the formation of A_s (see Eqs. (1.41), (1.45), and (1.46)). Considering the relation

$$k_{-1} C_o \gg k_{-2} C_I^{\mathrm{eq}} \tag{1.47}$$

and that V and I are in thermal equilibrium at the onset of diffusion, i.e., $\widetilde{C}_V(x,0) = \widetilde{C}_I(x,0) = 1$, the formation of A_s is mainly controlled by the dissociative mechanism (1.28). In this case the differential equation system (1.41), (1.42), (1.43), (1.44), (1.45), and (1.46) simplifies to equations for $\widetilde{C}_{\mathrm{A}_s}$, $\widetilde{C}_{\mathrm{A}_i}$, and $\widetilde{C}_V$ with in total six model parameters. A further reduction is achieved when diffusion in dislocation-free, i.e. $k_V = 0$, and highly dislocated Si is considered. These cases are treated in the following two paragraphs.

Diffusion in Dislocation-Free Crystals

The third term on the right hand side of Eq. (1.43), which expresses the contribution of internal sources and sinks to the formation of V, can be neglected for diffusion in a defect-free crystal ($k_V = 0$). In addition we assume that the transport capacity of interstitial foreign-atoms exceeds the transport capacity of V, i.e., $C^{\mathrm{eq}}_{\mathrm{A}_i} D_{\mathrm{A}_i} \gg C^{\mathrm{eq}}_{\mathrm{V}} D_{\mathrm{V}}$. These conditions lead to concentrations of A_i that approach thermal equilibrium

($\widetilde{C}_{\mathrm{A}_i} \approx 1$) for sufficient long diffusion times and Eqs. (1.41), (1.42), (1.43), and (1.45) can be reduced to the differential equation

$$\frac{C_V^{\mathrm{eq}}}{C_{\mathrm{A}_s}^{\mathrm{eq}}} \frac{\partial \widetilde{C}_V}{\partial t} = D_V^* \frac{\partial^2 \widetilde{C}_V}{\partial x^2} - \left(\frac{\partial \widetilde{C}_{\mathrm{A}_s}}{\partial t} \right)_V . \tag{1.48}$$

At sufficient long diffusion times, i.e. for $t \gg (k_{-1} C_o)^{-1}$, reaction (1.28) is in local equilibrium. According to the law of mass action, local equilibrium is expressed by

$$\frac{C_{\mathrm{A}_s}}{C_{\mathrm{A}_i} C_V} = \frac{C_{\mathrm{A}_s}^{\mathrm{eq}}}{C_{\mathrm{A}_i}^{\mathrm{eq}} C_V^{\mathrm{eq}}} \tag{1.49}$$

or

$$\frac{\widetilde{C}_{\mathrm{A}_s}}{\widetilde{C}_{\mathrm{A}_i} \widetilde{C}_V} = 1 \tag{1.50}$$

Assuming Eq. (1.50) and $\widetilde{C}_{\mathrm{A}_i} \approx 1$, $\widetilde{C}_V$ in Eq. (1.48) can be replaced by $\widetilde{C}_{\mathrm{A}_s}$. We obtain the single differential equation

$$\frac{\partial \widetilde{C}_{\mathrm{A}_s}}{\partial t} = D_V^{\mathrm{eff}} \frac{\partial^2 \widetilde{C}_{\mathrm{A}_s}}{\partial x^2} \tag{1.51}$$

with the effective diffusion coefficient

$$D_V^{\mathrm{eff}} = \frac{C_V^{\mathrm{eq}} D_V}{C_{\mathrm{A}_s}^{\mathrm{eq}} + C_V^{\mathrm{eq}}} \approx D_V^* \tag{1.52}$$

for $C_{\mathrm{A}_s}^{\mathrm{eq}} \gg C_V^{\mathrm{eq}}$. This relation holds for hybrid elements such as Au, Pt, and Zn in Si [41, 85, 86, 93–99] and Cu in Ge [78, 79, 81]. Moreover, these elements preferentially occupy the substitutional lattice site in the respective semiconductor, i.e., $C_{\mathrm{A}_s}^{\mathrm{eq}} \gg C_{\mathrm{A}_i}^{\mathrm{eq}}$ [50]. This ensures to measure mainly the distribution of A_s by means of both chemical and electrical profiling methods.

$D_V^{\mathrm{eff}} \approx D_V^* = C_V^{\mathrm{eq}} D_V / C_{\mathrm{A}_s}^{\mathrm{eq}}$ implies that the established diffusion profile of A_s is controlled by the diffusion of V or, strictly speaking, by the transport capacity $C_V^{\mathrm{eq}} D_V$. This diffusion mode is called native-defect controlled diffusion of A_s. In the case a constant surface concentration is established during annealing, the solution of Eq. (1.51) is given by a complementary error function (1.6) with $C_\mathrm{A}(x,t) = C_{\mathrm{A}_s}(x,t)$, $C_\mathrm{A}^\circ = C_{\mathrm{A}_s}^{\mathrm{eq}}$, and $D_\mathrm{A} = D_V^{\mathrm{eff}} \approx D_V^*$. Note, although Eq. (1.51) describes the diffusion of A_s, the apparent diffusion coefficient D_V^{eff} is interrelated with the properties of V and almost equals D_V^* that is one of the model parameters of the full differential equation system (1.41), (1.42), (1.43), (1.44), (1.45), and (1.46). Multiplying and dividing the parameter D_V^* with the boundary concentration $C_{\mathrm{A}_s}^{\mathrm{eq}}$ and the atom density C_o, respectively, yields the uncorrelated self-diffusion coefficient $C_V^{\mathrm{eq}} D_V / C_o$ (see Eq. (1.11)). Studies on Cu diffusion in dislocation-free Ge fully

reveal this correlation between Cu diffusion and the V-mediated Ge self-diffusion coefficient and thus confirm the dissociative mechanism for the diffusion of Cu in Ge [78, 79, 81].

In the following the dissociative diffusion of hybrid elements in highly dislocated crystals is described. Based on the full system of differential equations again one differential equation for A_s with an effective diffusivity can be deduced.

Diffusion in Highly Dislocated Crystals

We consider a crystal with a high density of dislocations or other extended defects that can serve as efficient sources of V. Vacancies consumed by the transformation of A_i to A_s via reaction (1.28) can now be supplied by these internal sources much faster than via diffusion from the surface. As a consequence, the thermal equilibrium concentration of V is maintained, i.e. $C_V(x,t) = C_V^{eq}$ or $\widetilde{C}_V \approx 1$. Local equilibrium of reaction (1.28) is established after sufficient long times ($t \gg 1/k_{-1}C_o$), i.e. $\widetilde{C}_{A_s} \approx \widetilde{C}_{A_i}$ according to Eq. (1.50). Following these approximations, Eqs. (1.41), (1.42), (1.43), and (1.45) can be replaced by a single differential equation

$$\frac{\partial \widetilde{C}_{A_s}}{\partial t} = D_{A_i}^{eff} \frac{\partial^2 \widetilde{C}_{A_s}}{\partial x^2} \tag{1.53}$$

with the effective diffusion coefficient

$$D_{A_i}^{eff} = \frac{C_{A_i}^{eq} D_{A_i}}{C_{A_s}^{eq} + C_{A_i}^{eq}}. \tag{1.54}$$

With the relation $C_{A_s}^{eq} \gg C_{A_i}^{eq}$, that holds for mainly substitutional dissolved hybrid elements such as Cu in Ge and Au, Zn, and Pt in Si [50], the effective diffusion coefficient $D_{A_i}^{eff}$ equals to a good approximation $D_{A_i}^* = C_{A_i}^{eq} D_{A_i} / C_{A_s}^{eq}$. This quantity represents again one model parameter of the full differential equation system (1.41), (1.42), (1.43), (1.44), (1.45), and (1.46). For constant surface concentrations $C_{A_s}^{eq}$, the solution of Eq. (1.53) is given by the complementary error function [47]

$$\widetilde{C}_{A_s}(x,t) = \operatorname{erfc} \frac{x}{2\sqrt{D_{A_i}^* t}}. \tag{1.55}$$

Multiplying the parameter $D_{A_i}^*$ with the boundary concentration $C_{A_s}^{eq}$ yields the transport capacity $C_{A_i}^{eq} D_{A_i}$. This diffusion mode is named the foreign-atom controlled diffusion of A_s since the formation of A_s via reaction (1.28) is controlled by the supply of A_i.

The investigation of Cu diffusion in highly dislocated Ge yields data for $C_{A_i}^{eq} D_{A_i}$ that exceed $C_V^{eq} D_V$ and thus the Ge self-diffusion coefficient (see [79, 81] and references therein). This result is consistent with the diffusion of Cu in dislocation-

free Ge that only provides information about the Ge self-diffusion when the relation $C^{eq}_{A_i} D_{A_i} \gg C^{eq}_V D_V$ is fulfilled (see Sect. 1.6.1.2) [78, 81].

In the following we consider that the kick-out mechanism (1.29) dominates the A_i-A_s exchange.

1.6.1.3 Dominance of the Kick-Out Mechanism

Again we consider that the concentrations of V and I are in thermal equilibrium at the onset of diffusion. The kick-out mechanism controls the formation of A_s in the case when the relation

$$k_{-2} C^{eq}_I \gg k_{-1} C_o \tag{1.56}$$

instead of Eq. (1.47) holds. Within this approximation the differential equation system (1.41), (1.42), (1.43), (1.44), (1.45), and (1.46) can be reduced to equations for $\widetilde{C}_{A_s}$, $\widetilde{C}_{A_i}$, and $\widetilde{C}_I$ with in total six model parameters. A further reduction is achieved for diffusion in dislocation-free, i.e. $k_I = 0$, and highly dislocated Si.

Diffusion in Dislocation-Free Crystals

Assuming a dislocation-free crystal, i.e. a crystal without internal sources of native point defects, self-interstitials can neither be formed nor annihilated at internal sources and sinks, respectively. Accordingly, the contribution on the right hand side of Eq. (1.44) that considers possible formation/annihilation of I at internal sources/sinks can be neglected ($k_I = 0$). A high transport capacity $C^{eq}_{A_i} D_{A_i}$ described by $C^{eq}_{A_i} D_{A_i} \gg C^{eq}_I D_I$ leads to $\widetilde{C}_{A_i} \approx 1$ for sufficient long times. With the condition for local equilibrium of reaction (1.29)

$$\frac{\widetilde{C}_{A_s} \widetilde{C}_I}{\widetilde{C}_{A_i}} = 1 \tag{1.57}$$

the differential equation

$$\frac{\partial \widetilde{C}_{A_s}}{\partial t} = \frac{\widetilde{C}_{A_s}{}^2}{\widetilde{C}^2_{A_s} + C^{eq}_I / C^{eq}_{A_s}} \frac{\partial}{\partial x} \frac{1}{\widetilde{C}^2_{A_s}} D^*_I \frac{\partial \widetilde{C}_{A_s}}{\partial x} \tag{1.58}$$

with the reduced diffusion coefficient

$$D^*_I = \frac{C^{eq}_I D_I}{C^{eq}_{A_s}} \tag{1.59}$$

is obtained. Gösele et al. [82] demonstrate that the relation

$$\widetilde{C}^2_{\mathrm{A}_s} \gg C^{\mathrm{eq}}_I / C^{\mathrm{eq}}_{\mathrm{A}_s} \tag{1.60}$$

is fulfilled for the diffusion of Au in thin Si samples after sufficient long diffusion times. Accordingly, Eq. (1.58) can be replaced by

$$\frac{\partial \widetilde{C}_{\mathrm{A}_s}}{\partial t} = \frac{\partial}{\partial x} D^{\mathrm{eff}}_I \frac{\partial \widetilde{C}_{\mathrm{A}_s}}{\partial x} \tag{1.61}$$

with

$$D^{\mathrm{eff}}_I = \frac{1}{\widetilde{C}^2_{\mathrm{A}_s}} D^*_I. \tag{1.62}$$

Equations (1.61) and (1.62) describe the native-defect controlled diffusion of A_s via the kick-out mechanism. The concentration dependence of D^{eff}_I leads to characteristic diffusion profiles that strongly differ from the native-defect controlled profiles of the dissociative model (see Eqs. (1.51) and (1.52)).

Based on Eq. (1.61) Gösele [82] deduced the relation

$$\widetilde{C}_{\mathrm{A}_s}(\frac{d}{2}, t) = \left(4\pi D^*_I \frac{t}{d^2}\right)^{\frac{1}{2}} \tag{1.63}$$

for the concentration of A_s in the center of the crystal with thickness d and the reduced diffusion coefficient D^*_I. Equation (1.63) shows that the uncorrelated, I-mediated Si self-diffusion coefficient $C^{\mathrm{eq}}_I D_I / C_o$ can be determined from the time evolution of the concentration of A_s in the center of the crystals after sufficient long diffusion times ($\widetilde{C}_{\mathrm{A}_i} \approx 1$). Data of $C^{\mathrm{eq}}_I D_I / C_o$ obtained from Au, Pt, and Zn diffusion studies (see e.g. [41, 83, 93, 100]) are in accord with the Si self-diffusion coefficients determined from direct tracer diffusion studies. This confirms the kick-out mechanism for the diffusion of these elements in Si and the contribution of I to Si self-diffusion [58].

Diffusion in Highly Dislocated Crystals

In crystals with a high density of dislocations or other efficient sources/sinks for self-interstitials, the thermal equilibrium concentration of I can be maintained during foreign-atom diffusion even when self-interstitials are consumed or formed via the kick-out reaction. Thus $\widetilde{C}_I(x,t) \approx 1$ holds and the differential equation system (1.41), (1.42), (1.43), (1.44), (1.45), and (1.46) can be reduced to

$$\frac{C^{\mathrm{eq}}_{\mathrm{A}_i}}{C^{\mathrm{eq}}_{\mathrm{A}_s}} \frac{\partial \widetilde{C}_i}{\partial t} = D^*_{\mathrm{A}_i} \frac{\partial^2 \widetilde{C}_{\mathrm{A}_i}}{\partial x^2} - \frac{\partial \widetilde{C}_{\mathrm{A}_s}}{\partial t}. \tag{1.64}$$

For sufficient long times ($(t \gg 1/k_{-2}C_I^{eq})$) the kick-out reaction (1.29) is in local equilibrium, i.e. $\widetilde{C}_{A_s} = \widetilde{C}_{A_i}$ (see Eq. (1.57)). Then the differential equation

$$\frac{\partial \widetilde{C}_{A_s}}{\partial t} = D_{A_i}^{eff} \frac{\partial^2 \widetilde{C}_{A_s}}{\partial x^2} \tag{1.65}$$

with the effective diffusion coefficient

$$D_{A_i}^{eff} = \frac{C_{A_i}^{eq} D_{A_i}}{C_{A_s}^{eq} + C_{A_i}^{eq}} \tag{1.66}$$

is obtained. The diffusion coefficient $D_{A_i}^{eff}$ equals $D_{A_i}^*$ for $C_{A_s}^{eq} \gg C_{A_i}^{eq}$. This, in particular, holds for both Au [86] and Zn [41] in Si. Concentration profiles of these elements measured after diffusion in highly dislocated Si fully confirm the impact of the defect density on the diffusion of these hybrid elements [41, 86]. The ratio $D_{A_i}^*/D_I^* = C_{A_i}^{eq} D_{A_i}/C_I^{eq} D_I$ clearly exceeds unity and thus confirms the native-defect controlled diffusion of these elements in dislocation-free Si that requires the validity of $D_{A_i}^* \gg D_I^*$. Note, diffusion in highly dislocated crystals via the kick-out and dissociative mechanisms provide the same effective diffusion coefficient $D_{A_i}^{eff}$ (see Eqs. (1.54) and (1.66)). This demonstrates that the type of native point defect involved in the interstitial-substitutional exchange can not be identified by means of diffusion studies with defect-rich materials because the concentration of V and I close to thermal equilibrium ($\widetilde{C}_{V,I} \approx 1$).

1.6.1.4 Occurrence of Both A_i-A_s Exchange Mechanisms

Both V and I exist in Si under thermal equilibrium conditions. Accordingly, beside the dissociative also the kick-out mechanisms can contribute to the native-defect controlled diffusion of hybrid foreign-atoms. The simultaneous occurrence of both A_i-A_s exchange mechanisms is considered in the following for local equilibrium and non-equilibrium conditions.

Diffusion Under Local Equilibrium Conditions

Assuming local equilibrium of reactions (1.28) and (1.29) described by Eqs. (1.50) and (1.57), respectively, and additionally $\widetilde{C}_{A_i} \approx 1$, the following differential equation can be derived from the full differential equation system (1.41), (1.42), (1.43), (1.44), (1.45), and (1.46) for a defect-free crystal (without one-, two-, or three-dimensional defects),

$$\left(1 + \frac{C_V^{eq}}{C_{A_s}^{eq}} + \frac{C_I^{eq}}{C_{A_s}^{eq}\left(\widetilde{C}_{A_s}\right)^2}\right) \frac{\partial \widetilde{C}_{A_s}}{\partial t} = \frac{\partial}{\partial x}\left(\frac{1}{\left(\widetilde{C}_{A_s}\right)^2} D_I^* + D_V^*\right) \frac{\partial \widetilde{C}_{A_s}}{\partial x}. \tag{1.67}$$

With the relations $C_{\mathrm{A}_s}^{\mathrm{eq}} \gg C_V^{\mathrm{eq}}$ and $\left(\widetilde{C}_{\mathrm{A}_s}\right)^2 \gg C_I^{\mathrm{eq}}/C_{\mathrm{A}_s}^{\mathrm{eq}}$, which hold for hybrid elements in Si under indiffusion conditions [82, 84], Eq. (1.67) reads

$$\frac{\partial \widetilde{C}_{\mathrm{A}_s}}{\partial t} = \frac{\partial}{\partial x}\left(\frac{1}{\left(\widetilde{C}_{\mathrm{A}_s}\right)^2} D_I^* + D_V^*\right)\frac{\partial \widetilde{C}_{\mathrm{A}_s}}{\partial x} = \frac{\partial}{\partial x} D_{I,V}^{\mathrm{eff}} \frac{\partial \widetilde{C}_{\mathrm{A}_s}}{\partial x} \tag{1.68}$$

with the effective diffusion coefficient

$$D_{I,V}^{\mathrm{eff}} = \frac{1}{\left(\widetilde{C}_{\mathrm{A}_s}\right)^2} D_I^* + D_V^*. \tag{1.69}$$

The concentration dependence of $D_{I,V}^{\mathrm{eff}}$ reveals that under in-diffusion conditions with $\widetilde{C}_{\mathrm{A}_s}(x,t) < 1$ the concentration profile of substitutional foreign-atoms is mainly characterized by diffusion via the kick-out mechanism even for $D_V^* \approx D_I^*$. In typical diffusion experiments where the hybrid-atom penetrates from the surface into the Si bulk the resulting diffusion profile is mainly controlled by the kick-out reaction (see e.g. [41]). Thus D_I^* can be determined from native-defect controlled in-diffusion profile whereas D_V^* is hardly extracted. On the other hand, the diffusion parameter D_V^* controls $D_{I,V}^{\mathrm{eff}}$ in the case when $\widetilde{C}_{\mathrm{A}_s} > 1$ holds (see Eq. (1.69)). This condition is realized in out-diffusion experiments where the concentration of the substitutional foreign-atom in the bulk exceeds its concentration at the surface (see e.g. [101, 102]).

The diffusion of hybrid atoms under local equilibrium conditions is characterized by the validity of Eqs. (1.50) and (1.57). This implies that

$$\widetilde{C}_I \widetilde{C}_V = 1. \tag{1.70}$$

is fulfilled. Equation (1.70) represents local equilibrium of the Frenkel-pair reaction (1.25). This interrelation between interstitial-substitutional exchange mechanisms and the Frenkel-pair reaction shows that local equilibrium between V and I can be established via the exchange reactions (1.28) and (1.29) even when direct recombination of V and I is a more moderate process due to an energy or entropy barrier [103]. Moreover, it is noted that foreign-atom profiles representing local equilibrium conditions can be described equally by any combination of two of the three reactions (1.25), (1.28), and (1.29). This actually holds for numerous Au and Pt diffusion profiles in Si. Thus these profiles do not provide definite information about the preferred way of interstitial-substitutional exchange.

The full differential equation system given by Eqs. (1.41), (1.42), (1.43), (1.44), (1.45), and (1.46) has been treated in the limit of either the dissociative or the kick-out mechanism for diffusion times that ensures local equilibrium conditions. Under these conditions the differential equations can be reduced to a single differential equation of the form of Eq. (1.5) with an effective diffusion coefficient that approximately equals the reduced diffusion coefficient $D_{\mathrm{X}}^* = C_{\mathrm{X}}^{\mathrm{eq}} D_{\mathrm{X}}/C_{\mathrm{A}_{\mathrm{s}}^{\mathrm{m}}}^{\mathrm{eq}}$ with $X \in \{\mathrm{A}_i, V, I\}$. This demonstrates that diffusion profiles of hybrid atoms

are mainly sensitive to D_X^*. The other model parameters involved in the full mathematical formulation of diffusion via interstitial-substitutional exchange play only a minor role. However, these parameters become significant in concentration profiles established after short and intermediate diffusion times (see Sect. 1.6.1.5).

Diffusion Under Non-equilibrium Conditions

Diffusion studies under experimental conditions deviating from local equilibrium of the point defects involved in defect reactions can, in principle, differentiate between the microscopic mechanisms of atomic transport (see e.g. [104–110]). Such studies provide valuable information about the model parameters entering the differential equations that describe the diffusion of dopant elements in Si via indirect diffusion mechanisms. In general, the solution of differential equations is only defined under specific initial and boundary conditions. These conditions must be in accord with the conditions realized experimentally. This is mandatory for direct comparison of experimental and calculated diffusion profiles that aims to determine the model parameters of the underlying diffusion equations. In the following section the impact of the model parameters on the temporal evolution of defect concentration profiles are described. It is shown that diffusion studies covering different time regimes are very advantageous to determine the mechanisms of diffusion and thus the underlying model parameters.

1.6.1.5 Numerical Simulation of Foreign-Atom Diffusion via Interstitial-Substitutional Exchange

The differential equations (1.41), (1.42), (1.43), (1.44), (1.45), and (1.46) representing diffusion in Si via interstitial-substitutional exchange are solved numerically to demonstrate the impact of the model parameters on the time evolution of the diffusion of hybrid atoms. The solutions reveal various diffusion regions that are differently sensitive to the settings of the model parameters.

Simulation of Kick-Out Diffusion

The simulation of foreign-atom diffusion via interstitial-substitutional is restricted for the sake of clarity to the kick-out mechanism. This limitation is justified because the in-diffusion of hybrid elements such as Au [82, 84, 86], Pt [95, 100], and Zn [41, 93] in Si is mainly controlled by this reaction (see Eqs. (1.68) and (1.69)). The

mathematical formulation of the kick-out mechanism is given by (see Eqs. (1.41), (1.42), (1.43), (1.44), (1.45), and (1.46) for comparison)

$$\frac{\partial \widetilde{C}_{\mathrm{A}_s}}{\partial t} = k_{-2} C_I^{\mathrm{eq}} \left(\widetilde{C}_{\mathrm{A}_i} - \widetilde{C}_{\mathrm{A}_s} \widetilde{C}_I \right) \tag{1.71}$$

$$\frac{C_{\mathrm{A}_i}^{\mathrm{eq}}}{C_{\mathrm{A}_s}^{\mathrm{eq}}} \frac{\partial \widetilde{C}_{\mathrm{A}_i}}{\partial t} = D_{\mathrm{A}_i}^* \frac{\partial^2 \widetilde{C}_{\mathrm{A}_i}}{\partial x^2} - \frac{\partial \widetilde{C}_{\mathrm{A}_s}}{\partial t} \tag{1.72}$$

$$\frac{C_I^{\mathrm{eq}}}{C_{\mathrm{A}_s}^{\mathrm{eq}}} \frac{\partial \widetilde{C}_I}{\partial t} = D_I^* \frac{\partial^2 \widetilde{C}_I}{\partial x^2} + \frac{\partial \widetilde{C}_{\mathrm{A}_s}}{\partial t} \tag{1.73}$$

and Eq. (1.31). The five model parameters $D_{\mathrm{A}_i}^*$, D_I^*, $C_{\mathrm{A}_i}^{\mathrm{eq}}/C_{\mathrm{A}_s}^{\mathrm{eq}}$, $C_I^{\mathrm{eq}}/C_{\mathrm{A}_s}^{\mathrm{eq}}$ and $k_{-2}C_I^{\mathrm{eq}}$ fully determine the solution of the differential equations under given initial- and boundary conditions. The boundary conditions

$$\widetilde{C}_{\mathrm{A}_i}(0, t) = \widetilde{C}_{\mathrm{A}_i}(d, t) = 1 \tag{1.74}$$

$$\widetilde{C}_I(0, t) = \widetilde{C}_I(d, t) = 1 \tag{1.75}$$

are considered for the numerical calculation of $\widetilde{C}_X$ with $X \in \{\mathrm{A}_s, \mathrm{A}_i, I\}$ in a finite crystal of thickness d. Equation (1.74) describes an infinite source of interstitial foreign-atoms at the surface. Moreover, Eq. (1.75) reflects an equilibrium concentration of I maintained at the surface. These equations represent conditions for in-diffusion of foreign-atoms that are deposited on top of or rapidly supplied via the gas phase to the sample surface. The boundary condition for A_s is given by the solution of Eq. (1.71) for $x = 0$ and $x = d$ taking into account Eqs. (1.74) and (1.75) to

$$\widetilde{C}_{\mathrm{A}_s}(0, t) = \widetilde{C}_{\mathrm{A}_s}(d, t) = 1 - \exp(-k_{-2} C_I^{\mathrm{eq}} t). \tag{1.76}$$

This solution indicates that the parameter $k_{-2}C_I^{\mathrm{eq}}$ controls the temporal increase of the A_s concentration at the surface.

The initial concentration of the diffusing element is generally very low prior to diffusion, i.e., below the detection limit of the method subsequently applied to measure the diffusion profile. Accordingly, the initial concentrations of interstitial and substitutional foreign-atoms within the semiconductor are lower than their equilibrium values $C_{\mathrm{A}_i}^{\mathrm{eq}}$ and $C_{\mathrm{A}_s}^{\mathrm{eq}}$ established at the surface in the course of diffusion. The following initial conditions are considered for the normalized concentrations of A_i and A_s

$$\widetilde{C}_{\mathrm{A}_s}(x, 0) = \widetilde{C}_{\mathrm{A}_i}(x, 0) = 10^{-10}. \tag{1.77}$$

The concentration of self-interstitials at the onset of diffusion, i.e., at time $t = 0$, is set to the equilibrium concentration C_I^{eq}

$$\widetilde{C}_I(x, 0) = 1. \tag{1.78}$$

These conditions described by Eqs. (1.77) and (1.78) fulfill local equilibrium of the kick-out reaction (see Eq. (1.57)) for $x > 0$ and $t = 0$.

The boundary and initial conditions formulated by Eqs. (1.74) (1.75), (1.76), (1.77), and (1.78) can be realized experimentally by Zn diffusion in Si [41, 111]. Equilibration of Si samples prior to Zn in-diffusion is achieved by separating the Zn-source from the Si samples and releasing Zn vapor after the equilibration process [111]. Corresponding diffusion profiles of substitutional Zn_s measured by means of the spreading resistance technique are presented in Sect. 1.7.1.

To demonstrate the impact of the model parameters on the diffusion of hybrid atoms via the kick-out mechanism, numerical solutions of Eqs. (1.71), (1.72), and (1.73) are presented in the following. We start from a set of model parameters that accurately describe the diffusion behavior of Zn in Si at 1481 K ($D^*_{\mathrm{A}_i} = 4 \cdot 10^{-07}\,\mathrm{cm}^2\mathrm{s}^{-1}$, $D^*_I = 8 \cdot 10^{-08}\,\mathrm{cm}^2\mathrm{s}^{-1}$, $C^{\mathrm{eq}}_{\mathrm{A}_i}/C^{\mathrm{eq}}_{\mathrm{A}_s} = 0.03$, $C^{\mathrm{eq}}_I/C^{\mathrm{eq}}_{\mathrm{A}_s} = 0.001$, $k_{-2}C^{\mathrm{eq}}_I = 0.1\,\mathrm{s}^{-1}$) [41]. Figures 1.8, 1.9, and 1.10 illustrate additional simulations with model parameters deviating from these reference values.

The significance and impact of the model parameter $k_{-2}C^{\mathrm{eq}}_I$ on the diffusion of hybrid elements via the kick-out mechanism is illustrated in Fig. 1.8. Increasing $k_{-2}C^{\mathrm{eq}}_I$ by one order of magnitude, i.e., from $0.1\,\mathrm{s}^{-1}$ to $1.0\,\mathrm{s}^{-1}$, mainly affects the normalized concentration $\widetilde{C}_{\mathrm{A}_s} = C_{\mathrm{A}_s}(x,t)/C^{\mathrm{eq}}_{\mathrm{A}_s}$ for diffusion times $t \leq 240$ s. For longer times no impact of $k_{-2}C^{\mathrm{eq}}_I$ on the diffusion profiles is evident. The parameter

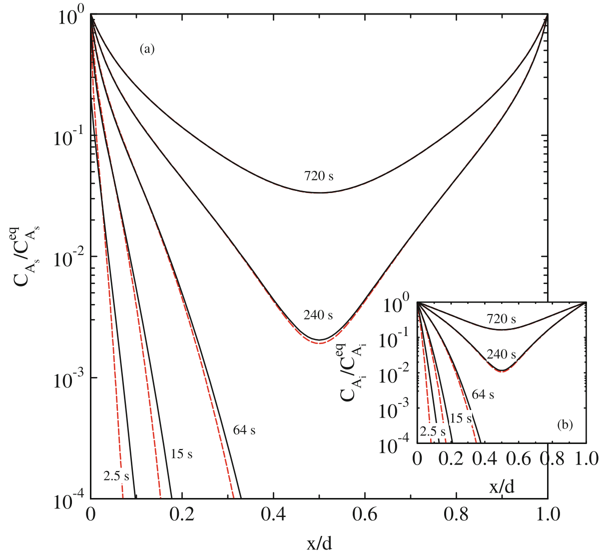

Fig. 1.8 Temporal evolution of the diffusion profiles of substitutional A_s (**a**) and interstitial A_i (**b**) foreign-atoms normalized by their respective thermal equilibrium concentration $C^{\mathrm{eq}}_{\mathrm{A}_s}$ and $C^{\mathrm{eq}}_{\mathrm{A}_i}$. The profiles illustrate the impact of the model parameter $k_{-2}C^{\mathrm{eq}}_I$ (—— : $k_{-2}C^{\mathrm{eq}}_I = 0.1\ \mathrm{s}^{-1}$) (- - - - : $k_{-2}C^{\mathrm{eq}}_I = 1.0\ \mathrm{s}^{-1}$)

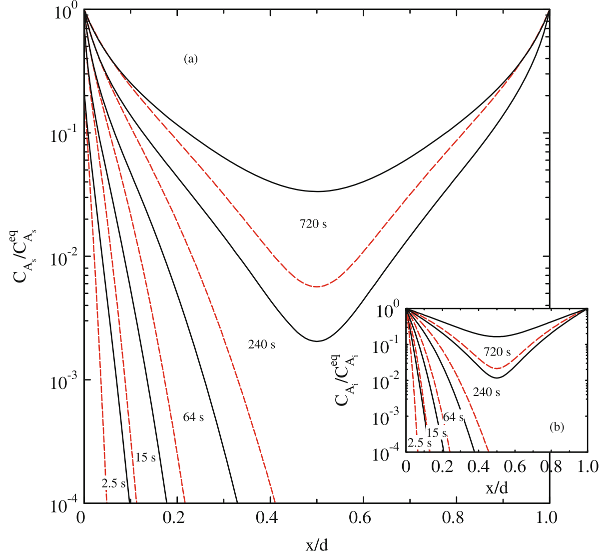

Fig. 1.9 Temporal evolution of the diffusion profiles of substitutional A_s (**a**) and interstitial A_i (**b**) foreign-atoms normalized by their respective thermal equilibrium concentration $C^{eq}_{A_s}$ and $C^{eq}_{A_i}$. The profiles illustrate the impact of the model parameter $C^{eq}_{A_i}/C^{eq}_{A_s}$. (—— : $C^{eq}_{A_i}/C^{eq}_{A_s} = 0.03$) (- - - - : $C^{eq}_{A_i}/C^{eq}_{A_s} = 0.3$)

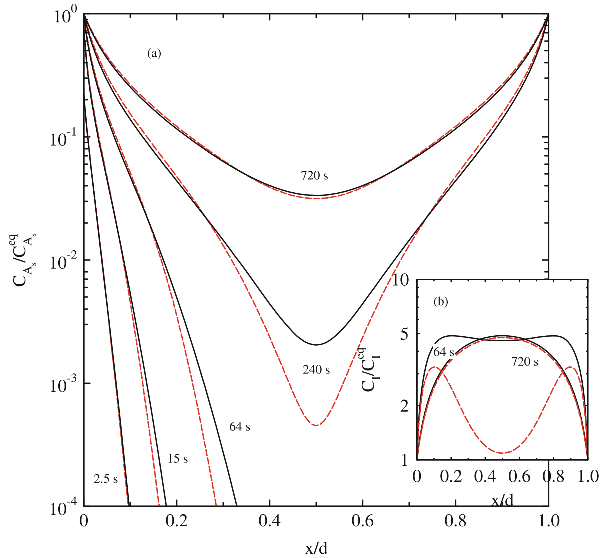

Fig. 1.10 Temporal evolution of the diffusion profiles of the substitutional A_s foreign-atom (**a**) and the self-interstitial I (**b**) normalized by their respective thermal equilibrium concentration $C^{eq}_{A_s}$ and C^{eq}_I. The profiles illustrate the impact of the model parameter $C^{eq}_I/C^{eq}_{A_s}$ (—— : $C^{eq}_I/C^{eq}_{A_s} = 0.001$) (- - - - : $C^{eq}_I/C^{eq}_{A_s} = 0.01$)

$k_{-2}C^{eq}_I$ reminds in Eq. (1.76) of the decay constant in the decay law of radioactive isotopes. In this analogy, $1/k_{-2}C^{eq}_I$ represents the time constant that describes the mean life-time for the transformation of interstitially to substitutionally dissolved foreign-atoms. In case the time constant is lowered, that is, $k_{-2}C^{eq}_I$ is increased, the mean time foreign-atoms stay on interstitial position decreases and accordingly, the penetration depth of both A_i and A_s is smaller due to the coupling between A_i and

A_s via the kick-out reaction. This is the main impact of $k_{-2}C_I^{\mathrm{eq}}$ on the diffusion profiles of $\widetilde{C}_{\mathrm{A}_s}$ and $\widetilde{C}_{\mathrm{A}_i}$ illustrated in Fig. 1.8.

Equation (1.76) describes that higher values of $k_{-2}C_I^{\mathrm{eq}}$ lead to increased A_s concentrations at the surface until the equilibrium concentration $C_{\mathrm{A}_s}^{\mathrm{eq}}$ is established. The interstitial-substitutional exchange via the kick-out reaction creates self-interstitials. Considering native-defect controlled diffusion of hybrid elements in dislocation-free crystals that prevails when $D_{\mathrm{A}_i}^* > D_I^*$ holds, a supersaturation of I is obtained, i.e. $\widetilde{C}_I > 1$. This supersaturation hampers the formation of additional A_s via the exchange mechanism. Further formation of A_s is governed by the transport of I to the sample surface that is limited by the parameter D_I^*. Close to the surface, the concentration of I is already reduced due to out-diffusion. However, in the bulk the I concentration till increases due to interstitial-substitutional exchange. This describes that the native defect-controlled mode of diffusion is reached earlier at the surface than in the bulk. Therefore diffusion profiles for longer times still reveal a dependence of $k_{-2}C_I^{\mathrm{eq}}$ at the diffusion front and/or at the center of the sample whereas the surface region is already insensitive to the parameter $k_{-2}C_I^{\mathrm{eq}}$ (see Fig. 1.8: t = 64 s and 240 s). Finally, when the supersaturation of I has reached its maximum, the formation of A_s is fully controlled by out-diffusion of I to the surface. At this stage of diffusion the entire A_s profile is insensitive to $k_{-2}C_I^{\mathrm{eq}}$ as supported by the $\widetilde{C}_{\mathrm{A}_s}$ profile in Fig. 1.8 for 720 s.

The impact of the model parameter $C_{\mathrm{A}_i}^{\mathrm{eq}}/C_{\mathrm{A}_s}^{\mathrm{eq}}$ on the time evolution of A_s and A_i profiles is shown by Fig. 1.9. At constant $D_{\mathrm{A}_i}^*$, an increase of $C_{\mathrm{A}_i}^{\mathrm{eq}}/C_{\mathrm{A}_s}^{\mathrm{eq}}$ is associated with a decrease of D_{A_i}. With increasing value of $C_{\mathrm{A}_i}^{\mathrm{eq}}/C_{\mathrm{A}_s}^{\mathrm{eq}}$ the penetration depth of A_i decreases and, due to the coupling between A_i and A_s via the kick-out reaction, also the penetration depth of A_s. The distribution of A_s is within a close surface region almost independent of this parameter. Here the removal of supersaturated self-interstitials by diffusion to the surface determines the profile shape. On the other hand, the supply of A_i and removal of I controls the formation of A_s at the transition region to the diffusion front. The diffusion front itself is affected both by diffusion and reaction processes. Finally, the diffusion of I fully controls further formation of A_s after sufficient long diffusion times that lead to $\widetilde{C}_{\mathrm{A}_i}(x,t) \approx 1$. At this stage the A_s profiles are insensitive to the model parameter $C_{\mathrm{A}_i}^{\mathrm{eq}}/C_{\mathrm{A}_s}^{\mathrm{eq}}$ and fully described by the solution of Eq. (1.61). Since this case was already discussed in Sect. 1.6.1.3, it is not illustrated in Fig. 1.9.

The impact of $C_I^{\mathrm{eq}}/C_{\mathrm{A}_s}^{\mathrm{eq}}$ on the diffusion of A_s for different times is illustrated by Fig. 1.10. The corresponding distributions of I for 64 s and 720 s are shown for comparison (see Fig. 1.10b). At the beginning of diffusion (after 2.5 s) the parameter does not affect the distribution of A_s. At this stage, the velocity of the formation of the reaction products is high and A_s and I are formed very shortly. With progressing formation of I via the kick-out reaction the impact of the backward reaction increases and the formation of the reaction products decreases, i.e., the formation of I per time unit decreases. At this stage of diffusion, which is characterized by times of 15 s to 240 s, the interstitial-substitutional exchange reaction controls the diffusion profiles and causes an increase in the I supersaturation. Since $C_I^{\mathrm{eq}}/C_{\mathrm{A}_s}^{\mathrm{eq}}$

is a measure of the supersaturation established via A_i-A_s exchange, the diffusion profiles are sensitive to this parameter. With increasing supersaturation the transport of I to the surface increases. The drop of the I concentration to thermal equilibrium ($\widetilde{C}_I = 1$) at $x = 0$, which is illustrated in the insert of Fig. 1.10, reflects the property of the surface as sink for I. Finally, after 720 s, the I supersaturation decreases. Now the formation of A_s is mainly controlled by the transport of I to the surface that is mainly mediated by D_I^*. Overall, the parameter $C_I^{eq}/C_{A_s}^{eq}$ affects the temporal evolution of A_s profiles for times varying between very short and effectively long times.

The Dirichlet boundary condition (1.74) for interstitial dissolved foreign atoms can be established experimentally by a constant vapor pressure p_A of the foreign atom (see e.g. sulfur: [112, 113]; zinc: [41, 93]). The vapor pressure determines the thermodynamic activity of the foreign atom A at the surface. Accordingly, the concentrations $C_{A_i}^{eq}$ and $C_{A_s}^{eq}$ correspond to equilibrium states that depend on p_A. In contrast, C_I^{eq} and the diffusion coefficients D_I and D_{A_i} describe properties of I and A_i that are independent of p_A. The parameters D_I^* and $C_I^{eq}/C_{A_s}^{eq}$ depend via $C_{A_s}^{eq}$ on p_A whereas $D_{A_i}^*$, $C_{A_i}^{eq}/C_{A_s}^{eq}$ and $k_{-2}C_I^{eq}$ are independent of p_A. This becomes evident by Eq. (1.31). The mass action constant K_2 is, like any other reaction constant, independent of p_A.

The impact of p_A on hybrid diffusion can be demonstrated by numerical simulations with varying values of D_I^* and $C_I^{eq}/C_{A_s}^{eq}$. Calculated $\widetilde{C}_{A_s}$ profiles for different parameters are illustrated in Fig. 1.11. The corresponding profiles of A_i and I are displayed in Figs. 1.12 and 1.13, respectively. Simulations for $\alpha \equiv D_{A_i}^*/D_I^* = 25$ reflect Zn diffusion profiles in dislocation-free and highly dislocated Si at 1388 K for 240 s [41]. The profiles belonging to $\alpha \in \{5, 1, 0.2, 0.04\}$ simulate the impact of a decreasing vapor pressure on diffusion in a sample with a thickness of 4 millimeter. The significance of $D_{A_i}^*/D_I^*$ on the shape of the A_s profiles is demonstrated by Fig. 1.11. A convex shape within the surface area is obtained for $\alpha > 1$. This reflects the native-defect controlled diffusion mode that holds for $C_{A_i}^{eq}D_{A_i} \gg C_I^{eq}D_I$. Within

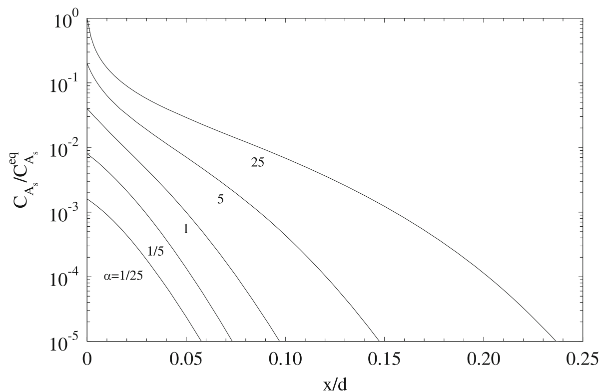

Fig. 1.11 Impact of the ratio $\alpha \equiv D_{A_i}^*/D_I^*$ on the normalized concentration profile of A_s

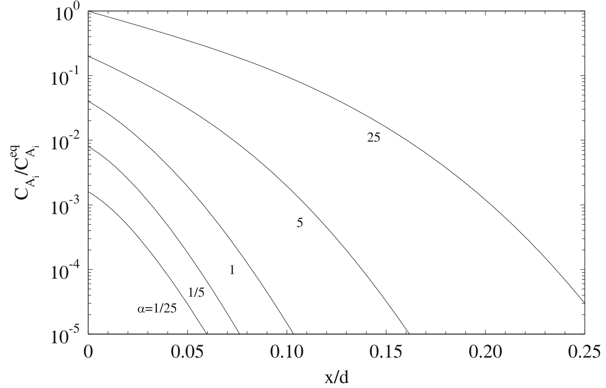

Fig. 1.12 Normalized concentration profiles of interstitial foreign-atoms A_i for different values of $\alpha \equiv D^*_{A_i}/D^*_I$

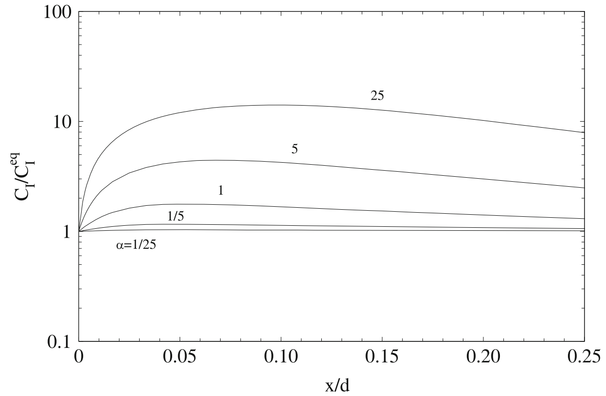

Fig. 1.13 Normalized concentration profile of self-interstitials I for different values of $\alpha \equiv D^*_{A_i}/D^*_I$

the approximation $\widetilde{C}_{A_i} \approx 1$, the relation

$$\widetilde{C}_{A_s} = \frac{1}{\widetilde{C}_I} \tag{1.79}$$

follows from Eq. (1.57). This is confirmed by the near-surface characteristic of the $\widetilde{C}_{A_s}$ and $\widetilde{C}_I$ profiles shown in Figs. 1.11 and 1.13 for $\alpha > 1$. Convex profiles reflect the significance of I for diffusion of the hybrid elements. In contrast, $\widetilde{C}_{A_s}$ profiles are concave for $D^*_{A_i} < D^*_I$ and are characterized by a negligible supersaturation of I, i.e. $\widetilde{C}_I \approx 1$. In this approximation Eq. (1.57) predicts $\widetilde{C}_{A_s} = \widetilde{C}_{A_i}$. The profiles shown in Figs. 1.11 and 1.12 for $\alpha < 1$ confirm this correlation.

Overall, Figs. 1.8, 1.9, 1.10, and 1.11 reveal a clear sensitivity of hybrid diffusion to all kick-out model parameters. This is summarized in Table 1.1 with $1/(k_{-2}C_I^{eq})$ as characteristic time for different diffusion stages. At the beginning of diffusion ($t < 1/(k_{-2}C_I^{eq})$) the A_s profiles not only depend on $D^*_{A_i}$ and D^*_I but are also sensitive to the parameters $k_{-2}C_I^{eq}$ and $C_{A_i}^{eq}/C_{A_s}^{eq}$. At intermediate times ($t \geq 1/(k_{-2}C_I^{eq})$) both $C_{A_i}^{eq}/C_{A_s}^{eq}$ and $C_I^{eq}/C_{A_s}^{eq}$ characterize the $\widetilde{C}_{A_s}$ profile. The near-surface curvature of $\widetilde{C}_{A_s}$ is a measure of the ratio $D^*_{A_i}/D^*_I$ that in particular affects the profiles for

Table 1.1 Dependence of $\widetilde{C}_{A_s}$ profiles in dislocation-free ($\star$) and dislocated ($*$) crystals on the model parameters of the kick-out mechanism

Diffusion stage	$D^*_{A_i}$	D^*_I	$\frac{C^{eq}_{A_i}}{C^{eq}_{A_s}}$	$\frac{C^{eq}_I}{C^{eq}_{A_s}}$	$k_{-2}C^{eq}_I$
$t < \frac{1}{k_{-2}C^{eq}_I}$	$\star$ ($*$)	$\star$	$\star$	–	$\star$ ($*$)
$t \geq \frac{1}{k_{-2}C^{eq}_I}$	$\star$ ($*$)	$\star$	$\star$	$\star$	$\star$ ($*$)
$t \gg \frac{1}{k_{-2}C^{eq}_I}$	$\star$ ($*$)	$\star$	$\star$	–	–
$\widetilde{C}_{A_i} \approx 1$	–	$\star$	–	–	–

$t \gg 1/(k_{-2}C^{eq}_I)$. Finally, according to Eq. (1.63), D^*_I can be obtained from the time evolution of the A_s concentration established in the center of the crystal after sufficient long diffusion times ($\widetilde{C}_{A_i} \approx 1$). The simulations of hybrid diffusion in dislocation-free crystals demonstrate that full information about the model parameters of the underlying diffusion-reaction mechanism are accessible from the time evolution of hybrid diffusion provided that effective short up to long diffusion times are realized experimentally.

Compared to hybrid diffusion in dislocation-free crystals, simultaneously performed experiments with highly dislocated material provide independent information about the parameters $D^*_{A_i}$ and $k_{-2}C^{eq}_I$. $\widetilde{C}_{A_s}$ profiles established in dislocated crystals for long times ($t \gg 1/(k_{-2}C^{eq}_I)$) are fully described by means of a complementary error function with $D^*_{A_i}$ (see Eq. (1.55)). The concave $\widetilde{C}_{A_s}$ curves are not controlled by I. These profiles are also very advantageous to determine the parameter $k_{-2}C^{eq}_I$ from the increase of the A_s concentration at the surface (see Eq. (1.76)), because the A_s boundary concentration is more accurately deduced from concave profiles in dislocated crystals than from convex profiles in dislocation-free material. Accordingly, $\widetilde{C}_{A_s}$ profiles in dislocated crystals can provide additional information about $k_{-2}C^{eq}_I$ and $D^*_{A_i}$. In the case hybrid diffusion in both dislocation-free and highly dislocated materials is considered, experimental $\widetilde{C}_{A_s}$ profiles in dislocation-free crystal mainly serve to determine D^*_I, $C^{eq}_{A_i}/C^{eq}_{A_s}$, and $C^{eq}_I/C^{eq}_{A_s}$. This is indicated in Table 1.1 where $k_{-2}C^{eq}_I$ and $D^*_{A_i}$ are also accessible by diffusion experiments in dislocated material. Experimental studies on this kind of hybrid diffusion in dislocation-free and highly dislocated Si are presented in Sect. 1.7.1 (see also [41]).

The numerical simulations presented in this section show that comprehensive diffusion experiments under equilibrium and non-equilibrium conditions are required to determine all model parameters of a diffusion-reaction system.

In the following the atomic mechanisms that mediate the diffusion of dopant elements are treated. Since the doping level of common p- and n-type dopants such as B, P, and As exceeds the intrinsic carrier concentration of Si and Ge, the impact of electronically extrinsic conditions on dopant diffusion must be considered. Again the classification into native-defect and foreign-atom controlled diffusion of A_s is used to describe the effective dopant diffusion coefficient.

1.6.2 Diffusion of Dopant Atoms

We consider that the solubility of substitutionally dissolved dopants A_s at diffusion temperature exceeds the intrinsic carrier concentration $n_{\rm in}$. As a consequence, the Fermi level E_f deviates from its intrinsic position $E_f^{\rm in}$ and the material is denoted electronically extrinsic. Moving the Fermi level from its intrinsic position to a position under extrinsic conditions, the formation of charged point defects X is affected and therewith their equilibrium concentrations $C_{\rm X}^{\rm eq}$ and transport capacities $C_{\rm X}^{\rm eq} D_{\rm X}$ [114]. Moreover, the dopant profile creates an electric field that affects the diffusion of charged mobile defects. Accordingly, the charge states of defects must be added to the reaction mechanisms. Since dopant diffusion is mediated by indirect diffusion mechanisms such as the vacancy-, interstitialcy-, kick-out-, and dissociative mechanisms, only these mechanisms are considered exemplary in the following and analytical solutions of the underlying diffusion equations are derived for specific experimental conditions.

1.6.2.1 Reaction Mechanisms with Charge States

Indirect diffusion mechanisms that are relevant for dopant diffusion in Si are the vacancy-, interstitialcy-, dissociative-, and kick-out mechanisms that, respectively, are described by the following reactions

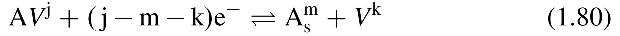

$$\mathrm{A}V^{\rm j} + (\mathrm{j-m-k})\mathrm{e}^- \rightleftharpoons \mathrm{A}_{\rm s}^{\rm m} + V^{\rm k} \tag{1.80}$$

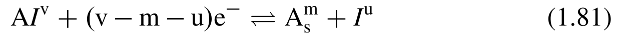

$$\mathrm{A}I^{\rm v} + (\mathrm{v-m-u})\mathrm{e}^- \rightleftharpoons \mathrm{A}_{\rm s}^{\rm m} + I^{\rm u} \tag{1.81}$$

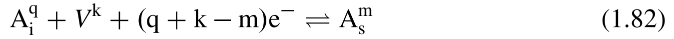

$$\mathrm{A}_{\rm i}^{\rm q} + V^{\rm k} + (\mathrm{q+k-m})\mathrm{e}^- \rightleftharpoons \mathrm{A}_{\rm s}^{\rm m} \tag{1.82}$$

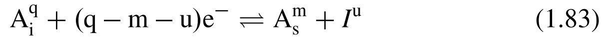

$$\mathrm{A}_{\rm i}^{\rm q} + (\mathrm{q-m-u})\mathrm{e}^- \rightleftharpoons \mathrm{A}_{\rm s}^{\rm m} + I^{\rm u} \tag{1.83}$$

with the charge states $\mathrm{j, k, m, q, u, v} \in \{0, \pm 1, \pm 2, \ldots\}$ and the electrons e^-.

In addition other reactions between point defects and defect pairs can be considered. Beside the Frenkel-pair reaction,

$$V^{\rm k} + I^{\rm u} + (\mathrm{k+u})\mathrm{e}^- \rightleftharpoons \phi, \tag{1.84}$$

which describes the annihilation (formation) of charged $V^{\rm k}$ and $I^{\rm u}$ into (from) self-atoms on regular lattice sites, the reactions

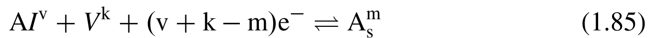

$$\mathrm{A}I^{\rm v} + V^{\rm k} + (\mathrm{v+k-m})\mathrm{e}^- \rightleftharpoons \mathrm{A}_{\rm s}^{\rm m} \tag{1.85}$$

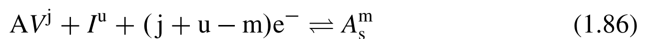

$$\mathrm{A}V^{\rm j} + I^{\rm u} + (\mathrm{j+u-m})\mathrm{e}^- \rightleftharpoons A_{\rm s}^{\rm m} \tag{1.86}$$

describe the dopant-defect pair assisted recombination of $V^{\rm k}$ and $I^{\rm u}$.

Generally, reactions (1.80), (1.81), (1.82), (1.83), (1.84), (1.85), and (1.86) are fast processes compared to the time scale of diffusion. For these conditions local equilibrium is established. Local equilibrium in the case of the vacancy (1.80), dissociative (1.82), and kick-out mechanisms (1.83) is characterized by

$$\frac{C_{\mathrm{A_s^m}}\, C_{V^\mathrm{k}}}{C_{\mathrm{A}V^\mathrm{j}}\, n^{(\mathrm{j-m-k})}} = \frac{C^{\mathrm{eq}}_{\mathrm{A_s^m}}\, C^{\mathrm{eq}}_{V^\mathrm{k}}}{C^{\mathrm{eq}}_{\mathrm{A}V^\mathrm{j}}\, (n^{\mathrm{eq}})^{(\mathrm{j-m-k})}} \tag{1.87}$$

$$\frac{C_{\mathrm{A_s^m}}}{C_{\mathrm{A_i^q}}\, C_{V^\mathrm{k}}\, n^{(\mathrm{q+k-m})}} = \frac{C^{\mathrm{eq}}_{\mathrm{A_s^m}}}{C^{\mathrm{eq}}_{\mathrm{A_i^q}}\, C^{\mathrm{eq}}_{V^\mathrm{k}}\, (n^{\mathrm{eq}})^{(\mathrm{q+k-m})}} \tag{1.88}$$

$$\frac{C_{\mathrm{A_s^m}}\, C_{I^\mathrm{u}}}{C_{\mathrm{A_i^q}}\, n^{(\mathrm{q-m-u})}} = \frac{C^{\mathrm{eq}}_{\mathrm{A_s^m}}\, C^{\mathrm{eq}}_{I^\mathrm{u}}}{C^{\mathrm{eq}}_{\mathrm{A_i^q}}\, (n^{\mathrm{eq}})^{(\mathrm{q-m-u})}}. \tag{1.89}$$

Here C_X ($C^{\mathrm{eq}}_\mathrm{X}$) represents the (thermal equilibrium) concentration of the defect X with X $\in \{\mathrm{A}V^\mathrm{j}, \mathrm{A_i^q}, \mathrm{A_s^m}, I^\mathrm{u}, V^\mathrm{k}\}$. n (n^{eq}) denotes the (maximum) free electron concentration. Local equilibrium does *not* imply that the concentrations of self-interstitials and vacancies equal their thermal equilibrium values $C^{\mathrm{eq}}_{I^\mathrm{u}}$ and $C^{\mathrm{eq}}_{V^\mathrm{k}}$, locally the concentration of the native defects can deviate from thermal equilibrium but the reactions are in dynamic equilibrium. Introducing defect and electron concentrations normalized to their thermal equilibrium values, $\widetilde{C}_\mathrm{X} = C_\mathrm{X}/C^{\mathrm{eq}}_\mathrm{X}$ and $\tilde{n} = n/n^{\mathrm{eq}}$, Eqs. (1.88) and (1.89) yield

$$\frac{\widetilde{C}_{\mathrm{A_s^m}}}{\widetilde{C}_{\mathrm{A_i^q}}\, \widetilde{C}_{V^\mathrm{k}}\, \tilde{n}^{(\mathrm{q+k-m})}} = \frac{\widetilde{C}_{\mathrm{A_s^m}}\, \widetilde{C}_{I^\mathrm{u}}}{\widetilde{C}_{\mathrm{A_i^q}}\, \tilde{n}^{(\mathrm{q-m-u})}} \tag{1.90}$$

which simplifies to

$$\frac{1}{\widetilde{C}_{V^\mathrm{k}}\widetilde{C}_{I^\mathrm{u}}\tilde{n}^{(\mathrm{k+u})}} = 1 \tag{1.91}$$

and expresses local equilibrium of the Frenkel-pair reaction (1.84). Obviously, this equilibrium state is simultaneously established when the kick-out and dissociative reactions are in local equilibrium.

Reactions (1.80), (1.81), and (1.83) are mathematically equivalent among each other. The mobile dopant-defects $\mathrm{A}V^\mathrm{j}$, $\mathrm{A}I^\mathrm{v}$, and $\mathrm{A_i^q}$ transform to substitutional dopants $\mathrm{A_s^m}$ thereby creating a native point defect (either V^k or I^u). On the other hand, reactions (1.82), (1.85), and (1.86) are also mathematically equivalent, since a mobile dopant defect and isolated native defect on the left hand side of the reactions transform to $\mathrm{A_s^m}$. This similarity between the reaction mechanisms indicates that dopant diffusion alone can hardly distinguish between $\mathrm{A}V^\mathrm{j}$, $\mathrm{A}I^\mathrm{v}$, and $\mathrm{A_i^q}$. However, dopant diffusion in isotope heterostructures can, in principle, differentiate between interstitial foreign-atoms and dopant-defect pairs, because the latter defects also contribute to self-diffusion.

1.6.2.2 Mathematical Formulation of Dopant Diffusion

The formation of substitutional shallow dopants to concentrations exceeding the intrinsic carrier concentration give rise to an electric field that affects the diffusion of charged mobile defects. Accordingly, a drift of charged defects in the electric field must be added to Eq. (1.1), which, in one dimension, reads

$$J_\mathrm{X} = -D_\mathrm{X}\frac{\partial C_\mathrm{X}}{\partial x} + \mu_\mathrm{X} C_\mathrm{X} \epsilon(x). \tag{1.92}$$

μ and ϵ denote the mobility and the electric field, respectively. Taking into account that the electric field is the derivative of the potential ψ

$$\epsilon(x) = -\frac{\partial \psi(x)}{\partial x} \tag{1.93}$$

and that the free electron concentration is given by

$$n(x) = \mathrm{N_C} \exp\left(\frac{E_f - E_\mathrm{C} + e\psi(x)}{kT}\right) \tag{1.94}$$

with e being the elementary charge, the electric field can be written as

$$\epsilon(x) = -\frac{kT}{e}\frac{1}{n(x)}\frac{\partial n(x)}{\partial x}. \tag{1.95}$$

Substituting Eq. (1.95) in Eq. (1.92) and using the Einstein relation

$$\mu = \mathrm{z}\, e \frac{D_\mathrm{X}}{kT} \tag{1.96}$$

with the charge state z of the diffusing species, we obtain

$$J_\mathrm{X} = -D_\mathrm{X}\frac{\partial C_\mathrm{X}}{\partial x} - \mathrm{z}\, C_\mathrm{X} D_\mathrm{X} \frac{1}{n(x)}\frac{\partial n(x)}{\partial x}. \tag{1.97}$$

In the case that the electric field is caused by acceptors, the flux equation reads

$$J_\mathrm{X} = -D_\mathrm{X}\frac{\partial C_\mathrm{X}}{\partial x} + \mathrm{z}\, C_\mathrm{X} D_\mathrm{X} \frac{1}{p(x)}\frac{\partial p(x)}{\partial x} \tag{1.98}$$

where p denotes the free hole concentration. Additional terms enter Eq. (1.92) when besides chemical and electrical forces also mechanical strain and/or hydrostatic pressure affect the flux of a point defect.

In the following dopant diffusion via the vacancy and dissociative mechanisms (1.80) and (1.82) are treated representative for reactions (1.80) and (1.86)

in more detail. Starting from the full differential equation system, useful approximations are presented that describe the relation between the shape of the diffusion profile and the charge states of the point defects involved in the diffusion process. Understanding this relation is very helpful to identify the underlying mechanisms of dopant diffusion.

Dopant Diffusion via the Vacancy Mechanism

The vacancy mechanism is given by reaction (1.80) in a generalized form. Adding the forward and backward rate constants which are denoted k_+ and k_-, respectively, reaction (1.80) reads

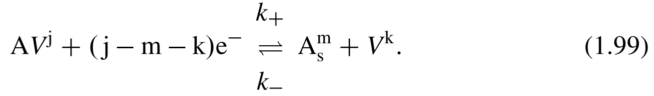

$$\mathrm{A}V^{\mathrm{j}} + (\mathrm{j}-\mathrm{m}-\mathrm{k})\mathrm{e}^- \underset{k_-}{\overset{k_+}{\rightleftharpoons}} \mathrm{A}_\mathrm{s}^\mathrm{m} + V^\mathrm{k}. \tag{1.99}$$

Taking into account Eq. (1.97), the following three coupled partial differential equations describe the diffusion and reaction of the point defects involved in reaction (1.99)

$$\frac{\partial C_{\mathrm{A}_\mathrm{s}^\mathrm{m}}}{\partial t} = \frac{\partial}{\partial x}\left(D_{\mathrm{A}_\mathrm{s}{}^\mathrm{m}} \frac{\partial C_{\mathrm{A}_\mathrm{s}{}^\mathrm{m}}}{\partial x} + \mathrm{m}\frac{C_{\mathrm{A}_\mathrm{s}{}^\mathrm{m}} D_{\mathrm{A}_\mathrm{s}{}^\mathrm{m}}}{n(x)}\frac{\partial n(x)}{\partial x}\right) + k_+ C_{\mathrm{A}V^\mathrm{j}}\, C_\mathrm{o}\, n^{(\mathrm{j}-\mathrm{m}-\mathrm{k})} - k_- C_{\mathrm{A}_\mathrm{s}^\mathrm{m}} C_{V^\mathrm{k}}\, n_\mathrm{in}^{(\mathrm{j}-\mathrm{m}-\mathrm{k})} \tag{1.100}$$

$$\frac{\partial C_{\mathrm{A}V^\mathrm{j}}}{\partial t} = \frac{\partial}{\partial x}\left(D_{\mathrm{A}V^\mathrm{j}} \frac{\partial C_{\mathrm{A}V^\mathrm{j}}}{\partial x} + \mathrm{j}\frac{C_{\mathrm{A}V^\mathrm{j}} D_{\mathrm{A}V^\mathrm{j}}}{n(x)}\frac{\partial n(x)}{\partial x}\right) - k_+ C_{\mathrm{A}V^\mathrm{j}}\, C_\mathrm{o}\, n^{(\mathrm{j}-\mathrm{m}-\mathrm{k})} + k_- C_{\mathrm{A}_\mathrm{s}^\mathrm{m}} C_{V^\mathrm{k}}\, n_\mathrm{in}^{(\mathrm{j}-\mathrm{m}-\mathrm{k})} \tag{1.101}$$

$$\frac{\partial C_{V^\mathrm{k}}}{\partial t} = \frac{\partial}{\partial x}\left(D_{V^\mathrm{k}} \frac{\partial C_{V^\mathrm{k}}}{\partial x} + \mathrm{k}\frac{C_{V^\mathrm{k}} D_{V^\mathrm{k}}}{n(x)}\frac{\partial n(x)}{\partial x}\right) + k_+ C_{\mathrm{A}V^\mathrm{j}}\, C_\mathrm{o}\, n^{(\mathrm{j}-\mathrm{m}-\mathrm{k})} - k_- C_{\mathrm{A}_\mathrm{s}^\mathrm{m}} C_{V^\mathrm{k}}\, n_\mathrm{in}^{(\mathrm{j}-\mathrm{m}-\mathrm{k})} \tag{1.102}$$

where C_X (D_X) with $\mathrm{X} \in \{\mathrm{A}_\mathrm{s}^\mathrm{m}, \mathrm{A}V^\mathrm{j}, V^\mathrm{k}\}$ is the concentration (diffusion coefficient) of the respective point defect. $D_{\mathrm{A}_\mathrm{s}{}^\mathrm{m}}$ equals the diffusivity of the substitutionally dissolved foreign atom via direct exchange. $C_\mathrm{o}(= 5{\times}10^{22}\ \mathrm{cm}^{-3}$ for Si) is the number density of substitutional lattice sites. The first term on the right hand side of reactions (1.100), (1.101), and (1.102) describes the change of the concentration of the point defect via diffusion and drift. The second term represents the formation/annihilation of the point defect via reaction (1.99).

Introducing normalized concentrations $\widetilde{C}_{\mathrm{X}} = C_{\mathrm{X}}/C_{\mathrm{X}}^{\mathrm{eq}}$ and $\tilde{n} = n/n^{\mathrm{eq}}$, reduced diffusivities $D_{\mathrm{X}}^{*} = C_{\mathrm{X}}^{\mathrm{eq}} D_{\mathrm{X}}/C_{\mathrm{A_s^m}}^{\mathrm{eq}}$, and the relationship between the rate constants k_{+} and k_{-}

$$\frac{k_{+}}{k_{-}} = \frac{C_{\mathrm{A_s^m}}^{\mathrm{eq}}\, C_{V^{\mathrm{k}}}^{\mathrm{eq}}\, n_{\mathrm{in}}^{(\mathrm{j-m-k})}}{C_{\mathrm{AV^j}}^{\mathrm{eq}}\, C_{\mathrm{o}}\, (n^{\mathrm{eq}})^{(\mathrm{j-m-k})}}, \tag{1.103}$$

due to the law of mass action, the differential equations (1.100), (1.101), and (1.102) read

$$\frac{\partial \widetilde{C}_{\mathrm{A_s^m}}}{\partial t} = \frac{\partial}{\partial x}\left(D_{\mathrm{A_s{}^m}} \frac{\partial \widetilde{C}_{\mathrm{A_s{}^m}}}{\partial x} + \mathrm{m} \frac{\widetilde{C}_{\mathrm{A_s{}^m}} D_{\mathrm{A_s{}^m}}}{\tilde{n}(x)} \frac{\partial \tilde{n}(x)}{\partial x}\right) + k_{-} C_{V^{\mathrm{k}}}^{\mathrm{eq}}\, n_{\mathrm{in}}^{(\mathrm{j-m-k})} \left(\widetilde{C}_{\mathrm{AV^j}}\, \tilde{n}^{(\mathrm{j-m-k})} - \widetilde{C}_{\mathrm{A_s^m}} \widetilde{C}_{V^{\mathrm{k}}}\right) \tag{1.104}$$

$$\frac{C_{\mathrm{AV^j}}^{\mathrm{eq}}}{C_{\mathrm{A_s^m}}^{\mathrm{eq}}} \frac{\partial \widetilde{C}_{\mathrm{AV^j}}}{\partial t} = \frac{\partial}{\partial x}\left(D_{\mathrm{AV^j}}^{*} \frac{\partial \widetilde{C}_{\mathrm{AV^j}}}{\partial x} + \mathrm{j} \frac{\widetilde{C}_{\mathrm{AV^j}} D_{\mathrm{AV^j}}^{*}}{\tilde{n}(x)} \frac{\partial \tilde{n}(x)}{\partial x}\right) - k_{-} C_{V^{\mathrm{k}}}^{\mathrm{eq}}\, n_{\mathrm{in}}^{(\mathrm{j-m-k})} \left(\widetilde{C}_{\mathrm{AV^j}}\, \tilde{n}^{(\mathrm{j-m-k})} - \widetilde{C}_{\mathrm{A_s^m}} \widetilde{C}_{V^{\mathrm{k}}}\right) \tag{1.105}$$

$$\frac{C_{V^{\mathrm{k}}}^{\mathrm{eq}}}{C_{\mathrm{A_s^m}}^{\mathrm{eq}}} \frac{\partial \widetilde{C}_{V^{\mathrm{k}}}}{\partial t} = \frac{\partial}{\partial x}\left(D_{V^{\mathrm{k}}}^{*} \frac{\partial \widetilde{C}_{V^{\mathrm{k}}}}{\partial x} + \mathrm{k} \frac{\widetilde{C}_{V^{\mathrm{k}}} D_{V^{\mathrm{k}}}^{*}}{\tilde{n}(x)} \frac{\partial \tilde{n}(x)}{\partial x}\right) + k_{-} C_{V^{\mathrm{k}}}^{\mathrm{eq}}\, n_{\mathrm{in}}^{(\mathrm{j-m-k})} \left(\widetilde{C}_{\mathrm{AV^j}}\, \tilde{n}^{(\mathrm{j-m-k})} - \widetilde{C}_{\mathrm{A_s^m}} \widetilde{C}_{V^{\mathrm{k}}}\right). \tag{1.106}$$

This system of differential equations describes the diffusion of A via the vacancy mechanism when $\mathrm{A_s^m}$ acts as donor. For $\mathrm{A_s^m}$ being an acceptor, $\tilde{n}$ and $\frac{1}{\tilde{n}}\frac{\partial \tilde{n}}{\partial x}$ are replaced by means of $np = n_{\mathrm{in}}^2$ with $1/\tilde{p}$ and $-\frac{1}{\tilde{p}}\frac{\partial \tilde{p}}{\partial x}$, respectively.

The electron and hole concentrations are related via the charge neutrality equation

$$n = p + \mathrm{m} C_{\mathrm{A_s^m}} + \mathrm{k} C_{V^{\mathrm{k}}} + \mathrm{j} C_{\mathrm{AV^j}} \tag{1.107}$$

with the concentrations of the point defects. For a substitutional donor $\mathrm{A_s^m}$ with $\mathrm{m} \in \{+1, +2, \ldots\}$, we obtain

$$\tilde{n}(x) = \frac{\left(\mathrm{m}\widetilde{C}_{\mathrm{A_s^m}} + \mathrm{j}\frac{C_{\mathrm{AV^j}}^{\mathrm{eq}}}{C_{\mathrm{A_s^m}}^{\mathrm{eq}}}\widetilde{C}_{\mathrm{AV^j}} + \mathrm{k}\frac{C_{V^{\mathrm{k}}}^{\mathrm{eq}}}{C_{\mathrm{A_s^m}}^{\mathrm{eq}}}\widetilde{C}_{V^{\mathrm{k}}}\right) + \sqrt{\left(\mathrm{m}\widetilde{C}_{\mathrm{A_s^m}} + \mathrm{j}\frac{C_{\mathrm{AV^j}}^{\mathrm{eq}}}{C_{\mathrm{A_s^m}}^{\mathrm{eq}}}\widetilde{C}_{\mathrm{AV^j}} + \mathrm{k}\frac{C_{V^{\mathrm{k}}}^{\mathrm{eq}}}{C_{\mathrm{A_s^m}}^{\mathrm{eq}}}\widetilde{C}_{V^{\mathrm{k}}}\right)^2 + 4\tilde{n}_{\mathrm{in}}^2}}{\left(\mathrm{m} + \mathrm{j}\frac{C_{\mathrm{AV^j}}^{\mathrm{eq}}}{C_{\mathrm{A_s^m}}^{\mathrm{eq}}} + \mathrm{k}\frac{C_{V^{\mathrm{k}}}^{\mathrm{eq}}}{C_{\mathrm{A_s^m}}^{\mathrm{eq}}}\right) + \sqrt{\left(\mathrm{m} + \mathrm{j}\frac{C_{\mathrm{AV^j}}^{\mathrm{eq}}}{C_{\mathrm{A_s^m}}^{\mathrm{eq}}} + \mathrm{k}\frac{C_{V^{\mathrm{k}}}^{\mathrm{eq}}}{C_{\mathrm{A_s^m}}^{\mathrm{eq}}}\right)^2 + 4\tilde{n}_{\mathrm{in}}^2}} \tag{1.108}$$

and

$$\frac{1}{\tilde{n}(x)}\frac{\partial \tilde{n}(x)}{\partial x} = \frac{1}{\sqrt{\left(\mathrm{m}\widetilde{C}_{\mathrm{A_s^m}} + \mathrm{j}\frac{C^{\mathrm{eq}}_{\mathrm{AV^j}}}{C^{\mathrm{eq}}_{\mathrm{A_s^m}}}\widetilde{C}_{\mathrm{AV^j}} + \mathrm{k}\frac{C^{\mathrm{eq}}_{V^{\mathrm{k}}}}{C^{\mathrm{eq}}_{\mathrm{A_s^m}}}\widetilde{C}_{V^{\mathrm{k}}}\right)^2 + 4\tilde{n}_{\mathrm{in}}^2}} \times \frac{\partial\left(\mathrm{m}\widetilde{C}_{\mathrm{A_s^m}} + \mathrm{j}\frac{C^{\mathrm{eq}}_{\mathrm{AV^j}}}{C^{\mathrm{eq}}_{\mathrm{A_s^m}}}\widetilde{C}_{\mathrm{AV^j}} + \mathrm{k}\frac{C^{\mathrm{eq}}_{V^{\mathrm{k}}}}{C^{\mathrm{eq}}_{\mathrm{A_s^m}}}\widetilde{C}_{V^{\mathrm{k}}}\right)}{\partial x} \tag{1.109}$$

with $\tilde{n}_{\mathrm{in}} = n_{\mathrm{in}}/C^{\mathrm{eq}}_{\mathrm{A_s^m}}$. Considering a substitutional acceptor $\mathrm{A_s^m}$ with $\mathrm{m} \in \{-1, -2, \ldots\}$ we get

$$\tilde{p}(x) = \frac{\left(-\mathrm{m}\widetilde{C}_{\mathrm{A_s^m}} - \mathrm{j}\frac{C^{\mathrm{eq}}_{\mathrm{AV^j}}}{C^{\mathrm{eq}}_{\mathrm{A_s^m}}}\widetilde{C}_{\mathrm{AV^j}} - \mathrm{k}\frac{C^{\mathrm{eq}}_{V^{\mathrm{k}}}}{C^{\mathrm{eq}}_{\mathrm{A_s^m}}}\widetilde{C}_{V^{\mathrm{k}}}\right) + \sqrt{\left(-\mathrm{m}\widetilde{C}_{\mathrm{A_s^m}} - \mathrm{j}\frac{C^{\mathrm{eq}}_{\mathrm{AV^j}}}{C^{\mathrm{eq}}_{\mathrm{A_s^m}}}\widetilde{C}_{\mathrm{AV^j}} - \mathrm{k}\frac{C^{\mathrm{eq}}_{V^{\mathrm{k}}}}{C^{\mathrm{eq}}_{\mathrm{A_s^m}}}\widetilde{C}_{V^{\mathrm{k}}}\right)^2 + 4\tilde{n}_{\mathrm{in}}^2}}{\left(-\mathrm{m} - \mathrm{j}\frac{C^{\mathrm{eq}}_{\mathrm{AV^j}}}{C^{\mathrm{eq}}_{\mathrm{A_s^m}}} - \mathrm{k}\frac{C^{\mathrm{eq}}_{V^{\mathrm{k}}}}{C^{\mathrm{eq}}_{\mathrm{A_s^m}}}\right) + \sqrt{\left(-\mathrm{m} - \mathrm{j}\frac{C^{\mathrm{eq}}_{\mathrm{AV^j}}}{C^{\mathrm{eq}}_{\mathrm{A_s^m}}} - \mathrm{k}\frac{C^{\mathrm{eq}}_{V^{\mathrm{k}}}}{C^{\mathrm{eq}}_{\mathrm{A_s^m}}}\right)^2 + 4\tilde{n}_{\mathrm{in}}^2}} \tag{1.110}$$

and

$$\frac{1}{\tilde{p}(x)}\frac{\partial \tilde{p}(x)}{\partial x} = \frac{1}{\sqrt{\left(-\mathrm{m}\widetilde{C}_{\mathrm{A_s^m}} - \mathrm{j}\frac{C^{\mathrm{eq}}_{\mathrm{AV^j}}}{C^{\mathrm{eq}}_{\mathrm{A_s^m}}}\widetilde{C}_{\mathrm{AV^j}} - \mathrm{k}\frac{C^{\mathrm{eq}}_{V^{\mathrm{k}}}}{C^{\mathrm{eq}}_{\mathrm{A_s^m}}}\widetilde{C}_{V^{\mathrm{k}}}\right)^2 + 4\tilde{n}_{\mathrm{in}}^2}} \times \frac{\partial\left(-\mathrm{m}\widetilde{C}_{\mathrm{A_s^m}} - \mathrm{j}\frac{C^{\mathrm{eq}}_{\mathrm{AV^j}}}{C^{\mathrm{eq}}_{\mathrm{A_s^m}}}\widetilde{C}_{\mathrm{AV^j}} - \mathrm{k}\frac{C^{\mathrm{eq}}_{V^{\mathrm{k}}}}{C^{\mathrm{eq}}_{\mathrm{A_s^m}}}\widetilde{C}_{V^{\mathrm{k}}}\right)}{\partial x}. \tag{1.111}$$

Equations (1.104), (1.105), and (1.106) together with Eq. (1.109) (Eq. (1.111)) represent the full set of equations to calculate diffusion profiles of donors (acceptors) $\mathrm{A_s^m}$ and other point defects involved in reaction (1.99) for specific initial and boundary conditions.

In the following approximations of the differential equation system (1.104), (1.105), and (1.106) are considered that lead to a single differential equation of the form

$$\frac{\partial C_{\mathrm{X}}}{\partial t} - \frac{\partial}{\partial x}\left(D_{\mathrm{X}}\frac{\partial C_{\mathrm{X}}}{\partial x}\right) = G_{\mathrm{X}}. \tag{1.112}$$

with $G_{\mathrm{X}} = 0$. Two different modes of dopant diffusion are distinguished, i.e., the native-defect and foreign-atom controlled modes. Each mode predicts characteristic profiles for $\mathrm{A_s^m}$. The characteristic shape of the profiles reflects the charge states of the point defects controlling the diffusion process.

Native-Defect Controlled Dopant Diffusion via the Vacancy Mechanism

The vacancy-controlled mode of dopant diffusion is established when the relationship $D^*_{\mathrm{AV^j}} \gg D^*_{V^\mathrm{k}}$ holds. The higher transport capacity $C^{\mathrm{eq}}_{\mathrm{AV^j}} D_{\mathrm{AV^j}}$ of the dopant-defect pair compared to $C^{\mathrm{eq}}_{V^\mathrm{k}} D_{V^\mathrm{k}}$ leads to an almost homogeneous distribution of the dopant-vacancy pairs after sufficiently long diffusion times, i.e., $\widetilde{C}_{\mathrm{AV^j}} \approx 1$. Accordingly, Eq. (1.105) can be neglected. The contribution of the direct diffusion of $\mathrm{A_s^m}$ to the diffusion of the dopant A is generally small compared to the indirect diffusion via AV pairs. Taking the difference between Eqs. (1.104) and (1.106) and assuming $C^{\mathrm{eq}}_{V^\mathrm{k}} \ll C^{\mathrm{eq}}_{\mathrm{A_s^m}}$ we obtain

$$\frac{\partial \widetilde{C}_{\mathrm{A_s^m}}}{\partial t} \approx -\frac{\partial}{\partial x}\left(D^*_{V^\mathrm{k}} \frac{\partial \widetilde{C}_{V^\mathrm{k}}}{\partial x} + \mathrm{k} \frac{\widetilde{C}_{V^\mathrm{k}} D^*_{V^\mathrm{k}}}{\tilde{n}(x)} \frac{\partial \tilde{n}(x)}{\partial x} \right). \tag{1.113}$$

For local equilibrium of reaction (1.99),

$$\frac{\widetilde{C}_{\mathrm{A_s^m}} \widetilde{C}_{V^\mathrm{k}}}{\widetilde{C}_{\mathrm{AV^j}}\ \tilde{n}^{\,(\mathrm{j-m-k})}} = 1, \tag{1.114}$$

and of reaction $\mathrm{A}V^\mathrm{j} + \mathrm{j}e^- \rightleftharpoons \mathrm{A}V^0$,

$$\frac{\widetilde{C}_{\mathrm{AV^0}}}{\widetilde{C}_{\mathrm{AV^j}}\ \tilde{n}^{\,\mathrm{j}}} = 1, \tag{1.115}$$

Eqs. (1.114) and (1.115) yield

$$\widetilde{C}_{V^\mathrm{k}} = \frac{\widetilde{C}_{\mathrm{AV^0}} \tilde{n}^{\,(-\mathrm{m-k})}}{\widetilde{C}_{\mathrm{A_s^m}}} \approx \frac{\tilde{n}^{\,(-\mathrm{m-k})}}{\widetilde{C}_{\mathrm{A_s^m}}} \tag{1.116}$$

because $\widetilde{C}_{\mathrm{AV^0}} \approx 1$. For high donor concentrations, i.e., $C^{\mathrm{eq}}_{\mathrm{A_s^m}}$ exceeds n_{in}, $\tilde{n} \approx \widetilde{C}_{\mathrm{A_s^m}}$ holds and Eq. (1.113) transforms with Eq. (1.116) to a differential equation of the form

$$\frac{\partial \widetilde{C}_{\mathrm{A_s^m}}}{\partial t} - \frac{\partial}{\partial x} D^{\mathrm{eff}}_{\mathrm{A_s^m}} \frac{\partial \widetilde{C}_{\mathrm{A_s^m}}}{\partial x} = 0 \tag{1.117}$$

with an effective diffusivity of $\mathrm{A_s^m}$ ($\mathrm{m} \in \{+1, +2, \ldots\}$) given by

$$D^{\mathrm{eff}}_{\mathrm{A_s^m}} = (\mathrm{m}+1) D^*_{V^\mathrm{k}} (\widetilde{C}_{\mathrm{A_s^m}})^{-\mathrm{m-k}-2}. \tag{1.118}$$

For high concentrations of acceptors $\mathrm{A_s^m}$ ($\mathrm{m} \in \{-1, -2, \ldots\}$) with $\tilde{p} \approx \widetilde{C}_{\mathrm{A_s^m}}$, Eq. (1.117) with

$$D^{\mathrm{eff}}_{\mathrm{A_s^m}} = (-\mathrm{m}+1) D^*_{V^\mathrm{k}} (\widetilde{C}_{\mathrm{A_s^m}})^{\mathrm{m+k}-2} \tag{1.119}$$

is obtained. Equations (1.118) and (1.119) reveal that in case of dopant diffusion via the vacancy mechanism the effective dopant diffusion coefficient $D^{\mathrm{eff}}_{\mathrm{A_s^m}}$ is interrelated to the reduced diffusion coefficient $D^*_{V^{\mathrm{k}}} = C^{\mathrm{eq}}_{V^{\mathrm{k}}} D_{V^{\mathrm{k}}} / C^{\mathrm{eq}}_{\mathrm{A_s^m}}$ and thus to the transport capacity of V^{k}. This interrelation reflects the V-controlled mode of dopant diffusion.

Foreign-Atom Controlled Dopant Diffusion via the Vacancy Mechanism

The foreign-atom controlled mode of dopant diffusion is established when the relationship $D^*_{\mathrm{A}V^{\mathrm{j}}} \ll D^*_{V^{\mathrm{k}}}$ holds. The higher transport capacity of V^{k} compared to that of $\mathrm{A}V^{\mathrm{j}}$ pairs leads to an almost homogeneous distribution of V^{k} after sufficiently long times, i.e., $\widetilde{C}_{V^{\mathrm{k}}} \approx 1$. Accordingly, Eq. (1.106) can be neglected. Taking into account that the direct diffusion of $\mathrm{A_s^m}$ is negligible compared to the indirect diffusion of $\mathrm{A_s^m}$ via $\mathrm{A}V$ pairs and that $C^{\mathrm{eq}}_{\mathrm{A}V^{\mathrm{j}}} \ll C^{\mathrm{eq}}_{\mathrm{A_s^m}}$ holds, the sum of Eqs. (1.104) and (1.105) yields

$$\frac{\partial \widetilde{C}_{\mathrm{A_s^m}}}{\partial t} \approx \frac{\partial}{\partial x}\left(D^*_{\mathrm{A}V^{\mathrm{j}}} \frac{\partial \widetilde{C}_{\mathrm{A}V^{\mathrm{j}}}}{\partial x} + \mathrm{j} \frac{\widetilde{C}_{\mathrm{A}V^{\mathrm{j}}} D^*_{\mathrm{A}V^{\mathrm{j}}}}{\tilde{n}(x)} \frac{\partial \tilde{n}(x)}{\partial x} \right). \tag{1.120}$$

Assuming local equilibrium of reaction (1.99) and of the reaction $V^{\mathrm{k}} + \mathrm{k}e^- \rightleftharpoons V^0$, which is expressed by Eq. (1.114) and

$$\frac{\widetilde{C}_{V^0}}{\widetilde{C}_{V^{\mathrm{k}}}\ \tilde{n}^{\mathrm{k}}} = 1, \tag{1.121}$$

respectively, one gets

$$\widetilde{C}_{\mathrm{A}V^{\mathrm{j}}} \approx \widetilde{C}_{\mathrm{A_s^m}} \tilde{n}^{(\mathrm{m-j})} = (\widetilde{C}_{\mathrm{A_s^m}})^{(\mathrm{m-j+1})}. \tag{1.122}$$

For donors $\mathrm{A_s^m}$ ($\mathrm{m} = +1, +2, \ldots$) with $\tilde{n} \approx \widetilde{C}_{\mathrm{A_s^m}}$, Eq. (1.120) transforms to Eq. (1.117) with

$$D^{\mathrm{eff}}_{\mathrm{A_s^m}} = (\mathrm{m}+1) D^*_{\mathrm{A}V^{\mathrm{j}}} (\widetilde{C}_{\mathrm{A_s^m}})^{\mathrm{m-j}}. \tag{1.123}$$

For acceptors $\mathrm{A_s^m}$ ($\mathrm{m} \in \{-1, -2, \ldots\}$) with $\tilde{p} \approx \widetilde{C}_{\mathrm{A_s^m}}$, the diffusion coefficient in Eq. (1.117) is given by

$$D^{\mathrm{eff}}_{\mathrm{A_s^m}} = (-\mathrm{m}+1) D^*_{\mathrm{A}V^{\mathrm{j}}} (\widetilde{C}_{\mathrm{A_s^m}})^{-\mathrm{m+j}}. \tag{1.124}$$

Equations (1.123) and (1.124) reveal that in case of the foreign-atom controlled mode of dopant diffusion via the vacancy mechanism the effective dopant diffusion coefficient $D^{\mathrm{eff}}_{\mathrm{A_s^m}}$ is interrelated to the reduced diffusion coefficient $D^*_{\mathrm{A}V^{\mathrm{j}}} = C^{\mathrm{eq}}_{\mathrm{A}V^{\mathrm{j}}} D_{\mathrm{A}V^{\mathrm{j}}} / C^{\mathrm{eq}}_{\mathrm{A_s^m}}$ and thus to the transport capacity of $\mathrm{A}V^{j}$. This interrelation reflects the $\mathrm{A}V$-controlled mode of dopant diffusion.

1.6.2.3 Dopant Diffusion via the Dissociative Mechanism

The dissociative mechanism is representative for the mechanisms (1.82), (1.85) and (1.86), which all possess a similar reaction scheme. The partial differential equation system for modeling dopant diffusion via the dissociative mechanism is easily translated to the equation system for modeling diffusion via the dopant-defect pair assisted recombination mechanism (1.85) (mechanism (1.86)) by replacing the defect(s) $\mathrm{A_i^q}$ (A_i^q, V^k) with $\mathrm{A}I^\mathrm{v}$ ($\mathrm{A}V^\mathrm{j}$, I^u).

Introducing forward and backward rate constants k_f and k_b, respectively, the dissociative mechanism reads

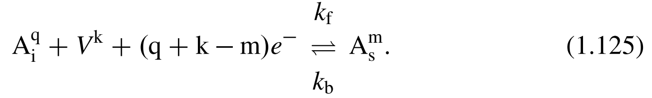

$$\mathrm{A_i^q} + V^\mathrm{k} + (\mathrm{q}+\mathrm{k}-\mathrm{m})e^- \underset{k_\mathrm{b}}{\overset{k_\mathrm{f}}{\rightleftharpoons}} \mathrm{A_s^m}. \tag{1.125}$$

k_f and k_b are related via the law of mass action according to

$$\frac{k_\mathrm{f}}{k_\mathrm{b}} = \frac{C^\mathrm{eq}_{\mathrm{A_s^m}}\, C'_\mathrm{o}\, n_\mathrm{in}^{(\mathrm{q}+\mathrm{k}-\mathrm{m})}}{C^\mathrm{eq}_{\mathrm{A_i^q}} C^\mathrm{eq}_{V^\mathrm{k}} (n^\mathrm{eq})^{(\mathrm{q}+\mathrm{k}-\mathrm{m})}}\,, \tag{1.126}$$

where C'_o is the number density of interstitial sites. Taking into account normalized concentrations and reduced diffusivities, the differential equation system for modeling dopant diffusion via the dissociative mechanism (1.125) is

$$\frac{\partial \widetilde{C}_{\mathrm{A_s^m}}}{\partial t} = \frac{\partial}{\partial x}\left(D_{\mathrm{A_s}^\mathrm{m}} \frac{\partial \widetilde{C}_{\mathrm{A_s}^\mathrm{m}}}{\partial x} + \mathrm{m}\frac{\widetilde{C}_{\mathrm{A_s}^\mathrm{m}} D_{\mathrm{A_s}^\mathrm{m}}}{\tilde{n}(x)}\frac{\partial \tilde{n}(x)}{\partial x}\right) + k_\mathrm{b}\, C'_\mathrm{o}\, n_\mathrm{in}^{(\mathrm{q}+\mathrm{k}-\mathrm{m})}\left(\widetilde{C}_{\mathrm{A_i^q}} \widetilde{C}_{V^\mathrm{k}}\, \tilde{n}^{(\mathrm{q}+\mathrm{k}-\mathrm{m})} - \widetilde{C}_{\mathrm{A_s^m}}\right) \tag{1.127}$$

$$\frac{C^\mathrm{eq}_{\mathrm{A_i^q}}}{C^\mathrm{eq}_{\mathrm{A_s^m}}} \frac{\partial \widetilde{C}_{\mathrm{A_i^q}}}{\partial t} = \frac{\partial}{\partial x}\left(D^*_{\mathrm{A_i^q}} \frac{\partial \widetilde{C}_{\mathrm{A_i^q}}}{\partial x} + \mathrm{q}\frac{\widetilde{C}_{\mathrm{A_i^q}} D^*_{\mathrm{A_i^q}}}{\tilde{n}(x)}\frac{\partial \tilde{n}(x)}{\partial x}\right) - k_\mathrm{b}\, C'_\mathrm{o}\, n_\mathrm{in}^{(\mathrm{q}+\mathrm{k}-\mathrm{m})}\left(\widetilde{C}_{\mathrm{A_i^q}} \widetilde{C}_{V^\mathrm{k}}\, \tilde{n}^{(\mathrm{q}+\mathrm{k}-\mathrm{m})} - \widetilde{C}_{\mathrm{A_s^m}}\right) \tag{1.128}$$

$$\frac{C^\mathrm{eq}_{V^\mathrm{k}}}{C^\mathrm{eq}_{\mathrm{A_s^m}}} \frac{\partial \widetilde{C}_{V^\mathrm{k}}}{\partial t} = \frac{\partial}{\partial x}\left(D^*_{V^\mathrm{k}} \frac{\partial \widetilde{C}_{V^\mathrm{k}}}{\partial x} + \mathrm{k}\frac{\widetilde{C}_{V^\mathrm{k}} D^*_{V^\mathrm{k}}}{\tilde{n}(x)}\frac{\partial \tilde{n}(x)}{\partial x}\right) - k_\mathrm{b}\, C'_\mathrm{o}\, n_\mathrm{in}^{(\mathrm{q}+\mathrm{k}-\mathrm{m})}\left(\widetilde{C}_{\mathrm{A_i^q}} \widetilde{C}_{V^\mathrm{k}}\, \tilde{n}^{(\mathrm{q}+\mathrm{k}-\mathrm{m})} - \widetilde{C}_{\mathrm{A_s^m}}\right). \tag{1.129}$$

The diffusion of a donor $\mathrm{A_s^m}$ ($\mathrm{m} \in \{+1, +2, \ldots\}$) is described by Eqs. (1.127), (1.128), and (1.129) and by equations for $\tilde{n}$ and $\frac{1}{\tilde{n}(x)}\frac{\partial \tilde{n}(x)}{\partial x}$ that are similar to

Eqs. (1.108) and (1.109). For an acceptor $\mathrm{A_s^m}$ ($\mathrm{m} \in \{-1, -2, \ldots\}$), $\tilde{n}$ and $\frac{1}{\tilde{n}} \frac{\partial \tilde{n}}{\partial x}$ are replaced with $1/\tilde{p}$ and $-\frac{1}{\tilde{p}} \frac{\partial \tilde{p}}{\partial x}$, respectively, and substituted by expressions similar to Eqs. (1.110) and (1.111).

Native-Defect Controlled Dopant Diffusion via the Dissociative Mechanism

The native-defect controlled mode of dopant diffusion holds for $D^*_{\mathrm{A_i^q}} \gg D^*_{V^\mathrm{k}}$. The higher transport capacity $C^{\mathrm{eq}}_{\mathrm{A_i^q}} D_{\mathrm{A_i^q}}$ compared to $C^{\mathrm{eq}}_{V^\mathrm{k}} D_{V^\mathrm{k}}$ leads to $\widetilde{C}_{\mathrm{A_i^q}} \approx 1$ after sufficiently long times. Under this condition we can neglect Eq. (1.128). Taking the sum of Eqs. (1.127) and (1.129) and assuming that the diffusion of $\mathrm{A_s^m}$ via direct exchange is small compared to the indirect diffusion of $\mathrm{A_s^m}$ via $\mathrm{A_i^q}$ and that $C^{\mathrm{eq}}_{V^\mathrm{k}} \ll C^{\mathrm{eq}}_{\mathrm{A_s^m}}$ is fulfilled, we obtain

$$\frac{\partial \widetilde{C}_{\mathrm{A_s^m}}}{\partial t} \approx \frac{\partial}{\partial x} \left(D^*_{V^\mathrm{k}} \frac{\partial \widetilde{C}_{V^\mathrm{k}}}{\partial x} + \mathrm{k} \frac{\widetilde{C}_{V^\mathrm{k}} D^*_{V^\mathrm{k}}}{\tilde{n}(x)} \frac{\partial \tilde{n}(x)}{\partial x} \right). \tag{1.130}$$

Considering local equilibrium of reaction (1.125) and $\mathrm{A_i^q} + \mathrm{q}e^- \rightleftharpoons \mathrm{A_i^0}$,

$$\frac{\widetilde{C}_{\mathrm{A_s^m}}}{\widetilde{C}_{\mathrm{A_i^q}} \widetilde{C}_{V^\mathrm{k}} \ \tilde{n}^{(\mathrm{q+k-m})}} = 1 \tag{1.131}$$

$$\frac{\widetilde{C}_{\mathrm{A_i^0}}}{\widetilde{C}_{\mathrm{A_i^q}} \ \tilde{n}^{\mathrm{q}}} = 1, \tag{1.132}$$

we obtain

$$\widetilde{C}_{V^\mathrm{k}} \approx \widetilde{C}_{\mathrm{A_s^m}} \ \tilde{n}^{(\mathrm{m-k})}. \tag{1.133}$$

For donors $\mathrm{A_s^m}$ ($\mathrm{m} \in \{+1, +2, \ldots\}$) with $\tilde{n}(x) \approx \widetilde{C}_{\mathrm{A_s^m}}$, Eq. (1.130) transforms to Eq. (1.117) with

$$D^{\mathrm{eff}}_{\mathrm{A_s^m}} = (\mathrm{m}+1) D^*_{V^\mathrm{k}} (\widetilde{C}_{\mathrm{A_s^m}})^{-\mathrm{k}}. \tag{1.134}$$

For acceptors $\mathrm{A_s^m}$ ($\mathrm{m} \in \{-1, -2, \ldots\}$) with $\tilde{p} \approx \widetilde{C}_{\mathrm{A_s^m}}$, Eq. (1.117) with

$$D^{\mathrm{eff}}_{\mathrm{A_s^m}} = (-\mathrm{m}+1) D^*_{V^\mathrm{k}} (\widetilde{C}_{\mathrm{A_s^m}})^{-\mathrm{m}+\mathrm{k}} \tag{1.135}$$

is obtained.

Foreign-Atom Controlled Dopant Diffusion via the Dissociative Mechanism

The foreign-atom controlled mode of dopant diffusion via the dissociative mechanism is established in the case when $D^*_{\mathrm{A_i^q}} \ll D^*_{V^\mathrm{k}}$ holds. Considering sufficiently long times, thermal equilibrium of V^k is established, i.e., $\widetilde{C}_{V^\mathrm{k}} \approx 1$. Thus we can neglect Eq. (1.129). Taking the sum of Eqs. (1.127) and (1.128) and assuming $C^{\mathrm{eq}}_{\mathrm{A_i^q}} \ll C^{\mathrm{eq}}_{\mathrm{A_s^m}}$ and $D_{\mathrm{A_s^m}} (= D^{\mathrm{ex}}_{\mathrm{A_s^m}}) \approx 0$, we obtain

$$\frac{\partial \widetilde{C}_{\mathrm{A_s^m}}}{\partial t} \approx \frac{\partial}{\partial x}\left(D^*_{\mathrm{A_i^q}} \frac{\partial \widetilde{C}_{\mathrm{A_i^q}}}{\partial x} + \mathrm{q} \frac{\widetilde{C}_{\mathrm{A_i^q}} D^*_{\mathrm{A_i^q}}}{\tilde{n}(x)} \frac{\partial \tilde{n}(x)}{\partial x} \right). \tag{1.136}$$

With

$$\widetilde{C}_{\mathrm{A_i^q}} \approx \widetilde{C}_{\mathrm{A_s^m}}\, \tilde{n}^{\,(\mathrm{m-q})} \tag{1.137}$$

which results from Eqs. (1.121) and (1.131), Eq. (1.136) reduces to Eq. (1.117) with

$$D^{\mathrm{eff}}_{\mathrm{A_s^m}} = (\mathrm{m}+1) D^*_{\mathrm{A_i^q}} (\widetilde{C}_{\mathrm{A_s^m}})^{\mathrm{m-q}}\,. \tag{1.138}$$

This effective diffusivity holds for donors $\mathrm{A_s^m}$ ($\mathrm{m} \in \{+1, +2, \ldots\}$) with $\tilde{n}(x) \approx \widetilde{C}_{\mathrm{A_s^m}}$.

For acceptors $\mathrm{A_s^m}$ ($\mathrm{m} \in \{-1, -2, \ldots\}$) with $\tilde{p} \approx \widetilde{C}_{\mathrm{A_s^m}}$, $D^{\mathrm{eff}}_{\mathrm{A_s^m}}$ in Eq. (1.117) is given by

$$D^{\mathrm{eff}}_{v\mathrm{A_s^m}} = (-\mathrm{m}+1) D^*_{\mathrm{A_i^q}} (\widetilde{C}_{\mathrm{A_s^m}})^{-\mathrm{m+q}}. \tag{1.139}$$

Characteristics of Dopant Diffusion in Semiconductors

The effective diffusion coefficients $D^{\mathrm{eff}}_{\mathrm{A_s^m}}$ for the vacancy (dissociative) mechanism in the native-defect controlled mode given by Eqs. (1.118) and (1.119) (Eqs. (1.134) and (1.135)) reveal that dopant diffusion is affected by the charge states m and k of $\mathrm{A_s^m}$ and V^k. On the other hand, within the foreign-atom controlled mode of dopant diffusion via the vacancy mechanism (dissociative mechanism) $D^{\mathrm{eff}}_{\mathrm{A_s^m}}$ is determined by the charge states m and j (q) of $\mathrm{A_s^m}$ and $\mathrm{A}V^\mathrm{j}$ ($\mathrm{A_i^q}$) (see Eqs. (1.123) and (1.124) (Eqs. (1.138) and (1.139))). Generally, the foreign-atom controlled mode of dopant diffusion via reactions (1.80), (1.81), (1.82) and reactions (1.85) and (1.86) is *not* sensitive to the charge states of the native point defects. The equations derived for $D^{\mathrm{eff}}_{\mathrm{A_s^m}}$ in the native-defect and foreign-atom controlled diffusion mode confirm expressions for the effective dopant diffusion coefficient given by Gösele [115].

Table 1.2 Effective diffusion coefficients $D^{\mathrm{eff}}_{\mathrm{A^m_s}}$ of the substitutional foreign-atoms $\mathrm{A^m_s}$ obtained on the basis of the vacancy mechanism (1.80) for (a) the native-defect controlled mode (see Eqs. (1.118) and (1.119)) and (b) the foreign-atom controlled mode (see Eqs. (1.123) and (1.124)) of dopant diffusion. The concentration dependence of $D^{\mathrm{eff}}_{\mathrm{A^m_s}}$ determines the shape of the dopant profile. Typical diffusion profiles of an element A are shown in Fig. 1.14

Vacancy mechanism: $\mathrm{A}V^{\mathrm{j}} + (\mathrm{j}-\mathrm{m}-\mathrm{k})e^- \rightleftharpoons \mathrm{A^m_s} + V^{\mathrm{k}}$		
With m =1+(donor)		
Reaction	(a) $D^{\mathrm{eff}}_{\mathrm{A^m_s}}$	(b) $D^{\mathrm{eff}}_{\mathrm{A^m_s}}$
$\mathrm{A}V^0 + e^- \rightleftharpoons \mathrm{A^+_s} + V^{2-}$	$2\,D^*_{V^{2-}}\,(\widetilde{C}_{\mathrm{A^+_s}})^{-1}$	$2\,D^*_{\mathrm{A}V^0}\,(\widetilde{C}_{\mathrm{A^+_s}})^{1}$
$\mathrm{A}V^0 \rightleftharpoons \mathrm{A^+_s} + V^{1-}$	$2\,D^*_{V^-}\,(\widetilde{C}_{\mathrm{A^+_s}})^{-2}$	$2\,D^*_{\mathrm{A}V^0}\,(\widetilde{C}_{\mathrm{A^+_s}})^{1}$
$\mathrm{A}V^0 - e^- \rightleftharpoons \mathrm{A^+_s} + V^0$	$2\,D^*_{V^0}\,(\widetilde{C}_{\mathrm{A^+_s}})^{-3}$	$2\,D^*_{\mathrm{A}V^0}\,(\widetilde{C}_{\mathrm{A^+_s}})^{1}$
$\mathrm{A}V^- \rightleftharpoons \mathrm{A^+_s} + V^{2-}$	$2\,D^*_{V^{2-}}\,(\widetilde{C}_{\mathrm{A^+_s}})^{-1}$	$2\,D^*_{\mathrm{A}V^-}\,(\widetilde{C}_{\mathrm{A^+_s}})^{2}$
$\mathrm{A}V^- - e^- \rightleftharpoons \mathrm{A^+_s} + V^-$	$2\,D^*_{V^-}\,(\widetilde{C}_{\mathrm{A^+_s}})^{-2}$	$2\,D^*_{\mathrm{A}V^-}\,(\widetilde{C}_{\mathrm{A^+_s}})^{2}$
$\mathrm{A}V^- - 2e^- \rightleftharpoons \mathrm{A^+_s} + V^0$	$2\,D^*_{V^0}\,(\widetilde{C}_{\mathrm{A^+_s}})^{-3}$	$2\,D^*_{\mathrm{A}V^-}\,(\widetilde{C}_{\mathrm{A^+_s}})^{2}$
With m =1−(acceptor)		
Reaction	(a) $D^{\mathrm{eff}}_{\mathrm{A^m_s}}$	(b) $D^{\mathrm{eff}}_{\mathrm{A^m_s}}$
$\mathrm{A}V^0 + e^- \rightleftharpoons \mathrm{A^-_s} + V^0$	$2\,D^*_{V^0}\,(\widetilde{C}_{\mathrm{A^-_s}})^{-3}$	$2\,D^*_{\mathrm{A}V^0}\,(\widetilde{C}_{\mathrm{A^-_s}})^{1}$
$\mathrm{A}V^0 \rightleftharpoons \mathrm{A^-_s} + V^+$	$2\,D^*_{V^+}\,(\widetilde{C}_{\mathrm{A^-_s}})^{-2}$	$2\,D^*_{\mathrm{A}V^0}\,(\widetilde{C}_{\mathrm{A^-_s}})^{1}$
$\mathrm{A}V^0 - e^- \rightleftharpoons \mathrm{A^-_s} + V^{2+}$	$2\,D^*_{V^{2+}}\,(\widetilde{C}_{\mathrm{A^-_s}})^{-1}$	$2\,D^*_{\mathrm{A}V^0}\,(\widetilde{C}_{\mathrm{A^-_s}})^{1}$
$\mathrm{A}V^+ + 2e^- \rightleftharpoons \mathrm{A^-_s} + V^0$	$2\,D^*_{V^0}\,(\widetilde{C}_{\mathrm{A^-_s}})^{-3}$	$2\,D^*_{\mathrm{A}V^+}\,(\widetilde{C}_{\mathrm{A^-_s}})^{2}$
$\mathrm{A}V^+ + e^- \rightleftharpoons \mathrm{A^-_s} + V^+$	$2\,D^*_{V^+}\,(\widetilde{C}_{\mathrm{A^-_s}})^{-2}$	$2\,D^*_{\mathrm{A}V^+}\,(\widetilde{C}_{\mathrm{A^-_s}})^{2}$
$\mathrm{A}V^+ \rightleftharpoons \mathrm{A^-_s} + V^{2+}$	$2\,D^*_{V^{2+}}\,(\widetilde{C}_{\mathrm{A^-_s}})^{-1}$	$2\,D^*_{\mathrm{A}V^+}\,(\widetilde{C}_{\mathrm{A^-_s}})^{2}$

Tables 1.2 and 1.3 summarize the concentration dependence of $D^{\mathrm{eff}}_{\mathrm{A^m_s}}$ for the vacancy mechanism and dissociative mechanism, respectively, taking into account charge states of point defects, that are relevant for dopant diffusion in semiconductors. The charge state m of $\mathrm{A^m_s}$ was chosen 1+ (1−) because singly ionized donors (acceptors) are commonly used for high n-type (p-type) doping of both elemental and compound semiconductors. It is emphasized that the concentration dependence of $D^{\mathrm{eff}}_{\mathrm{A^m_s}}$ deduced for the vacancy mechanism also holds for the interstitialcy (kick-out) mechanism given by reaction (1.81) (reaction (1.83)). $D^{\mathrm{eff}}_{\mathrm{A^m_s}}$ for the interstitialcy (kick-out) mechanism is given by Table 1.2 when AV is changed to AI ($\mathrm{A_i}$) and V is changed to I whereas the charge states of the defects are kept unchanged. On the other hand $D^{\mathrm{eff}}_{\mathrm{A^m_s}}$ deduced for the dissociative mechanism and given in Table 1.3 also reflects $D^{\mathrm{eff}}_{\mathrm{A^m_s}}$ of the dopant-defect pair assisted recombination mechanisms (1.85) and (1.86). This shows that Tables 1.2 and 1.3 are generally applicable to predict the concentration dependence of $D^{\mathrm{eff}}_{\mathrm{A^m_s}}$ for dopant diffusion via one of the mechanisms given by reactions (1.80), (1.81), (1.82), and (1.83) and reactions (1.85) and (1.86).

Table 1.2 reveals that $D^{\mathrm{eff}}_{\mathrm{A^m_s}}$ is proportional to $(C_{\mathrm{A^m_s}})^{\mathrm{r}}$ with $\mathrm{r} \in \{-1, -2, -3\}$ for the native-defect controlled mode of dopant diffusion via the vacancy mechanism. This power dependence is a consequence of the charge states of V^{k} under high n-type or p-type doping. Diffusion profiles of an element A with concentration dependent

Table 1.3 Effective diffusion coefficients $D^{\text{eff}}_{A_s^m}$ of the substitutional foreign-atoms A_s^m obtained on the basis of the dissociative mechanism (1.82) for (a) the native-defect controlled mode (see Eqs. 1.134 and 1.135) and (b) the foreign-atom controlled mode (see Eqs. 1.138 and 1.139) of dopant diffusion. The concentration dependence of $D^{\text{eff}}_{A_s^m}$ determines the shape of the dopant diffusion profile. Typical diffusion profiles of an element A are shown in Fig. 1.14

Dissociative mechanism: $A_i^q + V^k + (q+k-m)e^- \rightleftharpoons A_s^m$		
With m = 1+(donor)		
Reaction	(a) $D^{\text{eff}}_{A_s^m}$	(b) $D^{\text{eff}}_{A_s^m}$
$A_i^0 + V^{2-} - 3e^- \rightleftharpoons A_s^+$	$2\,D^*_{V^{2-}}\,(\widetilde{C}_{A_s^+})^3$	$2\,D^*_{A_i^0}\,(\widetilde{C}_{A_s^+})^1$
$A_i^0 + V^- - 2e^- \rightleftharpoons A_s^+$	$2\,D^*_{V^-}\,(\widetilde{C}_{A_s^+})^2$	$2\,D^*_{A_i^0}\,(\widetilde{C}_{A_s^+})^1$
$A_i^0 + V^0 - e^- \rightleftharpoons A_s^+$	$2\,D^*_{V^0}\,(\widetilde{C}_{A_s^+})^1$	$2\,D^*_{A_i^0}\,(\widetilde{C}_{A_s^+})^1$
$A_i^- + V^{2-} - 4e^- \rightleftharpoons A_s^+$	$2\,D^*_{V^{2-}}\,(\widetilde{C}_{A_s^+})^3$	$2\,D^*_{A_i^-}\,(\widetilde{C}_{A_s^+})^2$
$A_i^- + V^- - 3e^- \rightleftharpoons A_s^+$	$2\,D^*_{V^-}\,(\widetilde{C}_{A_s^+})^2$	$2\,D^*_{A_i^-}\,(\widetilde{C}_{A_s^+})^2$
$A_i^- + V^0 - 2e^- \rightleftharpoons A_s^+$	$2\,D^*_{V^0}\,(\widetilde{C}_{A_s^+})^1$	$2\,D^*_{A_i^-}\,(\widetilde{C}_{A_s^+})^2$
With m = 1−(acceptor)		
Reaction	(a) $D^{\text{eff}}_{A_s^m}$	(b) $D^{\text{eff}}_{A_s^m}$
$A_i^0 + V^0 + e^- \rightleftharpoons A_s^-$	$2\,D^*_{V^0}\,(\widetilde{C}_{A_s^-})^1$	$2\,D^*_{A_i^0}\,(\widetilde{C}_{A_s^-})^1$
$A_i^0 + V^+ + 2e^- \rightleftharpoons A_s^-$	$2\,D^*_{V^+}\,(\widetilde{C}_{A_s^-})^2$	$2\,D^*_{A_i^0}\,(\widetilde{C}_{A_s^-})^1$
$A_i^0 + V^{2+} + 3e^- \rightleftharpoons A_s^-$	$2\,D^*_{V^{2+}}\,(\widetilde{C}_{A_s^-})^3$	$2\,D^*_{A_i^0}\,(\widetilde{C}_{A_s^-})^1$
$A_i^+ + V^0 + 2e^- \rightleftharpoons A_s^-$	$2\,D^*_{V^0}\,(\widetilde{C}_{A_s^-})^1$	$2\,D^*_{A_i^+}\,(\widetilde{C}_{A_s^-})^2$
$A_i^+ + V^+ + 3e^- \rightleftharpoons A_s^-$	$2\,D^*_{V^+}\,(\widetilde{C}_{A_s^-})^2$	$2\,D^*_{A_i^+}\,(\widetilde{C}_{A_s^-})^2$
$A_i^+ + V^{2+} + 4e^- \rightleftharpoons A_s^-$	$2\,D^*_{V^{2+}}\,(\widetilde{C}_{A_s^-})^3$	$2\,D^*_{A_i^+}\,(\widetilde{C}_{A_s^-})^2$

diffusion coefficients D_A proportional to $(C_A)^r$ with $r \in \{-2, 0, 1, 2\}$ are illustrated in Fig. 1.14. For $r < 0$ the shape of the dopant profile is concave. On the other hand, convex dopant profiles result in case of foreign-atom controlled mode of dopant diffusion via the vacancy mechanism, i.e., $D^{\text{eff}}_{A_s^m}$ is proportional to $(C_{A_s^m})^r$ with $r \in \{1, 2\}$. This power dependence is a consequence of the charge states of A_s^m and AV^j.

In contrast to the vacancy mechanism, the dissociative mechanism predicts box-shaped diffusion profiles for singly ionized donors (acceptors) both for the native defect and foreign-atom controlled diffusion mode in the case that neutral and negatively (positively) charged vacancies are favored under n-type (p-type) conditions (see Table 1.3). More specifically, $D^{\text{eff}}_{A_s^m}$ is proportional to $(C_{A_s^m})^r$ with $r \in \{1, 2, 3\}$ in the case when V^k with $k \in \{0, 1-, 2-\}$ ($k \in \{0, 1+, 2+\}$) mediates donor (acceptor) diffusion. In the foreign-atom controlled mode $D^{\text{eff}}_{A_s^m}$ is also proportional to $(C_{A_s^m})^r$ with $r \in \{1+, 2+\}$ when A_i^q is neutral and singly ionized, respectively. The power dependence results from the difference in the charge states between A_s^m and A_i^q, in the same way as for the vacancy mechanism.

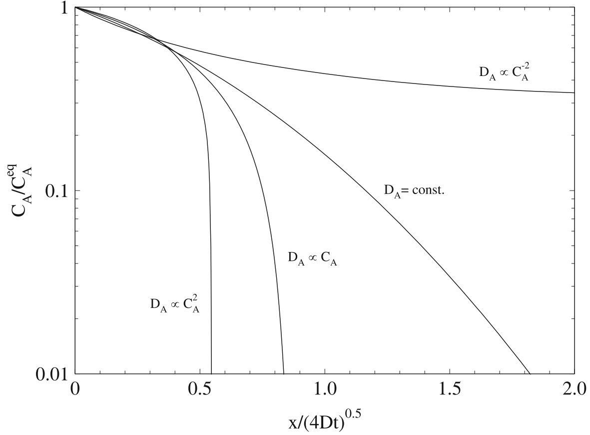

Fig. 1.14 Concentration profiles of an element A normalized by its equilibrium concentration $C_{\mathrm{A}}^{\mathrm{eq}}$ versus the normalized penetration depth $x/\sqrt{4D_{\mathrm{A}}t}$. The profiles represent solutions of Eq. (1.112) with $G_{\mathrm{X}} = 0$ and $X = \mathrm{A}$ for different concentration dependent diffusion coefficients D_{A} as indicated

This demonstrates that the shape of dopant profile alone can not tell which diffusion mode is operative.

Nonetheless, the scheme of the concentration dependence of $D_{\mathrm{A_s^m}}^{\mathrm{eff}}$ given by Tables 1.2 and 1.3 is very helpful for the understanding of dopant profiles in Si, Ge and its alloys. Moreover, the scheme also holds for dopant diffusion in compound semiconductors such as SiC, GaAs, GaSb, ... assuming the diffusion process is restricted to one sublattice (see e.g. [116–125] and references therein). Also charge states of point defects other than those considered in Tables 1.2 and 1.3 may become important. Then the corresponding concentration dependence of $D_{\mathrm{A_s^m}}^{\mathrm{eff}}$ is given by Eqs. (1.118), (1.119), (1.134) and (1.135) for the native-defect controlled mode and by Eqs. (1.123), (1.124), (1.138), and (1.139) for the foreign-atom controlled diffusion mode.

In order to identify the mechanisms of diffusion, a direct comparison of experimental profiles with numerical solutions of the full partial differential equation system that represent the assumed diffusion model and a comparison of the reduced diffusion coefficients D_{X}^{*} with self-diffusion data is required. Generally, several mechanisms can contribute to the diffusion coefficient D_{A} of a mainly substitutionally dissolved element A. We expect

$$D_{\mathrm{A}} = D_{\mathrm{A}}^{(1)} + D_{\mathrm{A}}^{(2)} + D_{\mathrm{A}}^{(3)} + \ldots \tag{1.140}$$

where the number in the exponent represents contributions due to various indirect diffusion mechanisms. Each diffusion coefficient can be a complicated function of the concentration and diffusion coefficient of the defects involved in the particular reaction (see above). Equation (1.140) shows that it can be difficult to identify the diffusion mechanisms when several mechanisms contribute simultaneously.

As example we consider the diffusion of an element A under isoconcentration condition. Under this condition the diffusion is not affected by internal electric fields and/or chemical concentration gradients and thus always proceeds in thermal

equilibrium, that is, the concentrations of V and I are in thermal equilibrium. Accordingly, diffusion under isoconcentration conditions represents the foreign-atom controlled mode. Assuming $\mathrm{A_i^q}$, $\mathrm{A}V^{\mathrm{j}}$, and $\mathrm{A}I^{\mathrm{v}}$ of reactions (1.80), (1.81), (1.82), and (1.83) as the possible mobile defects, D_A for isoconcentration conditions is

$$D_\mathrm{A} = \frac{C^\mathrm{eq}_{\mathrm{A_i^q}} D_{\mathrm{A_i^q}}}{C^\mathrm{eq}_{\mathrm{A_s^m}} + C^\mathrm{eq}_{\mathrm{A_i^q}}} + \frac{C^\mathrm{eq}_{\mathrm{A}V^\mathrm{j}} D_{\mathrm{A}V^\mathrm{j}}}{C^\mathrm{eq}_{\mathrm{A_s^m}} + C^\mathrm{eq}_{\mathrm{A}V^\mathrm{j}}} + \frac{C^\mathrm{eq}_{\mathrm{A}I^\mathrm{v}} D_{\mathrm{A}I^\mathrm{v}}}{C^\mathrm{eq}_{\mathrm{A_s^m}} + C^\mathrm{eq}_{\mathrm{A}I^\mathrm{v}}}. \tag{1.141}$$

This follows from the differential equation system of the underlying reactions for the foreign-atom controlled diffusion mode (see e.g. Sects. 1.6.1.2 or 1.6.1.3). In the case when A is mainly dissolved on interstitial sites, i.e., $C^\mathrm{eq}_{\mathrm{A_i^q}} \gg C^\mathrm{eq}_{\mathrm{A_s^m}}, C^\mathrm{eq}_{\mathrm{A}V^\mathrm{j}}, C^\mathrm{eq}_{\mathrm{A}I^\mathrm{v}}$, and $D_{\mathrm{A_i^q}} \gg D_{\mathrm{A}V^\mathrm{j}}, D_{\mathrm{A}I^\mathrm{v}}$, we get $D_\mathrm{A} \approx D_{\mathrm{A_i^q}}$ as expected for the diffusion via the direct interstitial mechanism. For a mainly substitutionally dissolved element ($C^\mathrm{eq}_{\mathrm{A_s^m}} \gg C^\mathrm{eq}_{\mathrm{A_i^q}}, C^\mathrm{eq}_{\mathrm{A}V^\mathrm{j}}, C^\mathrm{eq}_{\mathrm{A}I^\mathrm{v}}$) the diffusivity D_A is given by the sum of the reduced diffusion coefficients $D^*_\mathrm{X} = C^\mathrm{eq}_\mathrm{X} D_\mathrm{X} / C^\mathrm{eq}_{\mathrm{A_s^m}}$ with $\mathrm{X} \in \{\mathrm{A_i^q}, \mathrm{A}V^\mathrm{j}, \mathrm{A}I^\mathrm{v}\}$.

Equation (1.141) also describes the diffusion of hybrid elements in dislocation-free crystals under isoconcentration conditions [119]. In this case the first term on the right hand side of Eq. (1.141) dominates. In order to identify the mechanisms of diffusion of an element A, complementary diffusion experiments under different experimental condition have to be performed [126]. In this respect also studies on the impact of self-interstitial and vacancy perturbations on self- and dopant diffusion are advantageous. Such experiments were extensively performed with Si (see references in [49]). Oxidation (nitridation) of a bare Si surface is known to inject self-interstitials (vacancies). The results considerably contributed to our present understanding of dopant diffusion in Si (see e.g. [127–136]).

The availability of highly enriched stable isotopes of Si and Ge combined with modern epitaxial deposition techniques such as chemical vapor deposition and molecular beam epitaxy enabled the preparation of isotopically controlled semiconductor layer structures. By means of such isotopically controlled heterostructures not only self-diffusion experiments in Si and Ge could be performed over a wide range of temperatures but also the impact of dopant diffusion on self-diffusion could be investigated directly [137–141]. Modeling of the simultaneous self- and dopant diffusion is a bit more complex than modeling of the separate processes but is a worthwhile effort because more information about the underlying mechanisms and properties of the point defects is obtained than from self- and dopant diffusion experiments studied separately [64, 75].

In the following section typical experimental diffusion profiles of hybrid and dopant atoms in Si are presented that provide strong evidence for different indirect diffusion mechanisms in Si.

1.7 Experimental Diffusion Profiles

Experimental diffusion profiles of Zn in Si [41] are presented in the following as an example on the diffusion behavior of hybrid atoms in Si. Similar profiles are observed for Au [83–86] and Pt [95, 96, 98–100]. In addition to Zn profiles in dislocation-free and highly dislocated Si, also experimental profiles are illustrated that reveal the impact of a reduced Zn vapor pressure on Zn diffusion and the time evolution of Zn diffusion. The Zn diffusion behavior under the different experimental conditions is consistently described on the basis of the kick-out mechanism constituting crucial evidence that Zn in Si mainly diffuses via the kick-out mechanism [41, 94].

As an example on the diffusion behavior of dopants in Si experimental profiles obtained after dopant diffusion in isotopically controlled Si heterostructures are shown [64, 137–139]. These concurrent self- and dopant diffusion experiments reveal the impact of both point-defect reactions and doping on self- and dopant diffusion. Such diffusion studies are very valuable to determine the charge states of the point defects involved in the diffusion process [76].

1.7.1 Diffusion Profiles of Hybrid Atoms

Diffusion of hybrid elements in defect-free and highly dislocated crystals provide the effective diffusion coefficients $D^{\mathrm{eff}}_{V,I}$ and $D^{\mathrm{eff}}_{\mathrm{A}_i}$, respectively, that strongly differ from each other. An impact of the defect structure on the diffusion of hybrid elements via the dissociative and kick-out mechanism is only expected when the relation $C^{\mathrm{eq}}_{\mathrm{A}_i} D_{\mathrm{A}_i} \gg C^{\mathrm{eq}}_{\mathrm{V,I}} D_{\mathrm{V,I}}$ is fulfilled. This condition implies that the transformation of A_i to A_s via reaction (1.26) and (1.27) is controlled by the diffusion of either V, I or A_i. In the case when $C^{\mathrm{eq}}_{\mathrm{A}_i} D_{\mathrm{A}_i} \ll C^{\mathrm{eq}}_{\mathrm{V,I}} D_{\mathrm{V,I}}$ holds, the A_i-A_s transformation is controlled by the diffusion of A_i. Accordingly, the property of dislocations acting as source and sink of native defects will not affect the diffusion of hybrid elements. However, the presence of dislocations can procure additional defect reactions such as trapping of hybrid atoms at dislocations that alters their diffusion behavior [94, 142, 143]. Experiments on the diffusion of Ag and Au in Ge reveal that their diffusion is independent of the defect density, i.e., equal diffusion data are obtained from profiles in dislocation-free and highly dislocated Ge [81]. Even for Zn diffusion in Si experimental conditions can be realized that provide similar diffusion profiles in dislocation-free and highly dislocated Si. Figure 1.15 illustrates $\mathrm{Zn_s}$ concentration profiles $C_{\mathrm{Zn_s}}(x)$ resulting from spreading-resistance (SR) measurements on dislocation-free (profile (+)) and highly dislocated Si samples (profile (×)) that were simultaneously diffused with Zn at 1115 °C for 2880 s [41].

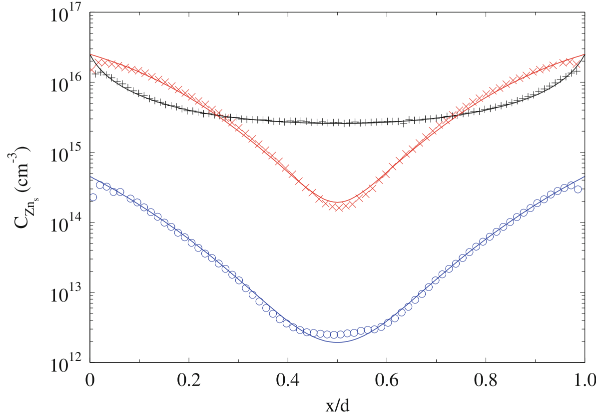

Fig. 1.15 Concentration profiles of substitutional Zn resulting from spreading resistance measurements performed on dislocation-free (+) and highly dislocated (×) Si samples after zinc diffusion at 1115 °C for 2880 s using elemental Zn as diffusion source. Profile (◯) indicates a Zn_s profile in dislocation-free Si measured after Zn diffusion at 1115 °C for 1620 s using $ZnCl_2$ as diffusion source. *Solid lines*: theoretical kick-out profiles simultaneously fitted to the data by optimizing the two essential model parameters $D^*_{Zn_i} = C^{eq}_{Zn_i} D_{Zn_i} / C^{eq}_{Zn_s}$ and $D^*_I = C^{eq}_I D_I / C^{eq}_{Zn_s}$ [41]

The boundary concentration of about $C_{Zn_s}(x = 0) = 2.5 \times 10^{16}\,cm^{-3}$ established at this temperature with a pure Zn source equals the Zn solubility [41, 93]. Also shown in Fig. 1.15 is a Zn_s concentration profile in dislocation-free Si obtained after 1620 s of Zn diffusion at 1115 °C using $ZnCl_2$ as diffusion source (profile: (◯)) [41]. This source yields $C_{Zn_s}(x = 0) = 4.5 \times 10^{14}\,cm^{-3}$ which is a factor 55 smaller than the solubility limit at 1115 °C attained in equilibrium with the elemental vapor source. The shape of the profiles in Fig. 1.15 reveals that the profile (+) in dislocation-free Si is convex whereas the profile (×) in the simultaneously diffused highly dislocated Si is concave. Also the lower profile (◯) has a concave curvature. Obviously, in dislocation-free Si the profile shape changes from convex to concave when the thermodynamic activity of the Zn source is lowered. This shows that the diffusion of Zn in Si is not only sensitive to the defect structure but also to the prevailing Zn vapor pressure (see Sect. 1.6.1.5 and Fig. 1.11). These results together with the time evolution of Zn diffusion in dislocation-free Si which is illustrated by the profiles in Fig. 1.16 provide strong evidence that Zn in Si mainly diffuses via the kick-out mechanism. Only this mechanism yields a consistent description of all profiles in Figs. 1.15 and 1.16 as illustrated by the solid lines [41]. The profiles of Zn_i and I corresponding to the calculated Zn_s profiles of Fig. 1.16 are shown in Figs. 1.17 and 1.18, respectively.

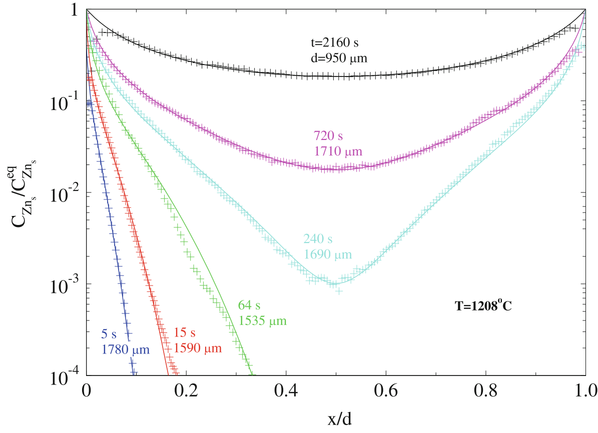

Fig. 1.16 Concentration profiles of substitutional Zn_s measured by means of the spreading resistance technique after Zn diffusion at 1208 °C for times listed in the figure. The penetration depth *x* is normalized to the thickness *d* of the particular sample given in the figure. *Solid lines* show calculated profiles based on the kick-out model with one set of parameters [41]

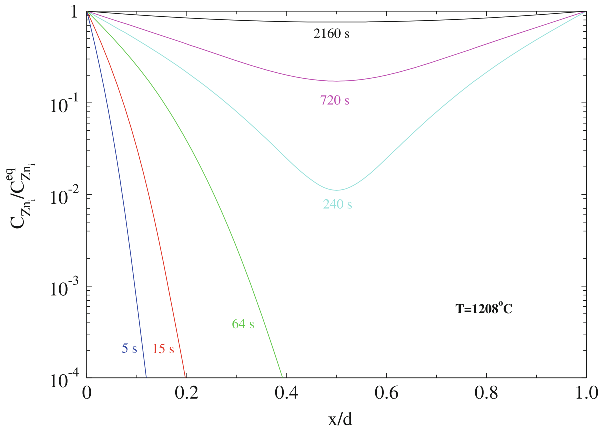

Fig. 1.17 Calculated normalized concentration profiles of interstitial Zn_i corresponding to the calculated Zn_s profiles shown in Fig. 1.16

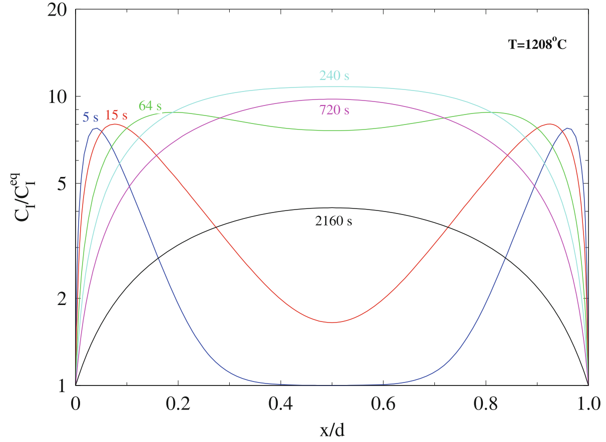

Fig. 1.18 Calculated normalized concentration profiles of self-interstitials *I* corresponding to the calculated Zn_s profiles shown in Fig. 1.16

1.7.2 Diffusion Profiles of Dopant Atoms

Numerous experiments on dopant diffusion in Si were performed over the past decades to determine the atomic mechanisms of diffusion [49]. The studies were motivated by the demand to control the diffusion and activation of dopants in the fabrication of Si-based electronic devices. Dopant diffusion in semiconductors can be rather complex since doping affects the position of the Fermi level and thus the formation of charged defects [114]. Moreover, dopant diffusion can induce native defect concentrations deviating from thermal equilibrium. The impact of the doping level on the shape of dopant profiles in Si is e.g. impressively demonstrated by the P diffusion experiments reported by Yoshida et al. [144, 145]. Most recently performed experiments on dopant diffusion in Si isotope structures not only confirm the concentration dependence of dopant diffusion but also reveal additional insight on the mechanisms of dopant diffusion and on the charge states of the native point defects involved [64, 76].

Concentration profiles of ^{11}B, ^{75}As, and ^{31}P and the corresponding ^{30}Si profiles measured with SIMS after diffusion annealing are illustrated in Fig. 1.19. Figure 1.19a shows the As-implanted Si isotope structure that reflects exemplary also B- and P-implanted isotope structures. The reduced concentration of ^{30}Si within the enriched ^{28}Si layers compared to the adjacent ^{nat}Si layers gives rise to a strong gradient at the ^{nat}Si/^{28}Si interface. Accordingly, the isotopically modulated structure is ideally suited for studying self-diffusion and the impact of dopant diffusion on self-diffusion. The dopant diffuses from the top implanted amorphous Si layer into the isotope structure. All Si profiles obtained after concurrent self- and dopant diffusion reveal a depth-dependent broadening. The concentration profiles of P and Si within the topmost ion-implanted amorphous Si layer are missing in Fig. 1.19d because this layer was removed prior to SIMS profiling (see Ref. [64]). The depth-dependent broadening of the Si isotope structure observed after dopant diffusion is due to charged point defects whose thermal equilibrium concentration depends on

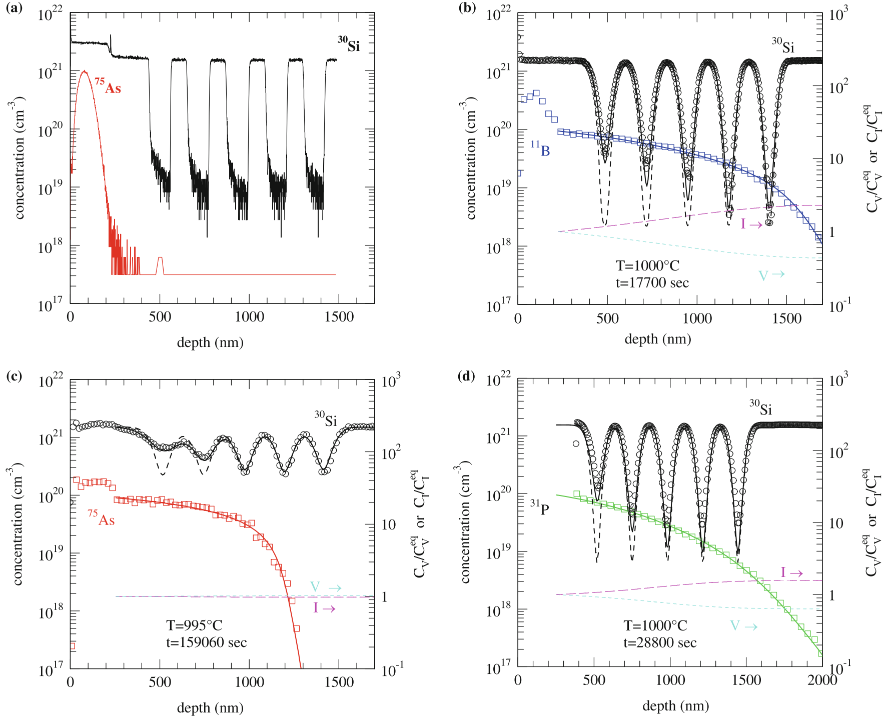

Fig. 1.19 Concentration profiles of ^{30}Si of a ^{nat}Si/^{28}Si isotope multilayer structures with a top amorphous Si layer (about 250 nm *thick*) implanted with either boron (^{11}B), arsenic (^{75}As), and phosphorous (^{31}P) and subsequently annealed at the temperatures and times indicated. The profiles were measured by means of secondary ion mass spectrometry. (**a**): ^{30}Si and ^{75}As profiles of the As-implanted Si isotope multilayer structure. (**b**), (**c**), and (**d**) illustrate, respectively, the ^{11}B, ^{75}As, and ^{31}P diffusion profiles and corresponding self-diffusion profiles. The *solid lines* in (**b**)–(**d**) are best fits to the experimental dopant and self-atom profiles obtained on the basis of indirect diffusion mechanisms [64]. The *lower dashed lines* show the corresponding concentrations $C_{V,I}$ of V (*short-dashed line*) and I (*long-dashed line*) normalized to their thermal equilibrium concentration $C_{V,I}^{eq}$ (see right ordinate). The diffusion of B and P leads to a super- and undersaturation of I and V, respectively, whereas As does not induce any significant deviation from the equilibrium concentration of I and V. The *upper thin dashed lines* in (**b**), (**c**), and (**d**) show ^{30}Si profiles that are expected for self-diffusion under electronic intrinsic and thermal equilibrium conditions. The top amorphous layer of the P-diffused Si isotope structure was removed by chemical-mechanical polishing before SIMS profiling

the position of the Fermi level [76]. As a consequence self-diffusion is altered by doping. Moreover dopant diffusion can lead to concentrations of native point defects that deviate from thermal equilibrium. This, in particular, holds for the native-defect controlled mode of dopant diffusion. These two effects of doping and dopant diffusion on self-diffusion are unraveled by the simultaneous self- and dopant-atom diffusion experiments. These experiments also provide information about possible contributions of AV and AI pairs to self-diffusion. Whether such pairs contribute

significantly to self-diffusion depends on the magnitude of the transport coefficients $C_{AV}^{eq}D_{AV}$ and $C_{AI}^{eq}D_{AI}$ compared to those of the native defects and on the correlation factors for self-diffusion via AV and AI. A comprehensive mathematical treatment of the simultaneous diffusion of self- and dopant atoms and of the impact of the Fermi level on the concentration of charged point defects is given in Refs. [64, 76].

Figure 1.19b shows that the Si profile associated with the in-diffusion of B reveals a faster Si diffusion for high B concentrations close to the amorphous/crystalline interface than at the B diffusion front. Comparison of the Si profile obtained by in-diffusion of B with that expected for electronically intrinsic and thermal equilibrium conditions reveals a higher Si diffusivity under B in-diffusion even at the deepest ^{28}Si/^{nat}Si interface. This points to a supersaturation of native point defects established by B diffusion. Additional results on B diffusion in Si isotope structures obtained at different temperatures, on enhanced (retarded) B diffusion under I (V) injection [129, 132] and of isoconcentration diffusion experiments [133] reveal the charge states of the mobile B-related defect and of the native point defects involved in B diffusion. Altogether, B diffusion in Si under various experimental conditions is consistently described by the following reactions [64]

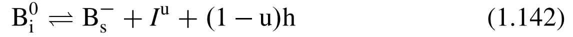

$$B_i^0 \rightleftharpoons B_s^- + I^u + (1-u)h \tag{1.142}$$

$$B_i^0 + V^k \rightleftharpoons B_s^- + (1+k)h \tag{1.143}$$

with neutral (I^0), singly and doubly positively (I^+, I^{2+}) charged self-interstitials and neutral (V^0), singly positive (V^+), and singly and doubly negative (V^-, V^{2-}) vacancies. h denotes a hole to satisfy charge neutrality of the reactions. The dissociative mechanism assures local equilibrium between I and V after sufficient long diffusion times. For a more detailed discussion on B diffusion in Si the interested reader is referred to Refs. [64, 105, 146, 147].

Si profiles obtained by As diffusion (see Fig. 1.19c) show an enhanced Si diffusion within the topmost isotope layers. Here the As doping concentration exceeds the intrinsic carrier concentration. The Si profile at the deepest interface is accurately described with the diffusion coefficient for intrinsic and thermal equilibrium conditions [64]. This and the shape of the As diffusion profiles points to a foreign-atom controlled mode of dopant diffusion. Indeed available experimental results on As diffusion in Si, which comprise As diffusion experiments under native defect injection [68, 132], under isoconcentration conditions [148], and on the simultaneous self- and dopant-atom diffusion [64], are accurately described by the defect reactions

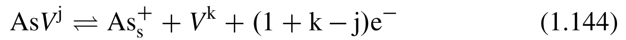

$$AsV^j \rightleftharpoons As_s^+ + V^k + (1+k-j)e^- \tag{1.144}$$

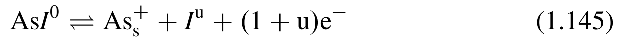

$$AsI^0 \rightleftharpoons As_s^+ + I^u + (1+u)e^- \tag{1.145}$$

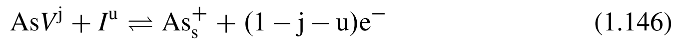

$$AsV^j + I^u \rightleftharpoons As_s^+ + (1-j-u)e^- \tag{1.146}$$

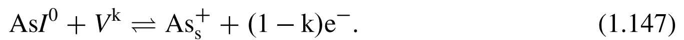

$$AsI^0 + V^k \rightleftharpoons As_s^+ + (1-k)e^-. \tag{1.147}$$

Various charge states for V ($\in \{V^+, V^0, V^-, V^{2-}\}$ and I ($\in \{I^{2+}, I^+, I^0, I^-\}$) were assumed as well as neutral and singly negatively charged dopant-vacancy pairs AsV^0 and AsV^-. The parameters deduced from modeling As diffusion reveal a foreign-atom controlled mode of diffusion, i.e., the equilibrium concentration of V and I is not disturbed by the diffusion of As. This is also demonstrated by the normalized concentration of V and I shown in Fig. 1.19c. A comprehensive discussion on As diffusion in Si is given in Ref. [64].

Self-diffusion profiles associated with the diffusion of P also indicate an enhanced self-atom diffusion at the topmost natural and isotopically enriched layers (see Fig. 1.19d)). On the other hand the diffusion of Si at the deepest ^{28}Si/^{nat}Si interface is described with a diffusion coefficient that is close to the value determined for intrinsic and thermal equilibrium conditions. This was a surprising result because the pronounced tail of P profiles which are clearly at variance with the box-shaped As profiles were generally assumed to be due to a supersaturation of Si self-interstitials [146, 149]. The broadening of the Si profiles demonstrates that the I supersaturation due to P diffusion is significantly lower than expected on the basis of the previous considered P diffusion models. Taking into account additional results on P diffusion in Si obtained under different experimental conditions that comprise diffusion studies under intrinsic and extrinsic doping [150, 151], under defect injection [129, 132, 152], and under isoconcentration conditions [150], the following reactions were determined to accurately describe P diffusion in Si [64]

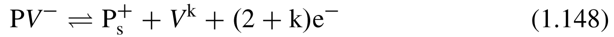

$$\mathrm{P}V^- \rightleftharpoons \mathrm{P}_\mathrm{s}^+ + V^\mathrm{k} + (2+\mathrm{k})\mathrm{e}^- \tag{1.148}$$

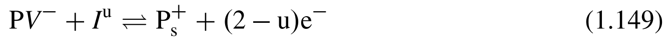

$$\mathrm{P}V^- + I^\mathrm{u} \rightleftharpoons \mathrm{P}_\mathrm{s}^+ + (2-\mathrm{u})\mathrm{e}^- \tag{1.149}$$

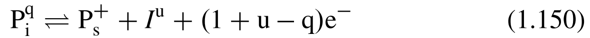

$$\mathrm{P}_\mathrm{i}^\mathrm{q} \rightleftharpoons \mathrm{P}_\mathrm{s}^+ + I^\mathrm{u} + (1+\mathrm{u}-\mathrm{q})\mathrm{e}^- \tag{1.150}$$

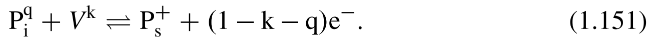

$$\mathrm{P}_\mathrm{i}^\mathrm{q} + V^\mathrm{k} \rightleftharpoons \mathrm{P}_\mathrm{s}^+ + (1-\mathrm{k}-\mathrm{q})\mathrm{e}^-. \tag{1.151}$$

$\mathrm{P}_\mathrm{i}^\mathrm{q}$ exists as neutral and singly positively charged defect. The charge states of V^k and I^u are the same as those considered in reactions (1.142), (1.143), (1.144), (1.145), (1.146), and (1.147) for modeling B and As diffusion.

Successful modeling of the simultaneous P and Si diffusion requires a contribution of singly positively charged mobile P defects to P diffusion. Generally, the extended tail of the P profiles compared to the much steeper As profile at the diffusion front was explained with an I-supersaturation established during P diffusion. Experiments on P diffusion in isotope multilayer structures clearly showed that this interpretation can not be correct. The supersaturation required to explain extended P profiles would predict an enhanced self-diffusion in the tail region that is not observed experimentally. In order to unravel this discrepancy, a mobile P species was proposed whose effective diffusivity is concentration independent. According to Eqs. (1.123) and (1.138), the charge difference between substitutional P_s^+ and the mobile P must be zero. Therefore a singly positively charged interstitial phosphorus defect P_i^+ is considered in reactions (1.150) and (1.151).

1.8 Concluding Remarks

Direct and indirect mechanisms of diffusion in semiconductors are discussed with particular emphasizes on the charge state of the point defects involved. Continuum theoretical calculations of atomic diffusion in semiconductors based on differential equations are presented that offer a robust and fast approach to describe experimental diffusion profiles. With this approach not only the diffusion of hybrid foreign-atoms that occupy both interstitial and substitutional lattice sites but also the impact of doping on self- and foreign-atom diffusion can be treated. Computer simulations reveal the significance of the various model parameters on the shape of foreign-atom profiles. In many cases the diffusion process is mainly determined by the transport coefficients $C_X^{eq} D_X$ of the point defects X involved in the diffusion process. Basically two different diffusion modes, the foreign-atom and native-defect controlled modes, can be distinguished. These modes are characterized by specific relations between the experimentally apparent effective diffusion coefficient of the foreign atom and the native point defect that controls the formation of the substitutional dopant A_s^m. This relation is crucial for the understanding of dopant diffusion in semiconductors.

With the availability of isotopically controlled semiconductor multilayer structures, advanced diffusion studies became possible that provide more detailed insight on the diffusion mechanisms and properties of defects involved than earlier studies [64, 76, 140]. The advantage of isotopically controlled semiconductors for diffusion studies is demonstrated by experiments and simulations of the simultaneous diffusion of self- and foreign-atoms in isotope multilayer structures. These experiments enable to determine the charge states of native point defects and help to distinguish between doping effects, i.e., Fermi level effect, and effects due to defect reactions on self- and dopant diffusion. Together with diffusion studies under various experimental conditions a consistent set of defect reactions are derived that accurately describe the diffusion of the most common dopants boron, phosphorous, and arsenic in Si.

With the availability of high-purity, isotopically enriched Si [153] sophisticated diffusion studies can be performed with well designed layered structures. Moreover, the computing capacity of today's personal computers is sufficient to solve the complex diffusion equations within acceptable times. Although, numerous diffusion studies have been performed with silicon, basic questions concerning the properties of self-interstitials and vacancies are still unsolved [65–67].

Today the continuous down-scaling of CMOS (complementary metal-oxide-semiconductors) devices reached 2D/3D device structures in nanometer size. Associated with this high level of integration is the need to control the dopant distribution and its activation [154]. Further miniaturization is intimately connected with an improved understanding of the properties and interaction of atomic defects. This interaction concerns the interaction of defects in the volume but also the interaction of defects with surfaces and interfaces since the surface/interface-to-volume ratio increases with decreasing size of electronic devices. The properties

of point defects in bulk Si, i.e., their type, mobility, interaction and electronic behavior are well understood to some extent, thanks to the progress achieved in spectroscopic and diffusion studies over the past decades and recently by means of isotopically controlled Si structures (see e.g. [49, 50, 64, 147, 155, 156]). However, the properties of dopants and self-atoms determined for bulk materials are not necessarily applicable to nanoscale Si structures because in small dimensions the thermodynamics and kinetics of point defects can be different from that in the bulk [157, 158]. Surface and interface states can affect the behavior of point defects in the whole nanostructure due to the high surface/interface-to-volume ratio.

Finite size, surface, and interface effects on atomic transport in nanosized semiconductors are technologically of fundamental significance to control and engineer the electronic properties of nanoelectronic devices and to successfully implement novel transistor concepts (see e.g. Ref. [159]). Atomistic calculations are increasingly used to predict defect types, defect interactions, their stability, mobility, and electronic properties. Finally, however, the relevance of these calculations needs to be verified experimentally.

The characterization of atomic defects and their interaction with other point defects, surfaces and interfaces in nanosized materials is very challenging. Not only experiments under well-defined conditions with two (2D) and/or three dimensional (3D) nanostructures must be performed but also appropriate analyses techniques are necessary to resolve nanosized 2D/3D structures and their properties.

References

1. Ammon, W.: Defects in Monocrystalline silicon. In: Kasap, S., Capper, P. (eds.) Springer Handbook of Electronic and Photonic Materials, pp. 101–120. Springer, New York (2007). doi:10.1007/978-0-387-29185-7_5
2. Car, R., Kelly, P.J., Oshiyama, A., Pantelides, S.T.: Microscopic theory of atomic diffusion mechanisms in silicon. Phys. Rev. Lett. **52**, 1814 (1984). doi:10.1103/PhysRevLett.52.1814
3. Bar-Yam, Y., Joannopoulos, J.D.: Barrier to migration of the silicon self-interstitial. Phys. Rev. Lett. **52**, 1129 (1984). doi:10.1103/PhysRevLett.52.1129
4. Blöchl, P.E., Smargiassi, E., Car, R., Laks, D.B., Andreoni, W., Pantelides, S.T.: First-principles calculations of self-diffusion constants in silicon. Phys. Rev. Lett. **70**, 2435 (1993). doi:10.1103/PhysRevLett.70.2435
5. Clark, S.J., Ackland, G.J.: Ab initio calculations of the self-interstitial in silicon. Phys. Rev. B. **56**, 47 (1997). doi:10.1103/PhysRevB.56.47
6. Sadigh, B., Lenosky, Th.J., Theiss, S.K., Caturla, M.-J., de la Rubia, T.D., Foad, M.A.: Mechanism of boron diffusion in silicon: an ab initio and Kinetic Monte Carlo study. Phys. Rev. Lett. **83**, 4341 (1999). doi:10.1103/PhysRevLett.83.4341
7. Leung, W.-K., Needs, R.J., Rajagopal, G., Itoh, S., Ihara, S.: Calculations of silicon self-interstitial defects. Phys. Rev. Lett. **83**, 2351 (1999). doi:10.1103/PhysRevLett.83.2351
8. Windl, W., Bunea, M.M., Stumpf, R., Dunham, S.T., Masquelier, M.P.: First-principles study of boron diffusion in silicon. Phys. Rev. Lett. **83**, 4345 (1999). doi:10.1103/PhysRevLett.83.4345
9. Jeong, J.-W., Oshiyama, A.: Atomic and electronic structures of a Boron impurity and its diffusion pathways in crystalline Si. Phys. Rev. B. **64**, 235204 (2001). doi:10.1103/PhysRevB.64.235204

10. Liu, X.-Y., Windl, W., Beardmore, K.M., Masquelier, M.P.: First-principles study of phosphorus diffusion in silicon: interstitial- and vacancy-mediated diffusion mechanisms. Appl. Phys. Lett. **82**, 1839 (2003). doi:10.1063/1.1562342
11. Al-Mushadani, O.K., Needs, R.J.: Free-energy calculations of intrinsic point defects in silicon. Phys. Rev. B **68**, 235205 (2003). doi:10.1103/PhysRevB.68.235205
12. Lopez, G.M., Fiorentini, V.: Structure, energetics, and extrinsic levels of small self-interstitial clusters in silicon. Phys. Rev. B **69**, 155206 (2004). doi:10.1103/PhysRevB.69.155206
13. El-Mellouhi, F., Mousseau, N., Ordejón, P.: Sampling the diffusion paths of a neutral vacancy in silicon with quantum mechanical calculations. Phys. Rev. B **70**, 205202 (2004). doi:10.1103/PhysRevB.70.205202
14. Jones, R., Briddon, P.R.: The ab initio cluster method and the dynamics of defects in semiconductors. In: Willardson, R.K., Weber, E.R., Stavola, M. (eds.) Identification of Defects in Semiconductors. Semiconductors and Semimetals. Academic Press, San Diego (1998)
15. Coutinho, J.: Density functional modeling of defects and impurities in silicon materials. In: Yoshida, Y., Langouche, G. (eds.) Defects and Impurities in Silicon Materials: An Introduction to Atomic-Level Silicon Engineering. Springer, Tokyo (2016)
16. Song, E.G., Kim, E., Lee, Y.H., Hwang, Y.G.: Fully relaxed point defects in crystalline silicon. Phys. Rev. B **48**, 1486 (1993). doi:10.1103/PhysRevB.48.1486
17. Tang, M., Colombo, L., Zhu, J., de la Rubia, T.D.: Intrinsic point defects in crystalline silicon: tight-binding molecular dynamics studiesof self-diffusion, interstitial-vacancy recombination, and formation volumes. Phys. Rev. B **55**, 14279 (1997). doi:10.1103/PhysRevB.55.14279
18. Alippi, P., Colombo, L., Ruggerone, P., Sieck, A., Seifert, G., Frauenheim, Th.: Atomic-scale characterization of boron diffusion in silicon. Phys. Rev. B **64**, 075207 (2001). doi:10.1103/PhysRevB.64.075207
19. Jääskeläinen, A., Colombo, L., Nieminen, R.: Silicon self-diffusion constants by tight-binding molecular dynamics. Phys. Rev. B **64**, 233203 (2001). doi:10.1103/PhysRevB.64.233203
20. Schober, H.R.: Extended interstitials in silicon and germanium. Phys. Rev. B **39**, 13013(R) (1989). doi:10.1103/PhysRevB.39.13013
21. Maroudas, D., Brown, R.A.: Atomistic calculation of the self-interstitial diffusivity in silicon. Appl. Phys. Lett. **62**, 172 (1993). doi:10.1063/1.109361
22. Maroudas, D., Brown, R.A.: Calculation of thermodynamic and transport properties of intrinsic point defects in silicon. Phys. Rev. B **47**, 15562 (1993). doi:10.1103/PhysRevB.47.15562
23. Posselt, M., Gao, F., Zwicker, D.: Atomistic study of the migration of di- and tri-interstitials in silicon. Phys. Rev. B **71**, 245202 (2005). doi:10.1103/PhysRevB.71.245202
24. Watkins, G.D.: EPR and ENDOR studies of defects in semiconductors. In: Willardson, R.K., Weber, E.R., Stavola, M. (eds.) Identification of Defects in Semiconductors. Semiconductors and Semimetals. Academic Press, San Diego (1998)
25. Spaeth, J.-M.: Magneto-optical and electrical detection of paramagnetic resonance in semiconductors. In: Willardson, R.K., Weber, E.R., Stavola, M. (eds.) Identification of Defects in Semiconductors. Semiconductors and Semimetals. Academic Press, San Diego (1998)
26. Weil, J.A., Bolton, J.R.: Electron Paramagnetic Resonance: Elementary Theory and Practical Applications, 2nd edn. Wiley, Hoboken (2007)
27. Perkowitz, S.: Optical Characterization of Semiconductors: Infrared, Raman, and Photoluminescence Spectroscopy. Elsevier Science, Burlington (2012)
28. Lang, D.V.: Deep-level transient spectroscopy: a new method to characterize traps in semiconductors. J. Appl. Phys. **45**, 3023 (1974). doi:10.1063/1.1663719
29. Wichert, Th., Recknagel, E.: Perturbed angular correlation. In: Microscopic Methods in Metals. Topics in Current Physics, vol. 40, pp. 317–364. Springer, Berlin/Heidelberg (1986). doi:10.1007/978-3-642-46571-0_11
30. Siegel, R.W.: Positron annihilation spectroscopy. Ann. Rev. Mater. Sci. **10**, 393–425 (1980). doi:10.1146/annurev.ms.10.080180.002141

31. Saarinen, K., Hautojärvi, P., Corbel, C.: Positron annihilation spectroscopy of defects in semiconductors. In: Willardson, R.K., Weber, E.R., Stavola, M. (eds.) Identification of Defects in Semiconductors. Semiconductors and Semimetals. Academic Press, San Diego (1998)
32. Krause-Rehberg, R., Leipner, H.S.: Positron Annihilation in Semiconductors: Defect Studies. Springer, Berlin/Heidelberg (1999)
33. Greenwood, N.N., Gibb, T.C.: Mössbauer Spectroscopy. Chapman and Hall, London (1971). doi:10.1007/978-94-009-5697-1
34. Würschum, R., Bauer, W., Maier, K., Seeger, A., Schaefer, H.-E.: Defects in semiconductors after electron irradiation or in high-temperature thermal equilibrium, as studied by positron annihilation. J. Phys.: Condens. Matter **1**, SA33–SA48 (1989). doi:10.1088/0953-8984/1/SA/005
35. Langouche, G., Yoshida, Y.: Nuclear methods to study defects and impurities in Si materials. In: Yoshida, Y., Langouche, G. (eds.) Defects and Impurities in Silicon Materials: An Introduction to Atomic-Level Silicon Engineering. Springer, Tokyo (2016).
36. Ueki, T., Itsumi, M., Takeda, T.: Octahedral void defects observed in the bulk of Czochralski silicon. Appl. Phys. Lett. **70**, 1248 (1997). doi:10.1063/1.118543
37. Nishimura, M., Yamaguchi, Y., Nakamura, K., Jablonski, J., Wantanabe, M.: The role of oxygen impurities in the formation of grown-in laser scattering tomography defects in silicon single crystals. In: Claeys, C.L., Rai-Choudhury, P., Watanabe, M., Stallhofer, P., Dawson, H.J. (eds.) High Purity Silicon V, Proceedings Volume 98-13, pp. 188–199. The Electrochemical Society, Pennington (1998)
38. Abe, T., Kato, Y.: The effects of polishing damage and oxygen concentration on gate oxide integrity in silicon crystals. Jpn. J. Appl. Phys. **32**, 1879–1883 (1993). doi:10.1143/JJAP.32.1879
39. Sugra, H., Abe, H., Koya, H., Yoshimi, T., Suzuki, I., Yoshioka, H., Kagawa, N.: Proceedings of the 2nd Symposium on Physics and Chemistry of SiO_2 and Si-SiO_2 Interfaces, vol. 2, p. 279 (1993)
40. Ammon, W.v., Ehlert, A., Lambert, U., Gräf, D., Brohl, M., Wagner, P.: Gate oxide related bulk properties of oxygen doped floating zone and Czochralski silicon. In: Huff, H.R., Bergholz, W., Sumino, K. (eds.) Semiconductor Silicon/1994: Proceedings of the Seventh International Symposium on Silicon Materials Science and Technology. Electrochemical Society Proceedings vol. 94–10, pp. 136–147, Pennington (1994)
41. Bracht, H., Stolwijk, N.A., Mehrer, H.: Properties of intrinsic point defects in silicon determined by zinc diffusion experiments under nonequilibrium conditions. Phys. Rev. B **52**, 16542–16560 (1995). doi:10.1103/PhysRevB.52.16542
42. Edelin, G., Mathiot, D.: A model for the determination of the defect concentrations in III-V compounds. Philos. Mag. B **42**, 95–110 (1980). doi:10.1080/01418638008225641
43. Tan, T.Y.: Point defect thermal equilibria in GaAs. Mater. Sci. Eng. B **10**, 227–239 (1991). doi:10.1016/0921-5107(91)90130-N
44. Tan, T.Y., You, H.-M., Gösele, U.M.: Thermal equilibrium concentrations and effects of negatively charged Ga vacancies in n-type GaAs. Appl. Phys. A **56**, pp. 249–258 (1993). doi:10.1007/BF00539483
45. More generally, the diffusion flux is proportional to the gradient of the chemical potential (see e.g. [46]). For ideal solid solutions such as doped semiconductors the chemical potential is proportional to the concentration gradient. Accordingly, dopant diffusion in semiconductors is generally described in terms of concentration gradients. On the other hand, in case of e.g. binary diffusion couples the gradient in the chemical potential is considered for the treatment of the interdiffusion process
46. Mehrer, H.: Diffusion in Solids: Fundamentals, Methods, Materials, Diffusion-Controlled Processes. Springer Series in Solid-State Sciences. Springer, Berlin/New York (2007).
47. Crank, J.: The Mathematics of Diffusion. Oxford Science Publications/Clarendon Press, Oxford (1979)

48. Philibert, J.M., Atom Movements – Diffusion and Mass Transport in Solids, Hors Collection, EDP Sciences. Editions de Physique, Les Ulis (2012)
49. Beke, D.L., Landolt, H., Börnstein, R. (eds.): Diffusion in Semiconductors and Non-Metallic Solids. New Series, Group III, vol. 33A. Springer, Berlin (1998)
50. Schulz, M., Landolt, H., Börnstein, R. (eds.): Impurities and Defects in Group IV Elements, IV-IV and III-V Compounds. New Series, Group III, vol. 41A2, Part α. Springer, Berlin (2002)
51. Compaan, K., Haven, Y.: Correlation factors for diffusion in solids. Trans. Faraday Soc. **52**, 786–801 (1956). doi:10.1039/TF9565200786
52. Frank, W., Gösele, U., Mehrer, H., Seeger, A.: In: Murch, G.E., Nowick, A.S. (eds.) Diffusion in Crystalline Solids. Academic Press, New York (1984)
53. Landolt, H., Börnstein, R.: In: Mehrer, H. (ed.) Diffusion in Solids Metals and Alloys, New Series III, vol. 26. Springer, Berlin (1990)
54. Heumann, Th.: In: Ilschner, B. (ed.) Diffusion in Metallen, Werkstoff-Forschung und -Technik Bd., vol. 10. Springer, Berlin (1992)
55. Compaan, K., Haven, Y.: Correlation factors for diffusion in solids. Part 2. – indirect interstitial mechanism. Trans. Faraday Soc. **54**, 1498–1508 (1958). doi:10.1039/TF9585401498
56. Posselt, M., Gao, F., Bracht, H.: Correlation between self-diffusion in Si and the migration mechanisms of vacancies and self-interstitials: an atomistic study. Phys. Rev. B **78**, 035208 (2008). doi:10.1103/PhysRevB.78.035208
57. Chen, R., Dunham, S.T.: Correlation factors for interstitial-mediated self-diffusion in the diamond lattice: kinetic lattice Monte Carlo approach. Phys. Rev. B **83**, 134124, (2011). doi:10.1103/PhysRevB.83.134124
58. Bracht, H., Haller, E.E., Clark-Phelps, R.: Silicon self-diffusion in isotope heterostructures. Phys. Rev. Lett. **81**, 393 (1998). doi:10.1103/PhysRevLett.81.393
59. Ural, A., Griffin, P.B., Plummer, J.D.: Self-diffusion in silicon: similarity between the properties of native point defects. Phys. Rev. Lett. **83**, 3454 (1999). doi:10.1103/PhysRevLett.83.3454
60. Bracht, H., Haller, E.E.: Comment on "Self-Diffusion in silicon: similarity between the properties of native point defects". Phys. Rev. Lett. **85**, 4835 (2000). doi:10.1103/PhysRevLett.85.4835
61. Ural, A., Griffin, P.B., Plummer, J.D.: Ural, griffin, and plummer reply. Phys. Rev. Lett. **85**, 4836 (2000). doi:10.1103/PhysRevLett.85.4836
62. Aid, S.R., Sakaguchi, T., Toyonaga, K., Nakabayashi, Y., Matumoto, S., Sakuraba, M., Shimamune, Y., Hashiba, Y., Murota, J., Wada, K., Abe, T.: Si self-diffusivity using isotopically pure ^{30}Si epitaxial layers. Mater. Sci. Eng. B **114–115**, 330 (2004). doi:10.1016/j.mseb.2004.07.055
63. Shimizu, Y., Uematsu, M., Itoh, K.M.: Experimental evidence of the vacancy-mediated silicon self-diffusion in single-crystalline silicon. Phys. Rev. Lett. **98**, 095901 (2007). doi:10.1103/PhysRevLett.98.095901
64. Bracht, H., Silvestri, H.H., Sharp, I.D., Haller, E.E.: Self- and foreign-atom diffusion in semiconductor isotope heterostructures. II. Experimental results for silicon. Phys. Rev. B **75**, 035211 (2007). doi:10.1103/PhysRevB.75.035211
65. Kube, R., Bracht, H., Hüger, E., Schmidt, H., Lundsgaard Hansen, J., Nylandsted Larsen, A., Ager III, J.W., Haller, E.E., Geue, T., Stahn, J.: Contributions of vacancies and self-interstitials to self-diffusion in silicon under thermal equilibrium and nonequilibrium conditions. Phys. Rev. B. **88**, 085206 (2013). doi:10.1103/PhysRevB.88.085206
66. Suezawa, M., Iijima, Y., Yonenaga, I.: Comment on "Contributions of vacancies and self-interstitials to self-diffusion in silicon under thermal equilibrium and nonequilibrium conditions". Phys. Rev. B **90**, 117201 (2014). doi:10.1103/PhysRevB.90.117201
67. Kube, R., Bracht, H., Hüger, E., Schmidt, H., Lundsgaard Hansen, J., Nylandsted Larsen, A., Ager III, J.W., Haller, E.E., Geue, T., Stahn, J., Uematsu, M., Itoh, K.M.: Reply to "Comment on 'Contributions of vacancies and self-interstitials to self-diffusion in silicon under thermal equilibrium and nonequilibrium conditions"'. Phys. Rev. B **90**, 117202 (2014). doi:10.1103/PhysRevB.90.117202

68. Fahey, P.M., Griffin, P.B., Plummer, J.D.: Point defects and dopant diffusion in silicon. Rev. Mod. Phys. **61**, 289 (1989). doi:10.1103/RevModPhys.61.289
69. Watkins, G.D., Corbett, J.W.: Defects in irradiated silicon: electron paramagnetic resonance and electron-nuclear double resonance of the Si-E center. Phys. Rev. **134**, A1359 (1964). doi:10.1103/PhysRev.134.A1359
70. Manning, J.R.: Correlation factors for impurity diffusion. bcc, Diamond, and fcc Structures. Phys. Rev. **136**, A1758 (1964). doi:10.1103/PhysRev.136.A1758
71. Hu, S.M.: On interaction potential, correlation factor, vacancy mobility, and activation energy of impurity diffusion in diamond lattice. Phys. Stat. Sol. B **60**, 595 (1973). doi:10.1002/pssb.2220600215
72. Dunham, S.T., Wu, C.D.: Atomistic models of vacancy-mediated diffusion in silicon. J. Appl. Phys. **78**, 2362 (1995). doi:10.1063/1.360156
73. Brotzmann, S., Bracht, H.: Intrinsic and extrinsic diffusion of phosphorus, arsenic, and antimony in germanium. J. Appl. Phys. **103**, 033508 (2008). doi:10.1063/1.2837103
74. Chroneos, A., Bracht, H., Grimes, R.W., Uberuaga, B.P.: Vacancy-mediated dopant diffusion activation enthalpies for germanium. Appl. Phys. Lett. **92**, 172103 (2008). doi:10.1063/1.2918842
75. Brotzmann, S., Bracht, H., Lundsgaard Hansen, J., Nylandsted Larsen, A., Simoen, E., Haller, E.E., Christensen, J.S., Werner, P.: Diffusion and defect reactions between donors, C, and vacancies in Ge. I. Experimental results. Phys. Rev. B **77**, 235207 (2008). doi:10.1103/PhysRevB.77.235207
76. Bracht, H.: Self- and foreign-atom diffusion in semiconductor isotope heterostructures. I. Continuum theoretical calculations. Phys. Rev. B **75**, 035210 (2007). doi:10.1103/PhysRevB.75.035210
77. Frank, F.C., Turnbull, D.: Mechanism of diffusion of copper in germanium. Phys. Rev. **104**, 617 (1956). doi:10.1103/PhysRev.104.617
78. Stolwijk, N.A., Frank, W., Hölzl, J., Pearton, S.J., Haller, E.E.: Diffusion and solubility of copper in germanium. Appl. Phys. **57**, 5211 (1985). doi: 10.1063/1.335259
79. Bracht, H.: Copper related diffusion phenomena in germanium and silicon. Mater. Sci. Semicond. Process. **7**, 113 (2004). doi:10.1016/j.mssp.2004.06.001
80. Equation (4) in Ref. [79] should read $D^{\mathrm{eff}}_{\mathrm{Cu(1)}} = 7.8 \times 10^{-5} \exp\left(-\frac{0.084\,\mathrm{eV}}{k_{\mathrm{B}}T}\right)\,\mathrm{cm}^2\mathrm{s}^{-1}$
81. Bracht, H., Stolwijk, N.A., Mehrer, H.: Diffusion and solubility of copper, silver, and gold in germanium. Phys. Rev. B **43**, 14465 (1991). doi:10.1103/PhysRevB.43.14465
82. Gösele, U., Frank, W., Seeger, A.: Mechanism and kinetics of the diffusion of gold in silicon. Appl. Phys. **23**, 361 (1980). doi:10.1007/BF00903217
83. Stolwijk, N.A., Schuster, B., Hölzl, J., Mehrer, H., Frank, W.: Diffusion and solubility of gold in silicon. Physica B+C **116**, 335 (1983). doi:10.1016/0378-4363(83)90271-1
84. Morehead, F., Stolwijk, N.A., Meyberg, W., Gösele, U.: Self-interstitial and vacancy contributions to silicon self-diffusion determined from the diffusion of gold in silicon. Appl. Phys. Lett. **42**, 690 (1983). doi:10.1063/1.94074
85. Stolwijk, N.A., Schuster, B., Hölzl, J.: Diffusion of gold in silicon studied by means of neutron-activation analysis and spreading-resistance measurements. Appl. Phys. A **33**, 133 (1984). doi:10.1007/BF00617619
86. Stolwijk, N.A., Hölzl, J., Frank, W., Weber, E.R., Mehrer, H.: Diffusion of gold in dislocation-free or highly dislocated silicon measured by the spreading-resistance technique. Appl. Phys. A. **39**, 37 (1986). doi:10.1007/BF01177162
87. Hauber, J., Stolwijk, N.A., Tapfer, L., Mehrer, H., Frank, W.: U- and W-shaped diffusion profiles of gold in silicon. J. Phys. C; Solid State Phys. **19**, 5817 (1986). doi:10.1088/0022-3719/19/29/007
88. Stolwijk, N.A., Hölzl, J., Frank, W., Hauber, J., Mehrer, H.: Decoration of defects in silicon with gold, and related subjects. Phys. Stat. Sol. (A) **104**, 225 (1987). doi:10.1002/pssa.2211040117

89. Föll, H., Gösele, U., Kolbesen, B.O.: Microdefects in silicon and their relation to point defects. J. Cryst. Growth **52**, 907 (1981). doi:10.1016/0022-0248(81)90397-3
90. Meyberg, W., Frank, W., Seeger, A., Peretti, H.A., Mondino, M.A.: The migration of interstitials to immobile vacancies and dislocations, with application to plastically deformed tantalum. Cryst. Lattice Defects Amorph. Mater. **10**, 1 (1983)
91. Bracht, H., Overhof, H.: Kinetics of interstitial-substitutional exchange of Zn, Pt, and Au in Si: experimental results and theoretical calculations. Phys. Stat. Sol. (A) **158**, 47 (1996). doi:10.1002/pssa.2211580107
92. Perret, M., Stolwijk, N.A., Cohausz, L.: Kick-out diffusion of zinc in silicon at 1262 K. J. Phys.: Condens. Matter **1**, 6347 (1989). doi:10.1088/0953-8984/1/36/004
93. Grünebaum, D., Czekalla, Th., Stolwijk, N.A., Mehrer, H., Yonenaga, I., Sumino, K.: Diffusion and solubility of zinc in dislocation-free and plastically deformed silicon crystals. Appl. Phys. A **53**, 65 (1991). doi:10.1007/BF00323437
94. Bracht, H., Stolwijk, N.A., Yonenage, I., Mehrer, H.: Interstitial-substitutional diffusion kinetics and dislocation-induced trapping of zinc in plastically deformed silicon. Phys. Stat. Sol. (A) **137**, 499 (1993). doi:10.1002/pssa.2211370220
95. Hauber, J., Frank, W., Stolwijk, N.A.: Diffusion and solubility of platinum in silicon. Mater. Sci. Forum **38–41**, 707 (1989). doi:10.4028/www.scientific.net/MSF.38-41.707
96. Zimmermann, H., Ryssel, H.: Observation of inverse U-shaped profiles after platinum diffusion in silicon. Appl. Phys. Lett. **59**, 1209 (1991). doi:10.1063/1.105505
97. Zimmermann, H., Ryssel, H.: Gold and platinum diffusion: the key to the understanding of intrinsic point defect behavior in silicon. Appl. Phys. A **55**, 121 (1992). doi:10.1007/BF00334210
98. Zimmermann, H., Ryssel, H.: The modeling of platinum diffusion in silicon under non-equilibrium conditions. J. Electrochem. Soc. **139**, 256 (1992). doi:10.1149/1.2069180
99. Lerch, W., Stolwijk, N.A., Mehrer, H., Poisson, Ch.: Diffusion of platinum into dislocated and non-dislocated silicon. Semicond. Sci. Technol. **10**, 1257 (1995). doi:10.1088/0268-1242/10/9/009
100. Mantovani, S., Nava, F., Nobili, S., Ottaviani, G.: In-diffusion of Pt in Si from the PtSi/Si interface. Phys. Rev. B **33**, 5536 (1986). doi:10.1103/PhysRevB.33.5536
101. Giese, A., Bracht, H., Stolwijk, N.A., Walton, J.T.: Out-diffusion of Zn from Si: a method to study vacancy properties in Si. J. Appl. Phys. **83**, 8062 (1998). doi:10.1063/1.367900
102. Giese, A., Bracht, H., Stolwijk, N.A., Baither, D.: Microscopic defects in silicon induced by zinc out-diffusion. Mater. Sci. Eng. B **71**, 160 (2000). doi:10.1016/S0921-5107(99)00367-0
103. Gösele, U., Frank, W., Seeger, A.: An entropy barrier against vacancy-interstitial recombination in silicon. Solid State Commun. **45**, 31 (1983). doi:10.1016/0038-1098(83)90878-5
104. Cowern, N.E.B., Janssen, K.T.F., van de Walle, G.F.A., Gravesteijn, D.J.: Impurity diffusion via an intermediate species: the B-Si system. Phys. Rev. Lett. **65**, 2434 (1990). doi:10.1103/PhysRevLett.65.2434
105. Cowern, N.E.B., van de Walle, G.F.A., Gravesteijn, D.J., Vriezema, C.J.: Experiments on atomic-scale mechanisms of diffusion. Phys. Rev. Lett. **67**, 212 (1991). doi:10.1103/PhysRevLett.67.212
106. Gossmann, H.-J., Gilmer, G.H., Rafferty, C.S., Unterwald, F.C., Boone, T., Poate, J.M., Luftman, H.S., Frank, W.: Determination of Si self-interstitial diffusivities from the oxidation-enhanced diffusion in B doping-superlattices: the influence of the marker layers. J. Appl. Phys. **77**, 1948 (1995). doi:10.1063/1.358828
107. Stolk, P.A., Gossmann, H.-J., Eaglesham, D.J., Jacobson, D.C., Rafferty, C.S., Gilmer, G.H., Jaraíz, M., Poate, J.M., Luftman, H.S., Haynes, T.E.: Physical mechanisms of transient enhanced dopant diffusion in ion-implanted silicon. J. Appl. Phys. **81**, 6031 (1997). doi:10.1063/1.364452
108. Gossmann, H.-J.: Dopants and intrinsic point-defects during Si device processing. In: Huff, H.R., Gösele, U., Tsuya, H. (eds.) Silicon Materials Science and Technology. Electrochemical Society Proceedings, vol. 98-1, p. 884, Pennington (1998)

109. Ural, A., Griffin, P.B., Plummer, J.D.: Fractional contributions of microscopic diffusion mechanisms for common dopants and self-diffusion in silicon. J. Appl. Phys. **85**, 6440 (1999). doi:10.1063/1.370285
110. Cowern, N., Rafferty, C.: Enhanced diffusion in silicon processing. MRS Bull. **25**, 39 (2000). doi:10.1557/mrs2000.97
111. Bracht, H., Stolwijk, N.A., Mehrer, H., Yonenaga, I.: Short-time diffusion of zinc in silicon for the study of intrinsic point defects. Appl. Phys. Lett. **59**, 3559 (1991). doi:10.1063/1.106393
112. Stolwijk, N.A., Grünebaum, D., Perret, M., Brohl, M.: Zinc and sulfur in silicon, experimental evidence for kick-out diffusion behavior. Mater. Sci. Forum **38–41**, 701 (1989). doi:10.4028/www.scientific.net/MSF.38-41.701
113. Rollert, F., Stolwijk, N.A., Mehrer, H.: Diffusion of sulfur-35 into silicon using an elemental vapor source. Appl. Phys. Lett. **63**, 506 (1993). doi:10.1063/1.109987
114. Shockley, W., Moll, J.L.: Solubility of Flaws in Heavily-Doped Semiconductors. Phys. Rev. **119**, 1480 (1960). doi:10.1103/PhysRev.119.1480
115. Gösele, U.M.: Fast diffusion in semiconductors. Ann. Rev. Mater. Sci. **18**, 257 (1988). doi:10.1146/annurev.ms.18.080188.001353
116. Bracht, H., Stolwijk, N.A., Laube, M., Pensl, G.: Diffusion of boron in silicon carbide: evidence for the kick-out mechanism. Appl. Phys. Lett. **77**, 3188 (2000). doi:10.1063/1.1325390
117. Rüschenschmidt, K., Bracht, H., Laube, M., Stolwijk, N.A., Pensl, G.: Diffusion of boron in silicon carbide. Physica B **308–310**, 734 (2001). doi:10.1016/S0921-4526(01)00889-4
118. Rüschenschmidt, K., Bracht, H., Stolwijk, N.A., Laube, M., Pensl, G., Brandes, G.R.: Self-diffusion in isotopically enriched silicon carbide and its correlation with dopant diffusion. J. Appl. Phys. **96**, 1458 (2004). doi:10.1063/1.1766101
119. Yu, S., Tan, T.Y., Gösele, U.: Diffusion mechanism of chromium in GaAs. J. Appl. Phys. **70**, 4827 (1991). doi:10.1063/1.349049
120. Uematsu, M., Wada, K., Gösele, U.: Non-equilibrium point defect phenomena influencing beryllium and zinc diffusion in GaAs and related compounds. Appl. Phys. A **55**, 301 (1992). doi:10.1007/BF00324076
121. Uematsu, M., Werner, P., Schultz, M., Tan, T.Y., Gösele, U.M.: Sulfur diffusion and the interstitial contribution to arsenic self-diffusion in GaAs. Appl. Phys. Lett. **67**, 2863 (1995). doi:10.1063/1.114810
122. Tan, T.Y.: Point defects and diffusion mechanisms pertinent to the Ga sublattice of GaAs. Mater. Chem. Phys. **40**, 245 (1995). doi:10.1016/0254-0584(95)01488-8
123. Bösker, G., Stolwijk, N.A., Thordson, J.V., Södervall, U., Andersson, T.G.: Diffusion of nitrogen from a buried doping layer in gallium arsenide revealing the prominent role of as interstitials. Phys. Rev. Lett. **81**, 3443 (1998). doi:10.1103/PhysRevLett.81.3443
124. Bracht, H., Brotzmann, S.: Zinc diffusion in gallium arsenide and the properties of gallium interstitials. Phys. Rev. B **71**, 115216 (2005). doi:10.1103/PhysRevB.71.115216
125. Sunder, K., Bracht, H., Nicols, S.P., Haller, E.E.: Zinc and gallium diffusion in gallium antimonide. Phys. Rev. B **75**, 245210 (2007). doi:10.1103/PhysRevB.75.245210
126. Ural, A., Griffin, P.B., Plummer, J.D.: Atomic-scale diffusion mechanisms via intermediate species. Phys. Rev. B **65**, 134303 (2002). doi:10.1103/PhysRevB.65.134303
127. Mizuo, S., Higuchi, H.: Retardation of Sb Diffusion in Si during Thermal Oxidation. Jpn. J. Appl. Phys. **20**, 739 (1981). doi:10.1143/JJAP.20.739
128. Mizuo, S., Higuchi, H.: Effects of Oxidation on Aluminum Diffusion in Silicon. Jpn. J. Appl. Phys. **21**, 56 (1982). doi:10.1143/JJAP.21.56
129. Mizuo, S., Kusaka, T., Shintani, A., Nanba, M., Higuchi, H.: Effect of Si and SiO2 thermal nitridation on impurity diffusion and oxidation induced stacking fault size in Si. J. Appl. Phys. **54**, 3860 (1983). doi:10.1063/1.332611
130. Matsumoto, S., Ishikawa, Y., Niimi, T.: Oxidation enhanced and concentration dependent diffusions of dopants in silicon. J. Appl. Phys. **54**, 5049 (1983). doi:10.1063/1.332776
131. Ishikawa, Y., Tomisato, M., Honma, H., Matsumoto, S., Niimi, T.: The retarded diffusion of arsenic in silicon by thermal oxidation in extrinsic conditions. J. Electrochem. Soc. **130**, 2109 (1983). doi:10.1149/1.2119532

132. Fahey, P., Barbuscia, G., Moslehi, M., Dutton, R.W.: Kinetics of thermal nitridation processes in the study of dopant diffusion mechanisms in silicon. Appl. Phys. Lett. **46**, 784 (1985). doi:10.1063/1.95909
133. Miyake, M.: Oxidation-enhanced diffusion of ion-implanted boron in silicon in extrinsic conditions. J. Appl. Phys. **57**, 1861 (1985). doi:10.1063/1.334416
134. Ishikawa, Y., Nakamichi, I., Matsumoto, S., Niimi, T.: The effect of thermal oxidation of silicon on boron diffusion in extrinsic conditions. Jpn. J. Appl. Phys. **26**, 1602 (1987). doi:10.1143/JJAP.26.1602
135. Giles, M.D.: Extrinsic transient diffusion in silicon. Appl. Phys. Lett. **58**, 2399 (1991). doi:10.1063/1.104883
136. Gossmann, H.-J., Haynes, T.E., Stolk, P.A., Jacobson, D.C., Gilmer, G.H., Poate, J.M., Luftman, H.S., Mogi, T.K., Thompson, M.O.: The interstitial fraction of diffusivity of common dopants in Si. Appl. Phys. Lett. **71**, 3862 (1997). doi:10.1063/1.120527
137. Sharp, I.D., Bracht, H.A., Silvestri, H.H., Nicols, S.P., Beeman, J.W., Hansen, J., Nylandsted Larsen, A., Haller, E.E.: Self- and dopant diffusion in extrinsic boron doped isotopically controlled silicon multilayer structures. Mater. Res. Soc. Symp. Proc. **719**, F13.11 (2002). doi:10.1557/PROC-719-F13.11
138. Silvestri, H.H., Sharp, I.D., Bracht, H.A., Nicols, S.P., Beeman, J.W., Hansen, J., Nylandsted Larsen, A., Haller, E.E.: Dopant and Self-Diffusion in Extrinsic n-Type Silicon Isotopically Controlled Heterostructures. Mater. Res. Soc. Symp. Proc. **719**, F13.10 (2002). doi:10.1557/PROC-719-F13.10
139. Silvestri, H.H., Bracht, H., Sharp, I.D., Lundsgaard Hansen, J., Nylandsted Larsen, A., Haller, E.E.: Simultaneous phosphorus and Si self-diffusion in extrinsic, isotopically controlled silicon heterostructures. Mater. Res. Soc. Symp. Proc. **810**, C3.3. (2004) C3.3. doi:10.1557/PROC-810-C3.3
140. Bracht, H., Silvestri, H.H., Haller, E.E.: Advanced diffusion studies with isotopically controlled materials. Solid State Commun. **133**, 727 (2005). doi:10.1016/j.ssc.2004.12.024
141. Bracht, H., Diffusion mediated by doping and radiation-induced point defects. Physica B **376–377**, 11 (2006). doi:10.1016/j.physb.2005.12.006
142. Bracht, H., Rodriguez Schachtrup, A., Yonenaga, I.: Segregation of gold at dislocations confirmed by gold diffusion into highly dislocated silicon. Mater. Sci. Forum **258–263**, 1783 (1997)
143. Rodriguez, A., Bracht, H., Yonenaga, I.: Impact of high B concentrations and high dislocation densities on Au diffusion in Si. J. Appl. Phys. **95**, 7841 (2004). doi:10.1063/1.1751235
144. Yoshida, M., Arai, E., Nakamura, H., Terunuma, Y.: Excess vacancy generation mechanism at phosphorus diffusion into silicon. J. Appl. Phys. **45**, 1498 (1974). doi:10.1063/1.1663450
145. Yoshida, M.: Numerical solution of phosphorus diffusion equation in silicon. Jpn. J. Appl. Phys. **18**, 479 (1979). doi:10.1143/JJAP.18.479
146. Uematsu, M.: Simulation of boron, phosphorus, and arsenic diffusion in silicon based on an integrated diffusion model, and the anomalous phosphorus diffusion mechanism. J. Appl. Phys. **82**, 2228 (1997). doi:10.1063/1.366030
147. Mirabella, S., De Salvador, D., Napolitani, E., Bruno, E., Priolo, F.: Mechanisms of boron diffusion in silicon and germanium. J. Appl. Phys. **113**, 031101 (2013). doi:10.1063/1.4763353
148. Masters, B.J., Fairfield, J.M.: Arsenic isoconcentration diffusion studies in silicon. J. Appl. Phys. **40**, 2390 (1969). doi:10.1063/1.1658001
149. Yoshida, M., Tanaka, S.: Simulation of phosphorus diffusion profiles with different phosphorus surface concentration at the same diffusion temperature in silicon. Jpn. J. Appl. Phys. **41**, 5493 (2002). doi:10.1143/JJAP.41.5493
150. Makris, J.S., Masters, B.J.: Phosphorus isoconcentration diffusion studies in silicon. J. Electrochem. Soc. **120**, 1252 (1973). doi:10.1149/1.2403672
151. Fair, R.B., Tsai, J.C.C.: A Quantitative model for the diffusion of phosphorus in silicon and the emitter dip effect. J. Electrochem. Soc. **124**, 1107 (1977). doi:10.1149/1.2133492
152. Tan, T.Y., Gösele, U.: Point defects, diffusion processes, and swirl defect formation in silicon. Appl. Phys. A **37**, 1 (1985). doi:10.1007/BF00617863

153. Ager III, J.W., Beeman, J.W., Hansen, W.L., Haller, E.E., Sharp, I.D., Liao, C., Yang, A., Thewalt, M.L.W., Riemann, H.: High-purity, isotopically enriched bulk silicon. J. Electrochem. Soc. **152**, G448 (2005). doi:10.1149/1.1901674
154. see International Technology Roadmap for Semiconductors. http://www.itrs.net
155. Thewalt, M.L.W.: Spectroscopy of excitons and shallow impurities in isotopically enriched silicon-electronic properties beyond the virtual crystal approximation. Solid State Commun. **133**, 715 (2005). doi:10.1016/j.ssc.2004.12.023
156. Steger, M., Yang, A., Sekiguchi, T., Saeedi, K., Thewalt, M.L.W., Henry, M.O., Johnston, K., Riemann, H., Abrosimov, N.V., Churbanov, M.F., Gusev, A.V., Kaliteevskii, A.K., Godisov, O.N., Becker, P., Pohl, H.-J.: Photoluminescence of deep defects involving transition metals in Si: new insights from highly enriched 28Si. J. Appl. Phys. **110**, 081301 (2011). doi:10.1063/1.3651774
157. Gleiter, H.: Nanostructured materials: basic concepts and microstructure. Acta Mater. **48**, 1 (2000). doi:10.1016/S1359-6454(99)00285-2
158. Gleiter, H., Weissmüller, J., Wollersheim, O., Würschum, R.: Nanocrystalline materials: a way to solids with tunable electronic structures and properties. Acta mater. **49**, 737 (2001). doi:10.1016/S1359-6454(00)00221-4
159. Colinge, J.-P., Lee, C.-W., Afzalian, A., Akhavan, N.D., Yan, R., Ferain, I., Razavi, P., O'Neill, B., Blake, A., White, M., Kelleher, A.-M., McCarthy, B., Murphy, R.: Nanowire transistors without junctions. Nat. Nanotechnol. **5**, 225 (2010). doi:10.1038/nnano.2010.15